MODULATION OF THE TUMOR SUPPRESSOR PROGRAMMED CELL DEATH 4 BY THE PROTEIN ARGININE METHYL TRANSFERASE 5: FROM BIOLOGY TO BIOMARKER

by

Matthew A. Powers

A dissertation submitted to the faculty of
The University of Utah
in partial fulfillment of the requirements for the degree of

Doctor of Philosophy

Department of Oncological Sciences

University of Utah

December 2010

The University of Utah Graduate School

STATEMENT OF DISSERTATION APPROVAL

The dissertation of **Matthew A. Powers**

has been approved by the following supervisory committee members:

Katharine S. Ullman	, Chair	**10-19-2010** Date Approved
Eric L. Huang	, Member	**10-19-2010** Date Approved
David A. Jones	, Member	**10-19-2010** Date Approved
Matthew K. Topham	, Member	**10-19-2010** Date Approved
Alana L. Welm	, Member	**10-19-2010** Date Approved

and by **Barbara J. Graves**, Chair of the Department of **Oncological Sciences**

and by Charles A. Wight, Dean of The Graduate School.

ABSTRACT

Programmed cell death 4 (PDCD4) has been described as a tumor suppressor in multiple cancer cell types. *In vitro*, exogenous expression of PDCD4 results in decreased anchorage-independent cell growth and invasion. These anticancer phenotypes are attributed to inhibition of the translation initiation factor eIF4A when bound to PDCD4. In this dissertation, I report the discovery of novel interactions with the nuclear pore protein Nup153, the exon junction core protein eIF4AIII, and protein arginine methyltransferase 5 (PRMT5) that may modulate PDCD4 in a cancer context.

PDCD4 levels are often suppressed in cancerous cells compared to normal surrounding tissues, and elevated expression in tumors is correlated with better survival outcomes. Despite this, 20-30% of patients with tumors that express high levels of PDCD4 have poor outcomes, indicating that these cancers deactivate PDCD4. Our analyses of transcript expression in breast cancer patients show that simultaneous upregulation of *PRMT5* with *PDCD4* results in poor survival outcomes. Using an orthotopic tumor model, I demonstrate that simultaneous expression of PDCD4 and PRMT5 in the breast cancer cell line MCF7 causes accelerated tumor growth. This tumor growth phenotype is dependent on PRMT5 enzymatic activity and the PDCD4 N-terminal site that is modified by PRMT5. This demonstrates that PDCD4 tumor suppressor function is radically altered when modified by PRMT5. Furthermore, this provides a mechanism for poor outcomes in patients with tumors that express elevated

PDCD4. These findings show the utility of tracking both PDCD4 and PRMT5 as biomarkers and reveals PRMT5 as a potential target of chemotherapy.

Finally, PDCD4 acts as a tumor suppressor through inhibition of the RNA helicase activity of eIF4A, although the precise mechanism of how this is accomplished has been unknown. In this dissertation, I report that PDCD4 interferes with the ability of eIF4A to interact with RNA, thereby deactivating its RNA helicase function. This provides a clear *in vitro* mechanism for eIF4A inhibition by PDCD4.

To Annie

CONTENTS

LIST OF FIGURES

LIST OF TABLES

CHAPTER 1

INTRODUCTION

1.1 Broad issues in cancer

Despite significant advances in treatment and detection, cancer is still a leading cause of mortality, especially in developed countries. The American Cancer Society estimates that there are 11.6 million people who have had or are actively living with cancer in the United States (approximately 1 in 27 people). It is estimated that 1.5 million people will be diagnosed and 570,000 will die of the disease in 2010 which is on pace for 1,500 mortalities a day (1).

Unlike pathologies resulting from invasion of external pathogens with dissimilar physiology, cancer is a direct descendent of normal cells within the body. This characteristic makes cancer both challenging to differentiate from healthy cells, especially in early stages, and difficult to treat because of overlap in expression of targets of chemotherapy between normal and tumor cells. Advances in imaging and new diagnostic tests have increased the accuracy of detection of cancer at very early stages. This has lead to increased survival of many cancer patients but has also caused new dilemmas regarding aggressiveness of treatment and type of treatment. Historically, for instance, breast cancer prognosis has been defined by the tumor-node-metastasis (TNM) staging standards, which accounts only for the organ of origin, size and lymph node

involvement and metastasis. This prognostic standard does not account for markers that determine aggressiveness, treatment type and treatment sensitivity, especially in subclinical cancers detected by early screening (2). Unknown and/or unquantifiable risk assessments based on new detection methods can lead to over treatment of indolent disease, exposing patients to unwanted side effects and even new cancers, or under treatment of aggressive disease, risking recurrence (3). An example of this dilemma is a stage I-II breast cancer tumor with a negative lymph node biopsy. The decision to commit to adjuvant therapy after surgery and radiation remains difficult when weighing the possible side effects of chemotherapy/endocrine therapy versus unknown disease recurrence probability (3).

Increasingly, the molecular signatures of tumors are used to determine both outcomes and treatment options and have fueled intensive research into new prognostic indicators including microarray, RT-PCR and protein expression based tests. These tests have not only helped in patient risk assessments but have also yielded new targets for drug design. Cancer is an extremely diverse set of diseases with many types, and despite these new innovations in prognostic indicators and development of new drugs, there are numerous cancer types with little recourse. Expanding the use of new prognostic tools and adding new ones to the kit will help inform doctors and patients on treatment type and could provide new targets for chemotherapy.

1.2 Translation initiation and cancer

Cancers are defined by a lack of growth control, an ability to escape apoptosis, and the capability of invading new tissues. Many barriers at different cellular levels of

control are overcome in the process of malignant transformation and each one of these pathways is of interest for yielding new biomarkers and potential drug targets. Loss of regulation can occur in cell signaling, genomic stability, transcriptional control, transcript stability and translation. In the last few decades, protein translation has become increasingly understood as an important point of control, and disregulation, in oncogenesis (4, 5). The defining quality of uncontrolled cell growth is predicated on the ability of the cell to upregulate its normal capacity to synthesize building blocks necessary for cell division. Specifically, this node of regulation is at the rate-limiting step in the production of proteins, translation initiation, when the ribosome loads onto messenger RNA with the help of a protein complex and is accurately positioned at the start codon. Beyond "bulk" levels of translation, growth-related proteins have specific translational control mechanisms that can be targets of deregulation. These include sequences targeted by microRNAs and also structures within the 5' and 3' untranslated regions of growth-related mRNAs that allow for fine tuning of expression beyond transcription (5). Overall, disregulation of translation initiation during oncogenesis is now recognized as an important step to malignancy and is garnering broad interest as a source of prognostic indicators and targets for chemotherapy.

The initiation step of so-called "cap-dependent" translation occurs when the translation initiation complex eIF4F binds the 5' methyl cap. The 5' cap is a specialized structure containing a guanine nucleotide modified by a methyl group at position seven and connected to the mRNA strand by a 5', 5' triphosphate linkage (i.e. an inverted guanine that confers resistance to endonucleases). Cap-dependent translation makes up the bulk of protein synthesis but an alternative method using specialized mRNA

structures termed internal ribosome binding sites (IRES) is less dependent on the components that comprise eIF4F and is a major source of new protein synthesis during mitosis of the cell cycle when cap-dependent translation is inhibited (4, 5). Once loaded onto mRNA, the eIF4F complex recruits the 43S initiation complex (which is composed of the 40S ribosome, eIF5 and the ternary complex eIF2GTP-$tRNA_i$) then scans the 5'UTR, unwinding secondary RNA structures that are encountered, until it is positioned at the appropriate start AUG codon. The end of translation initiation is marked by hydrolysis of GTP to GDP, causing release of eIF2 and recruitment of the 60S ribosome to the 43S initiation complex. This forms the complete translation-competent 80S ribosome and that subsequently catalyzes the first peptide bond with help from eIF5A (4). Misregulation of any translation initiation factor is potentially relevant in cancer biology, but there is increased interest in the eIF4F complex as many of its components are implicated in oncogenesis.

The critical steps of recognizing the 5' methyl cap and scanning the 5'UTR is carried out by the three proteins that make up the eIF4F complex: eIF4E, eIF4G and eIF4A. eIF4E, the cap binding protein of the eIF4F complex, is overexpressed in numerous cancers and its overexpression is known to transform NIH3T3 cells (6). Phosphorylation of eIF4E at serine 209 is also associated with some cancers (5). In conjunction with overexpression, specialized inhibiting proteins –4E-binding proteins (4E-BPs)– are often deactivated, increasing the effective concentration of eIF4E in cancer (7). 4E-BP binds and inhibits association of eIF4E with the 5' methyl cap and incorporation into the eIF4F complex. The pro-cancer mTOR signal pathway hyper-phosphorylates 4E-BP, causing it to dissociate from eIF4E (5, 8).

eIF4G is a large scaffold protein that links eIF4E with eIF4A and the ribosome and additionally recruits kinases responsible for phosphorylation of eIF4E at serine 209. eIF4G is expressed in two isoforms, eIF4G1 and 2, with isoform 1 being the most common. eIF4G1 is overexpressed in some cancers, and exogenous upregulation of eIF4G1 can transform NIH3T3 cells in the absence of upregulated eIF4E (9-11). eIF4G was found to be highly elevated in inflammatory breast cancer, in the absence of changes in levels or phosphorylation of eIF4E (12). The ability of eIF4G to transform cells, and its upregulation in cancers in the absence of eIF4E upregulation, indicates that eIF4G may upregulate cap-independent translation. Cap-independent translation is mediated by special mRNA sequences that form internal ribosome entry sites (IRESs) and this specialized form of translation is often dependent on eIF4G (and in some cases eIF4A) but not on eIF4E (12). Despite these later findings, the small molecule inhibitor 4EG1-1 inhibits eIF4G1 and eIF4E interaction and has tumor killing properties in tissue culture (13, 14).

The last component of the eIF4F complex, eIF4A (or more specifically, the paralogues eIF4A1 and eIF4A2), is an ATP-dependent RNA helicase responsible for unwinding secondary structures in the 5'UTR of mRNAs thereby allowing efficient translation of these transcripts. eIF4A1 is upregulated in some hepatocellular carcinomas and tumor cell lines (15). The eIF4A small molecule inhibitor, silvestrol, blocks translation and also is a potent inhibitor of breast and prostate tumor growth in xenograft models (16).

Interestingly, the tumor suppressor programmed cell death 4 (PDCD4) has been reported to bind ribosomes, eIF4G, eIF4A and regulate eIF4E levels and phosphorylation

status (17-19). Moreover, the ability of PDCD4 to function as a tumor suppressor *in vitro* appears to be dependent on its ability to bind to eIF4A and inhibit translation (18, 19). PDCD4 is down-regulated in a number of cancers and is a prognostic indicator, with increased expression correlating with increased survival and lower tumor grade (20-24). Many studies place PDCD4 as a central player at the node of translation initiation and point to a critical role for PDCD4 levels in the generation/progression of numerous tumor types.

Although translation regulation is a strong theme in many studies centered on PDCD4, other functions, including RNA binding and transcriptional control (25, 26) that may be independent of translation, have been attributed to PDCD4 and may play a role in its tumor suppressor functions. I will review the major findings in the field to help synthesize what is known about PDCD4 function and regulation.

1.3 Discovery of PDCD4 and its role in tumor suppression

PDCD4 (also termed MA-3, TIS, DUG, and H731) was first described as a transcript up-regulated upon apoptotic stimuli in a variety of blood cell lines. These stimuli included ionomycin, phorbol myristate acetate, dexamethasone and removal of IL-3 or IL-2 (27). Notably, exogenous expression of PDCD4 in these same cell lines did not induce apoptosis, indicating that PDCD4 is not sufficient for cell death. PDCD4 is expressed in all mouse tissues tested, to varying degrees (27). Unlike the above reagents used to stimulate apoptosis, induction of apoptosis by camptothecin, which blocks topoisomerase function, caused downregulation of PDCD4. This down-regulation was attributed to elements in the *Pdcd4* promoter sensitive to topoisomerase inhibition and

resulted in loss of PDCD4 expression at the transcription level (28, 29). During murine embryogenesis, PDCD4 was found to be upregulated although it is unclear what role this plays since, later, a knockout mouse of PDCD4 had no visible developmental defects (30, 31).

PDCD4 was first connected to cancer in a murine epidermal cell model. In JB6 (P+) cells that are sensitive to phorbol ester-induced transformation, PDCD4 was down-regulated compared to the transformation-resistant JB6 (P-) cell line. The P- resistant cell line became susceptible to transformation when PDCD4 was reduced by anti-sense constructs, showing that PDCD4 was necessary for this resistance (32). PDCD4 was also found to confer transformation resistance to the JB6 (P+) cell line (33). Concomitant with upregulation of PDCD4 was a down- regulation of AP-1-dependent signaling although the mechanism of signal down-regulation was unclear (33).

Soon after, PDCD4 was discovered to bind the translation initiation protein eIF4A (34), blocking its ability to unwind RNA hairpins and decreasing translation of mRNA reporters containing structured 5'UTRs (18, 19). The ability of PDCD4 to block transformation in the JB6 mouse model was likewise found to be dependent on binding of eIF4A (19). Furthermore, PDCD4 blocked anchorage-independent cell growth in transformed mouse cells (35). Despite this connection, the molecular mechanism by which PDCD4 prevents eIF4A activity remained an open question (see Chapter 4).

1.4 Clinical and cancer-specific studies of PDCD4

1.4.1 Skin cancer

As stated above, PDCD4 was first recognized as a tumor suppressor in a transformed mouse epidermal cell line, when exogenous upregulation of PDCD4 suppressed the ability of transformed cells to grow in soft agar (35). Transgenic mice overexpressing PDCD4 in the epidermis exhibited a short hair phenotype due to shortened anagen (the growth phase of hair follicle) but had no other detectable defect. Treatment of the skin of these mice with tumor promoting agents resulted in papilloma formation with delayed kinetics and decreased burden compared to wildtype littermates. The development of squamous cell carcinoma from papilloma was also significantly decreased in these mice, indicating that PDCD4 inhibits both skin tumor development and progression *in vivo* (36). In a separate study, treating the skin of wild-type mice with the linoleic acid metabolite 13-HOA induced upregulation of PDCD4 concurrent with inhibition of tumor formation (37).

In the transgenic mouse model, PDCD4 up-regulation also correlated with down-regulation of endogenous CDK4 and ODC, both of which are expressed from mRNAs with 5'UTRs predicted to have structured hairpins. This observation reinforced the model that translation suppression may be critical to *in vivo* suppression of carcinogenesis (31).

1.4.2 Lung cancer

PDCD4 was first studied for clinical relevance in lung cancer. *PDCD4* mRNA expression was found to be lower in lung cancer cell lines than in human bronchial

epithelial cells (HBEC) or in small airway epithelial cells (SAEC) cultured *in vitro* (20). This was confirmed in lung cancer cells compared to surrounding normal cells by microarray, where *PDCD4* levels were markedly low in higher grade tumors. To follow this up, Chen *et al* probed a tissue microarray of 248 primary lung cancer samples from 124 patients for PDCD4 protein. Eighty three percent of the samples exhibited no staining whereas 17% had low nuclear and cytoplasmic staining. Normal lung tissue displayed strong nuclear PDCD4 staining. The tumors from the tissue microarray were further stratified into adenocarcinomas or squamous cell carcinomas. No correlation was made in the squamous cell carcinomas. Interestingly, PDCD4 was expressed at significantly lower levels in higher grade adenocarcinomas whereas no association was found with stage, side or nodal status. The most striking result was that the absence of PDCD4 protein expression was significantly correlated with adverse prognosis with a mean survival of patients with PDCD4 positive tumors reaching 47 months compared with 22 months in patients without expression (20). This was the first indication that PDCD4 was a relevant biomarker for patient outcome.

1.4.3 Colon cancer

In a study of colon cancer, 71 tumors were compared to 42 adenomas and 71 normal tissues. Overall PDCD4 levels assessed by immunohistochemistry showed a progressive decrease between normal to adenoma to tumor samples. Interestingly, normal tissue displayed high levels of nuclear PDCD4 whereas the adenomas had intermediate and tumors had low levels of staining. Kaplan-Meier analysis of disease free survival and overall survival showed that loss of PDCD4 was a prognostic indicator

of poor outcome. Notably, transition of PDCD4 from the nucleus to the cytoplasm was also correlated with poor outcome (21). In a separate study of 86 adenocarcinoma and carcinoma tissue samples, not linked to patient outcomes, PDCD4 was also observed to be down-regulated compared to normal tissue (38).

In tissue culture models related to colon cancer, overexpression of PDCD4 in the colorectal cancer cell line RKO caused a decrease in AP-1 transcription by downregulation of the MAPK signal pathway through repression of MAP4K1 expression. The overexpression of PDCD4 did not alter the cell's doubling time in culture but inhibited invasiveness of RKO cells by 50-60% in matrigel assays. This inhibition of invasion was attributed to lowered cell migration and loss of expression of matrix metallo-proteases (MMPs) (39). Later, PDCD4 was also found to downregulate u-PAR expression at the transcription level by inhibiting the *cis*-acting transcription factors Sp-1 and Sp-3 (40). u-PAR is also involved in breakdown of extracellular matrix and contributes to cell invasiveness when expressed. In a separate study, knockdown of PDCD4 in HT29 cells increased invasiveness by 11 fold and induced a fibroblast-like morphology of the cells. This knockdown was accompanied by suppression of E-cadherin, a molecule that increases cell-cell adhesion, and increases in active nuclear β-catenin, Tcf4 mediated transcription and AP-1 signaling (38).

An endogenous micro RNA, miRNA-21, was found to downregulate PDCD4 in colorectal cancer tissue culture cells. Exogenous expression of miRNA-21 caused a decrease in PDCD4 and an increase in cell invasion and extravasation using a chicken embryo based assay. miRNA-21 was also found to be expressed in a number of colon cancer cell lines and to be inversely correlated with PDCD4 expression (41).

These tissue culture results help explain, at least in part, the lower probability of survival when PDCD4 expression is lost in colon cancer patients. Tumors with lowered PDCD4 levels may have increased mobility due to down regulation of E-cadherin and increased invasiveness due to upregulation of u-PAR and MMPs. These changes, together with increased oncogenic signaling through AP-1 and β-catenin, could significantly alter cell physiology in a way that results in a more aggressive phenotype (higher grade) and increased potential for metastases.

1.4.4 Leukemia and lymphoma

PDCD4 was first implicated in hematologic malignancies in a knockout mouse model (31). The removal of exon 3 and 4 by targeted homologous recombination produced a mouse that lacked mRNA and protein expression of PDCD4. These mice had no gross phenotypic abnormalities such as body weight, temperature or oxygen consumption. Yet, 85% of the *Pdcd4* knockout mice developed B-cell lymphoma over the course of their life as opposed to 14% for wildtype C57BL/6 littermates. Interestingly, these knockout mice also had a reduced incidence of diabetes when induced by self-reactive lymphocytes upon treatment with streptozotocin. Further, the severity of experimental autoimmune encephalomyelitis induced by treatment with myelin oligodendrocyte glycoprotein was also reduced in *Pdcd4* knockout mice. Investigation into the cause of lowered immune response revealed that overall translation, along with IL-10, IL-4 and IFN-γ, were all upregulated in isolated cells from the knockout mice whereas ~ 50 other immune response molecules/cytokines were unaffected by PDCD4 status (31). This altered immune response indicates that the etiology of B-cell

lymphomas could be due in part to a dysfunctional immune system due to inappropriate expression of these three molecules; it would be of interest to transplant a mix of wild-type and *Pdcd4* knockout hematopoietic cells to evaluate the contribution of cell autonomous mechanisms.

Acute myeloid leukemia is characterized by accumulation of progenitor blood cells that are blocked in the ability to differentiate. Stimulation of these cells to differentiate by addition of drugs such as all-*trans* retinoic acid (ATRA) can be an effective treatment with minimal side effects. Ozpolat *et al.* found that treatment of the acute promyelocytic leukemia cell line NB4 with ATRA causes both differentiation and upregulation of PDCD4. NB4 cells transfected with siRNA to deplete PDCD4 failed to differentiate upon ATRA stimulation. Also, $p27^{kip1}$ and DAP5 (both necessary for differentiation) were down-regulated while c-myc and WT1 (both poor prognostic indicators and normally down-regulated by ATRA treatment) were upregulated concurrent with siRNA-mediated knockdown of PDCD4 and ATRA treatment. Both the upregulation and downregulation of these proteins were at a posttranslational level as mRNA concentrations remained constant indicating that PDCD4 may be directly regulating expression by translation inhibition (42).

The development of B-cell lymphoma in mice lacking PDCD4 strongly indicates its role in tumor suppression. PDCD4 also helps regulate the inflammatory response in mice. The inability of acute myeloid leukemia cells to respond to differentiation signals when PDCD4 is missing points to a possible role for PDCD4 in proper blood lineage development, although a gross phenotype may only appear under immune cell challenge. The downregulation of $p27^{kip1}$ and DAP5 at a post transcriptional-level may indicate that

PDCD4 also increases translation of some mRNAs making it a selective translation suppressor and activator. A pro-translation role of PDCD4 is one possible explanation for a pro-tumor growth phenotype attributed to PDCD4 that we have discovered (See Chapter 3).

1.4.5 Hepatocellular carcinoma

In a study of 18 samples from patients with hepatocellular carcinoma (HCC), PDCD4 protein was found to be down-regulated in tumors compared to adjacent normal hepatocytes. PDCD4 was expressed in the cytoplasm of both normal hepatocytes and HCC. As a follow-up, PDCD4 was transfected into the HCC cell line Hu7. DNA fragmentation was found to occur in cells where exogenously expressed PDCD4 accumulated in the nucleus. Well-known markers of apoptosis were present in cells which expressed PDCD4. HCC is known to undergo apoptosis with TGF-β1 treatment; TGF-β1 treatment of Hu7 cells caused an upregulation of PDCD4 concurrent with apoptosis. Finally, antisense knockdown of PDCD4 caused a loss of apoptosis upon TGF-β1 treatment. These results indicate that PDCD4 is sufficient to induce apoptosis in this hepatocellular carcinoma cell line and is necessary for TGF-β1 mediated HCC cell death (43). In contrast, a second study did not report apoptosis in MHCC-97H, MHCC-97L, or Hep3B HCC cell lines upon exogenous expression of PDCD4 but rather a block in matrigel invasion assays was found (44). Finally, a separate study indicated that overexpression of PDCD4 blocks both the upregulation and phosphorylation of eIF4E in MHCC-97L cells upon hydrogen peroxide treatment (a treatment known to induce metastatic potential in these cells) (17). There was no actual test of invasion or

translation in these cells and it is unclear what role eIF4E may play in metastasis of HCC. Follow up on the ability of PDCD4 to cause apoptosis in one cell line, Hu7, but not in others, MHCC-97H and L and Hep3B may provide clues of oncogenic addiction pathways in subcohorts of HCC and may also provide a better understanding of PDCD4 targets.

In a small study of 68 Chinese men with HCC, smokers and non smokers were stratified. Smokers were found to have significantly less PDCD4 expression in normal liver compared with nonsmokers but there was no difference in expression in carcinoma tissue in either cohort. On average, smokers developed HCC 10 years earlier than nonsmokers, raising the question of whether loss of PDCD4 in the liver, due to smoking, may play a role in early development of HCC (45).

1.4.6 Breast cancer

A study of 65 breast tumors compared to 15 cases of ductal carcinoma in situ (DCIS) and 5 samples of normal breast tissue found that PDCD4 was progressively lost, as assessed by immunohistochemistry, from normal to DCIS to ductal carcinoma. There was mixed subcellular localization with a primarily cytoplasmic localization of PDCD4 in normal breast tissue. PDCD4 was primarily localized in the cytoplasm in invasive ductile carcinoma but was at a much lower level than DCIS or normal tissue. Also of note, PDCD4 nuclear localization strongly correlated with ER^+ and $HER2/neu^+$ DCIS cells but there was no correlation with retinoic acid receptor or progesterone receptor expression (24). Interestingly, in a previous study from the same lab, culturing RAR^+ breast cancer cells with ATRA caused growth arrest and up regulation of PDCD4. This

held true in a neuroblastoma and acute myeloid leukemia cell lines also positive for RAR^+. Treating ER^+, $Her2/neu^+$ cell lines with the estrogen receptor antagonist ICI-182780, or with Herceptin, also up regulated PDCD4. This suggests a potentially complicated interplay between hormone receptors and HER2/neu signaling and PDCD4 expression in breast cancer.

1.4.7 Esophageal cancer

In esophageal cancer, loss of PDCD4 expression correlated with worse tumor grade. Normal tissue expressed nuclear PDCD4, which was down regulated or lost in cancerous tissue. Residual nuclear PDCD4 staining in tumors correlated with longer disease free survival and overall survival (46). This indicates that PDCD4 also is lost in the progression of esophageal cancer and that subcellular localization may play an important tumor suppressor role.

1.4.8 Ovarian cancer

In a study of ovarian tissue and tumors, PDCD4 was localized to the nucleus, as assessed by immunohistochemistry, in all normal tissue positive for expression (84% of normal samples expressed PDCD4). Of 44 tumor samples, 18 had PDCD4 expression. Of these, 6 expressed PDCD4 in the nucleus, 9 had predominantly cytoplasmic expression and 4 had mixed localization. Clinical follow-up established that high PDCD4 expression (those above the median for PDCD4 expression) correlated with longer disease free survival but not with age, stages of disease, histological types, grade, metastasis, disease specific and overall survival. This study also found good correlation

between protein and mRNA expression of PDCD4 (23). Overexpression of PDCD4 in SKOV3, 3AO, and CAOV3 ovarian cancer cells caused impaired proliferation, corresponding to cell cycle arrest at S and G2 phase and apoptosis. Subcutaneous injection of SKOV3 cells engineered to overexpress PDCD4 into nude mice resulted in tumors that grew significantly slower than control cells (47). The mouse model, clinical data and cell culture *in vitro* data all point to a role for PDCD4 inhibiting growth of ovarian cancer cells.

1.4.9 Bladder cancer

One study of multiple cancer types found that PDCD4 was upregulated in bladder cancer and breast cancer compared to normal cells using the monoclonal H731 antibody raised against partially purified bacterially expressed constructs (48). This result may indicate that PDCD4 is regulated differently in bladder although we know that PDCD4 is often down regulated in breast cancer (24) (Chapter 3). Although a clear result for the example provided, use of this H731 antibody for an immunoblot in a separate study shows multiple background bands other than PDCD4 and may indicate that the IHC results are tracking an alternative marker (32).

1.5 Regulation of PDCD4

To date, PDCD4 levels are known to be regulated by transcription, protein degradation, and miRNA targeting of mRNA. PDCD4 was originally defined as a transcript down regulated by topoisomerase inhibitor treatments and elements within the *Pdcd4* promoter were found responsible (28, 29). Gao *et al.* found that the *Pdcd4* region

was subject to DNA methylation and gene silencing in glioma (49), however, treatment of breast cancer cells with DNA methyltransferase inhibitors did not affect expression levels (24).

While gene silencing at this locus needs more thorough and critical assessment, different mechanisms may well be in play in different cancer types. A counterintuitive observation of PDCD4 regulation is its transcriptional upregulation by v-Myb (an oncogenic viral homologue of c-Myb), found in cultured chicken cells (50, 51). The significance of this regulation is unclear in light of not knowing if avian and human PDCD4 differ in function and regulation. Dorello *et al.* elegantly demonstrated that PDCD4 is a target for proteasomal degradation through activation of the mTOR pathway. This occurs following mitogen stimulation, subsequent phosphorylation of PDCD4 by S6K1, and ubiquitination catalyzed by β-TRCP (52). This proteasomal degradation pathway was also activated by treatment of cells with phorbol esters (53) and through BCR-ABL fusion oncogenic protein signaling (54). The oncogenic micro RNA, miR-21, was found to target PDCD4 mRNA, leading to a block in translation and transcript degradation (41, 55). miR-21 regulation of PDCD4 has been found in breast cancer, hepatocellular carcinoma, and colon cancer and may regulate PDCD4 across numerous other cancers (41, 55-58). Recently, PDCD4 was also found to be a target of miR-183 in hepatocellular carcinoma indicating that other micro RNAs also downregulate PDCD4 (59). In a study of *PDCD4* mRNA levels and protein expression in 14 squamous cell carcinomas (SSC), there was little correlation between mRNA levels and PDCD4 expression (60). This highlights that PDCD4 levels can be regulated independent of transcript levels, which is discussed later.

Subcellular localization may also regulate PDCD4 activity. High efficiency translation occurs when polyribosomes are loaded onto mRNAs in cytoplasm and the activity of PDCD4 as a translation inhibitor is thought to also occur in this subcellular compartment (19). In mouse skin and human breast tissue, PDCD4 is localized primarily to the cytoplasm (24, 36). Yet, PDCD4 is prevalent in the nucleus in healthy lung and colon cancer cells and is cytoplasmic in the corresponding cancers (20, 21, 61). In chicken cells, PDCD4 shuttles between the nucleus and the cytoplasm and has been shown to contain a putative nuclear localization signal (25). If PDCD4 functions as a tumor suppressor in the cytoplasm, sequestration of PDCD4 in the nucleus would effectively deactivate this function. Alternatively, the pioneer round of translation occurs in or en route from the nucleus and could be a target of PDCD4 activity that leads to tumor suppression (see Chapter 2). PDCD4 has also been reported to directly alter transcription leading to growth suppression and drug sensitivity in prostate cancer cells (26). Cytoplasmic localization would alter this function. It remains unclear where PDCD4 exerts its major tumor suppressor function and what role subcellular localization plays. Experiments testing the ability of PDCD4 to inhibit anchorage independent cell growth or matrigel invasion when trapped in the cytoplasm or nucleus may help clarify if either localization or shuttling is necessary for tumor suppressor function.

1.6 Roles of PDCD4 downstream of/or alternative to translation regulation

1.6.1 Cell growth/cell cycle

In many cell lines, overexpression of PDCD4 does not affect doubling times under normal tissue culture conditions (18, 19, 27, 35, 36, 39, 40). In an endocrine tumor cell line, Bon-1, transfection of rat PDCD4 caused an inhibition of cell growth. This was initially presumed to be through down-regulation of carbonic anhydrase type II at a posttranscriptional level. In a later study, however, $p21^{waf1/cip1}$ was found to be upregulated following overexpresison of PDCD4 in these cells, providing an alternative explanation for slower cell proliferation, as p21 inhibits the transition from G2 to M phase (61, 62). The reported links between PDCD4 and cell cycle regulators have been variable, perhaps due to cell type differences. For instance, stable knockdown of PDCD4 via siRNA in HeLa and HT116 cells *upregulated* $p21^{waf1/cip1}$ and no change in cell cycle timing was reported (63). In a glioblastoma cell line (T98G) starved for 72 hrs and then reactivated with serum, overexpression of degradation-resistant PDCD4 caused a delay in G1/S phase transition, with slower accumulation of cyclin D1, cyclin A, SKP2 and slower degradation of p27 (52). Overexpression of PDCD4 in MHCC-97H HCC cells caused a slower growth rate in culture and an accumulation of G1 and G2 phase with a reduction in S phase (44). Expresssion of PDCD4 in the prostate cancer cell line PC3 also inhibited proliferation in culture but was not analyzed for cell cycle arrest or apoptosis (26). PDCD4 was shown to down-regulate proliferation of ovarian cancer cell lines in culture, trapping them in S and G2 phase (47). It appears that the effects of PDCD4 on the cell cycle are variable between cell types. This is an important factor to

take into account in any experimental design; at the least, doubling times in culture should be tested in any experiment where levels of PDCD4 is altered in order to interpret changes in tumor growth of the same cells (i.e., is a decrease in tumor growth when PDCD4 levels are elevated accounted for by a slowed cell cycle or is it a tumor-specific phenomenon?).

1.6.2 Apoptosis

The ability of PDCD4 to directly cause apoptosis is also variable between studies. PDCD4 overexpression has been reported to cause apoptosis in MCF-7, MB-MDA-231 and T-47D breast cancer cells (reported up to 80%) (64) and in the Hu7 hepatocellular carcinoma cell line (43). But, overexpression of PDCD4 in MCF-7 and MB-MDA-231 cells was performed by Zhu *et al.* without any comment on induction of apoptosis. Although apoptosis was not directly tested, induction of cell death (especially at 80% frequency) would have significantly altered the interpretation of their conclusions and would have been difficult to miss if present (65). Interestingly, unlike in Hu7 HCC, overexpression of PDCD4 in MHCC-97H, MHCC-97L and Hep3G HCC cells did not cause apoptosis (44). This indicates that the direct induction of apoptosis by PDCD4 is not only variable between cell types but also cell lines of the same cancer. This may indicate oncogene addiction in certain cell types that are particularly sensitive to PDCD4 inhibition.

1.6.3 RNA binding

PDCD4 has been shown to bind RNA in chicken cells *in vitro (25)* and I have demonstrated that human PDCD4 also binds RNA (see Chapter 4). This function is not clearly understood but may play a role in positioning PDCD4 at the site of translation initiation. Alternatively, PDCD4 RNA interactions may play a secondary, unknown role in cancer biology. I show that PDCD4 RNA interactions are altered when PDCD4 is bound to eIF4A (Chapter 4). The role of RNA binding in PDCD4 tumor suppression or other unknown functions would be an interesting line of research to pursue.

1.7 Conclusions and unanswered questions

Clearly, PDCD4 plays an important tumor suppressor role in surrogate *in vitro* cell assays, such as invasion and migration experiments. These results are supported by clinical data through repeated correlations of low expression of PDCD4 with higher tumor grade and poor outcomes. Despite these findings, it is difficult to clearly distinguish which functions attributed to PDCD4 *in vitro* play a role in cancer etiology and progression since *in vivo* models to test these functions directly have not been used. One exception is a study using ovarian cancer cells, although this experiment was not an orthotopic tumor model and the cell line in question displayed decreased proliferation in culture. A decrease of tissue culture growth is an *in vitro* feature (then recapitulated in the xenograft model) and does not seem to be a generalizable affect of PDCD4 in cancers of other origins (47). In numerous other cases, however, alterations caused by PDCD4 expression in anchorage-independent cell growth and invasion assays have not been

tested in parallel with tumor growth or metastasis potential *in vivo*. This has left a large gap in our understanding of the fundamental role for PDCD4 in modulating tumor behavior. Moreover, the ability of PDCD4 to change the phenotypes of cultured cells may be significantly altered by a tissue microenvironment. This is particularly pertinent in breast cancer cells where PDCD4 levels are potentially regulated by hormone receptors and growth factor receptors. This is also a factor in blood cancers because PDCD4 expression may alter the extracellular cytokine milieu, changing the immune response to these cells. Finally, a major unaddressed question in this field is what accounts for poor clinical outcomes when tumors in fact do express PDCD4. Although 70-75% of patients with elevated PDCD4 levels have better prognosis and/or survival, the other 35% of patients with elevated levels of PDCD4 fair poorly. If we understood this discrepancy between the presence of a tumor suppressor and poor outcome, we could improve what is already a promising biomarker and potentially find ways to unmask the activity of PDCD4 in these tumors. This question ultimately became the central topic of my thesis research (see Chapter 3).

1.8 References

1. Jemal A, Siegel R, Xu J, Ward E. Cancer Statistics, 2010. CA Cancer J Clin 2010;60 (5):277-300.

2. Burke HB. Outcome prediction and the future of the TNM staging system. J Natl Cancer Inst 2004;96(19):1408-9.

3. Duffy MJ, Crown J. A personalized approach to cancer treatment: how biomarkers can help. Clin Chem 2008;54(11):1770-9.

4. Silvera D, Formenti SC, Schneider RJ. Translational control in cancer. Nat Rev Cancer 2010;10(4):254-66.

5. Sonenberg N, Hinnebusch AG. Regulation of translation initiation in eukaryotes: mechanisms and biological targets. Cell 2009;136(4):731-45.

6. Lazaris-Karatzas A, Montine KS, Sonenberg N. Malignant transformation by a eukaryotic initiation factor subunit that binds to mRNA 5' cap. Nature 1990;345(6275):544-7.

7. Armengol G, Rojo F, Castellvi J, *et al.* 4E-binding protein 1: a key molecular "funnel factor" in human cancer with clinical implications. Cancer Res 2007;67(16):7551-5.

8. Sonenberg N. eIF4E, the mRNA cap-binding protein: from basic discovery to translational research. Biochem Cell Biol 2008;86(2):178-83.

9. Comtesse N, Keller A, Diesinger I, *et al.* Frequent overexpression of the genes FXR1, CLAPM1 and EIF4G located on amplicon 3q26-27 in squamous cell carcinoma of the lung. Int J Cancer 2007;120(12):2538-44.

10. Bauer C, Diesinger I, Brass N, Steinhart H, Iro H, Meese EU. Translation initiation factor eIF-4G is immunogenic, overexpressed, and amplified in patients with squamous cell lung carcinoma. Cancer 2001;92(4):822-9.

11. Braunstein S, Karpisheva K, Pola C, *et al.* A hypoxia-controlled cap-dependent to cap-independent translation switch in breast cancer. Mol Cell 2007;28(3):501-12.

12. Silvera D, Arju R, Darvishian F, *et al.* Essential role for eIF4GI overexpression in the pathogenesis of inflammatory breast cancer. Nat Cell Biol 2009;11(7):903-8.

13. Moerke NJ, Aktas H, Chen H, *et al.* Small-molecule inhibition of the interaction between the translation initiation factors eIF4E and eIF4G. Cell 2007;128(2):257-67.

14. Tamburini J, Green AS, Bardet V, *et al.* Protein synthesis is resistant to rapamycin and constitutes a promising therapeutic target in acute myeloid leukemia. Blood 2009;114(8):1618-27.

15. Shuda M, Kondoh N, Tanaka K, *et al.* Enhanced expression of translation factor mRNAs in hepatocellular carcinoma. Anticancer Res 2000;20(4):2489-94.

16. Cencic R, Carrier M, Galicia-Vazquez G, *et al.* Antitumor activity and mechanism of action of the cyclopenta[b]benzofuran, silvestrol. PLoS One 2009;4(4):e5223.

17. Jiang Y, Zhang SH, Han GQ, Qin CY. Interaction of Pdcd4 with eIF4E inhibits the metastatic potential of hepatocellular carcinoma. Biomed Pharmacother 2010;64(6):424-9.

18. Yang HS, Cho MH, Zakowicz H, Hegamyer G, Sonenberg N, Colburn NH. A novel function of the MA-3 domains in transformation and translation suppressor Pdcd4 is essential for its binding to eukaryotic translation initiation factor 4A. Mol Cell Biol 2004;24(9):3894-906.

19. Yang HS, Jansen AP, Komar AA, *et al.* The transformation suppressor Pdcd4 is a novel eukaryotic translation initiation factor 4A binding protein that inhibits translation. Mol Cell Biol 2003;23(1):26-37.

20. Chen Y, Knosel T, Kristiansen G, *et al.* Loss of PDCD4 expression in human lung cancer correlates with tumour progression and prognosis. J Pathol 2003;200(5):640-6.

21. Mudduluru G, Medved F, Grobholz R, *et al.* Loss of programmed cell death 4 expression marks adenoma-carcinoma transition, correlates inversely with phosphorylated protein kinase B, and is an independent prognostic factor in resected colorectal cancer. Cancer 2007;110(8):1697-707.

22. Wang X, Wei Z, Gao F, *et al.* Expression and prognostic significance of PDCD4 in human epithelial ovarian carcinoma. Anticancer Res 2008;28(5B):2991-6.

23. Wei NA, Liu SS, Leung TH, *et al.* Loss of Programmed cell death 4 (Pdcd4) associates with the progression of ovarian cancer. Mol Cancer 2009;8:70.

24. Wen YH, Shi X, Chiriboga L, Matsahashi S, Yee H, Afonja O. Alterations in the expression of PDCD4 in ductal carcinoma of the breast. Oncol Rep 2007;18(6):1387-93.

25. Bohm M, Sawicka K, Siebrasse JP, Brehmer-Fastnacht A, Peters R, Klempnauer KH. The transformation suppressor protein Pdcd4 shuttles between nucleus and cytoplasm and binds RNA. Oncogene 2003;22(31):4905-10.

26. Shiota M, Izumi H, Tanimoto A, *et al.* Programmed cell death protein 4 down-regulates Y-box binding protein-1 expression via a direct interaction with Twist1 to suppress cancer cell growth. Cancer Res 2009;69(7):3148-56.

27. Shibahara K, Asano M, Ishida Y, Aoki T, Koike T, Honjo T. Isolation of a novel mouse gene MA-3 that is induced upon programmed cell death. Gene 1995;166(2):297-301.

28. Onishi Y, Hashimoto S, Kizaki H. Cloning of the TIS gene suppressed by topoisomerase inhibitors. Gene 1998;215(2):453-9.

29. Onishi Y, Kizaki H. Molecular cloning of the genes suppressed in RVC lymphoma cells by topoisomerase inhibitors. Biochem Biophys Res Commun 1996;228(1):7-13.

30. Jurisicova A, Latham KE, Casper RF, Casper RF, Varmuza SL. Expression and regulation of genes associated with cell death during murine preimplantation embryo development. Mol Reprod Dev 1998;51(3):243-53.

31. Hilliard A, Hilliard B, Zheng SJ, *et al.* Translational regulation of autoimmune inflammation and lymphoma genesis by programmed cell death 4. J Immunol 2006;177(11):8095-102.

32. Cmarik JL, Min H, Hegamyer G, *et al.* Differentially expressed protein Pdcd4 inhibits tumor promoter-induced neoplastic transformation. Proc Natl Acad Sci U S A 1999;96(24):14037-42.

33. Yang HS, Jansen AP, Nair R, *et al.* A novel transformation suppressor, Pdcd4, inhibits AP-1 transactivation but not NF-kappaB or ODC transactivation. Oncogene 2001;20(6):669-76.

34. Goke A, Goke R, Knolle A, *et al.* DUG is a novel homologue of translation initiation factor 4G that binds eIF4A. Biochem Biophys Res Commun 2002;297(1):78-82.

35. Yang HS, Knies JL, Stark C, Colburn NH. Pdcd4 suppresses tumor phenotype in JB6 cells by inhibiting AP-1 transactivation. Oncogene 2003;22(24):3712-20.

36. Jansen AP, Camalier CE, Colburn NH. Epidermal expression of the translation inhibitor programmed cell death 4 suppresses tumorigenesis. Cancer Res 2005;65(14):6034-41.

37. Yasuda M, Nishizawa T, Ohigashi H, *et al.* Linoleic acid metabolite suppresses skin inflammation and tumor promotion in mice: possible roles of programmed cell death 4 induction. Carcinogenesis 2009;30(7):1209-16.

38. Wang Q, Sun Z, Yang HS. Downregulation of tumor suppressor Pdcd4 promotes invasion and activates both beta-catenin/Tcf and AP-1-dependent transcription in colon carcinoma cells. Oncogene 2008;27(11):1527-35.

39. Yang HS, Matthews CP, Clair T, *et al.* Tumorigenesis suppressor Pdcd4 down-regulates mitogen-activated protein kinase kinase kinase kinase 1 expression to suppress colon carcinoma cell invasion. Mol Cell Biol 2006;26(4):1297-306.

40. Leupold JH, Yang HS, Colburn NH, Asangani I, Post S, Allgayer H. Tumor suppressor Pdcd4 inhibits invasion/intravasation and regulates urokinase receptor (u-PAR) gene expression via Sp-transcription factors. Oncogene 2007;26(31):4550-62.

41. Asangani IA, Rasheed SA, Nikolova DA, *et al.* MicroRNA-21 (miR-21) post-transcriptionally downregulates tumor suppressor Pdcd4 and stimulates invasion, intravasation and metastasis in colorectal cancer. Oncogene 2008;27(15):2128-36.

42. Ozpolat B, Akar U, Steiner M, *et al.* Programmed cell death-4 tumor suppressor protein contributes to retinoic acid-induced terminal granulocytic differentiation of human myeloid leukemia cells. Mol Cancer Res 2007;5(1):95-108.

43. Zhang H, Ozaki I, Mizuta T, *et al.* Involvement of programmed cell death 4 in transforming growth factor-beta1-induced apoptosis in human hepatocellular carcinoma. Oncogene 2006;25(45):6101-12.

44. Zhang S, Li J, Jiang Y, Xu Y, Qin C. Programmed cell death 4 (PDCD4) suppresses metastatic potential of human hepatocellular carcinoma cells. J Exp Clin Cancer Res 2009;28:71.

45. Jiang Y, Zhang SH, Han GQ, Qin CH. Association of programmed cell death factor 4 (PDCD4) with hepatocellular carcinoma and smoking in a Chinese male population. J Int Med Res 2009;37(4):1179-83.

46. Fassan M, Cagol M, Pennelli G, *et al.* Programmed cell death 4 protein in esophageal cancer. Oncol Rep 2010;24(1):135-9.

47. Wei ZT, Zhang X, Wang XY, *et al.* PDCD4 inhibits the malignant phenotype of ovarian cancer cells. Cancer Sci 2009;100(8):1408-13.

48. Yoshinaga H, Matsuhashi S, Fujiyama C, Masaki Z. Novel human PDCD4 (H731) gene expressed in proliferative cells is expressed in the small duct epithelial cells of the breast as revealed by an anti-H731 antibody. Pathol Int 1999;49(12):1067-77.

49. Gao F, Wang X, Zhu F, *et al.* PDCD4 gene silencing in gliomas is associated with 5'CpG island methylation and unfavourable prognosis. J Cell Mol Med 2009;13(10):4257-67.

50. Schlichter U, Burk O, Worpenberg S, Klempnauer KH. The chicken Pdcd4 gene is regulated by v-Myb. Oncogene 2001;20(2):231-9.

51. Schlichter U, Kattmann D, Appl H, Miethe J, Brehmer-Fastnacht A, Klempnauer KH. Identification of the myb-inducible promoter of the chicken Pdcd4 gene. Biochim Biophys Acta 2001;1520(1):99-104.

52. Dorrello NV, Peschiaroli A, Guardavaccaro D, Colburn NH, Sherman NE, Pagano M. S6K1- and betaTRCP-mediated degradation of PDCD4 promotes protein translation and cell growth. Science 2006;314(5798):467-71.

53. Schmid T, Jansen AP, Baker AR, Hegamyer G, Hagan JP, Colburn NH. Translation inhibitor Pdcd4 is targeted for degradation during tumor promotion. Cancer Res 2008;68(5):1254-60.

54. Carayol N, Katsoulidis E, Sassano A, Altman JK, Druker BJ, Platanias LC. Suppression of programmed cell death 4 (PDCD4) protein expression by BCR-ABL-regulated engagement of the mTOR/p70 S6 kinase pathway. J Biol Chem 2008;283(13):8601-10.

55. Frankel LB, Christoffersen NR, Jacobsen A, Lindow M, Krogh A, Lund AH. Programmed cell death 4 (PDCD4) is an important functional target of the microRNA miR-21 in breast cancer cells. J Biol Chem 2008;283(2):1026-33.

56. Liu C, Yu J, Yu S, *et al.* MicroRNA-21 acts as an oncomir through multiple targets in human hepatocellular carcinoma. J Hepatol 2010;53(1):98-107.

57. Li T, Li D, Sha J, Sun P, Huang Y. MicroRNA-21 directly targets MARCKS and promotes apoptosis resistance and invasion in prostate cancer cells. Biochem Biophys Res Commun 2009;383(3):280-5.

58. Lu Z, Liu M, Stribinskis V, *et al.* MicroRNA-21 promotes cell transformation by targeting the programmed cell death 4 gene. Oncogene 2008;27(31):4373-9.

59. Li J, Fu H, Xu C, *et al.* miR-183 inhibits TGF-beta1-induced apoptosis by downregulation of PDCD4 expression in human hepatocellular carcinoma cells. BMC Cancer 2010;10:354.

60. Kalinichenko SV, Kopantzev EP, Korobko EV, *et al.* Pdcd4 protein and mRNA level alterations do not correlate in human lung tumors. Lung Cancer 2008;62(2):173-80.

61. Goke R, Barth P, Schmidt A, Samans B, Lankat-Buttgereit B. Programmed cell death protein 4 suppresses CDK1/cdc2 via induction of p21(Waf1/Cip1). Am J Physiol Cell Physiol 2004;287(6):C1541-6.

62. Lankat-Buttgereit B, Gregel C, Knolle A, Hasilik A, Arnold R, Goke R. Pdcd4 inhibits growth of tumor cells by suppression of carbonic anhydrase type II. Mol Cell Endocrinol 2004;214(1-2):149-53.

63. Bitomsky N, Wethkamp N, Marikkannu R, Klempnauer KH. siRNA-mediated knockdown of Pdcd4 expression causes upregulation of p21(Waf1/Cip1) expression. Oncogene 2008;27(35):4820-9.

64. Afonja O, Juste D, Das S, Matsuhashi S, Samuels HH. Induction of PDCD4 tumor suppressor gene expression by RAR agonists, antiestrogen and HER-2/neu antagonist in breast cancer cells. Evidence for a role in apoptosis. Oncogene 2004;23(49):8135-45.

65. Zhu S, Wu H, Wu F, Nie D, Sheng S, Mo YY. MicroRNA-21 targets tumor suppressor genes in invasion and metastasis. Cell Res 2008;18(3):350-9.

CHAPTER 2

THE DISCOVERY OF NOVEL PDCD4 INTERACTING PARTNERS

2.1 Abstract

Interactions between molecules maintain cell homeostasis and are aberrantly regulated in disease states. The protein PDCD4 is a tumor suppressor that is often down-regulated in a variety of cancers. The underlying mechanism of PDCD4 tumor suppression is thought to occur through blocking the efficient translation of mRNAs with structured elements in the 5' UTR by binding the translation initiation factor eIF4A. Loss of PDCD4 in cancer deregulates translational control and would modulate functions of other potential binding partners. Here I describe the discovery of new PDCD4 interacting partners eIF4AIII, Nup153, and PRMT5, which may also play a part in oncogenesis upon alterations in PDCD4 expression.

2.2 Introduction

Interactions between biomolecules control cellular homeostasis and are disrupted in disease. Oncogenesis often manifests when genes are mutated or epigenetically silenced. The physiological cell phenomena accompanying these changes, however, such as uncontrolled growth and tissue invasion, are a direct result of gains or losses of interactions between cell components. The burgeoning field of cancer proteomics aims

to detect these interactions and the post-translational modifications that control their function (1). High throughput proteomic endeavors have been instrumental in determining networks of interactions involved in normal cell homeostasis and in disease development (1, 2). Small-scale protein/protein interaction studies using candidate approaches have also yielded valuable information on new disease pathways and are also necessary to confirm or inform experimental findings from large-scale analysis (3). Directed experiments detecting the network of protein/protein interactions of factors known to have oncogenic or tumor suppressor functions could be particularly useful in finding new drug targets or better prognostic indicators.

PDCD4 is a tumor suppressor that binds to eIF4A, disrupting the ability of eIF4A to interact with RNA and function in translation initiation (4) (Chapter 4). This results in inefficient translation of mRNAs that are dependent on eIF4A RNA helicase activity and is thought to be the mechanism of PDCD4 tumor suppressor function (5). In lung, colon, ovarian cancer, and esophageal cancer, the presence of PDCD4 is associated with better survival outcomes (6-10). Nevertheless, subpopulations of patients with high levels of PDCD4 expressed in tumors have poor survival outcomes, indicating the possibility of protein partners that negatively regulate PDCD4 tumor suppressor function. Alternatively, the patient population with high tumor levels of PDCD4 and extended survival outcomes may have interacting partners that enhance PDCD4 tumor suppressor function.

Interestingly, PDCD4 also exhibits features, such as nuclear localization and RNA binding, that hint at unknown functions, separate from translation regulation, that may also alter tumor growth (6, 11). Because interacting partners are such an integral

part of understanding the function of proteins, I chose to look for novel PDCD4 binding proteins that might illuminate alternative roles in tumor biology. Three approaches were used. The first was a candidate approach based on similarity to known PDCD4 binding partner eIF4A. The second was determining interactions of nuclear pore proteins found through a yeast-two-hybrid screen. Lastly, I looked at differential binding partners of PDCD4 in interphase versus mitotic cell cycle based on the known function of PDCD4 as a growth/cell cycle regulation molecule.

2.3 Experimental Procedures

2.3.1 Constructs and mutations

The open reading frame for human PDCD4 was purchased from Open Biosystems. eIF4AII and eIF4AIII were cloned out of a human cDNA library. All three constructs were PCR amplified using Gateway compatible primers and introduced into DONR-221 or DONR-321 vectors by BP reactions. eIF4AIII proline 67 was mutated to leucine by site directed mutagenesis. pGEX4T was converted to a Gateway compatible vector (pDEST-pGEX4T) using RFB primers (Invitrogen) and PDCD4, eIF4AII and eIF4AIII were all introduced into this vector by LR reactions. For bacterial His-tagged protein expression, constructs were introduced into pEXP1-DEST vector by LR reactions. For mammalian expression of V5-tagged proteins, eIF4AIII was introduced into pcDNA3.1/nV5-DEST vector by LR reaction.

2.3.2 Recombinant protein expression and purification

GST-tagged PDCD4, eIF4AII, eIF4AIII and eIF4AIII$_{P67L}$ were expressed as follows: Colonies were picked from agar plates of BL21/RIL cells transduced with GST recombinant constructs and spiked into 50 ml, 50 μg/ml Amp, LB broth. Overnight broth cultures were spiked into 700 ml, 50 μg/ml Amp, NZY media. Cultures were grown until they reached an OD_{600} of 0.8. GST-recombinant proteins were induced with 0.1 mM IPTG for 4 hrs at 22°C. The cultures were pelleted by centrifugation 5,000 x g 15 minutes at 4°C. The resulting pellets were resuspended in 10 ml chilled STE buffer (10 mM Tris pH 8.0, 150 mM NaCl, 1 mM EDTA) and re-pelleted by centrifugation as before. These pellets were frozen overnight at -80°C and thawed on ice the following day and resuspended in 20 ml, 1 x PBS, 2ug/ml leupeptin and aprotinin, 400 μM PMS and 0.04 to 0.1% deoxycholate. Lysates were prepared by sonicating pellets with three bursts of 30 seconds apiece on ice. Lysates were clarified by centrifugation 10,000 x g for 20 minutes at 4°C. 3 ml of 80% glutathione bead slurry (GE-healthcare) were equilibrated in PBS and were added to the clarified supernatants and incubated 2 hours at 4°C to conjugate GST proteins to glutathione beads. These beads bound with GST-proteins were washed five times with 10 ml of TBS. To elute GST proteins from glutathione beads, 10 ml elution buffer (100 mM Tris pH 8.0, 120 mM NaCl, 20 mM glutathioine) was added to each sample and incubated for 15 minutes at room temperature. The eluted beads were pelleted by low speed centrifugation 1 minute and the supernatant containing GST-proteins were concentrated in a Millipore 10,000 MWC concentrator to 1 ml by centrifugation at 2,000 x g for 70 min at 4°C. 9 ml of RNAse free TBS was added to concentrated proteins. Proteins were concentrated and resuspended in TBS as above for a

total of three times to exchange the elution buffer for TBS. The proteins were finally concentrated to 500-300 µl and 10% glycerol was added. This final protein concentration was aliquoted and stored at -80°C.

Expression and purification of His-recombinant proteins PDCD4 and tandem-GFP (2 x GFP) was performed as follows: Colonies were picked agar plates containing BL21/RIL colonies transduced with His-recombinant constructs. These isolates were spiked into 50 ml, 50 µg/ml Amp, LB broth and grown overnight at 37°C. Overnight liquid cultures were then spiked into 700 ml, 50 µg/ml Amp, NZY media. Cultures were grown until they reached an OD_{600} of 0.8 (2-4 hours a 37°C). Recombinant protein expression was induced three hours at 37°C with 1 mM IPTG. Induced bacteria was pelleted 5,000 x g for 7 minutes at 4°C and subsequently resuspended in 10 ml of native lysis buffer (500 mM NaCl, 5 mM imidizole, 20 mM TrisCl, pH 8.0 4 µg/ml leupeptin and aprotinin, 400 µM PMSF and 0.04% deoxycholate and 1 µg/ml lysozyme). Resuspended bacteria were lysed on ice by sonication for 3 bursts lasting 30 seconds apiece. Lysates were clarified by centrifugation at 10,000 x g for 20 minutes at 4°C. Three ml of Ni-NTA beads (Novagen) were equilibrated in native lysis buffer and added to clarified lysates. His-recombinant proteins were bound to the Ni-NTA beads 1.5 hours at room temperature. Protein bound beads were washed five times in 10 ml of Native Wash Buffer (500 mM NaCl, 10 mM tris-pH 8.0, 20 mM imidazole) 10 minutes per wash. The His-tagged proteins were eluted from the Ni-NTA beads by incubation in 10 ml of Native Elution Buffer (500 mM NaCl, 250 mM imidazole, 10 mM EDTA, 20 mM Tris pH 8.0) for 15 minutes at room temperature. The elution buffer was replaced by concentrating the eluted proteins in a Millipore 10,000 MWC 15 ml concentrator by

centrifuging at 2,000 x g 1.5 hours at 4°C to 1 ml and adding back 9 ml freezer storage buffer (500 mM NaCl, 20 mM Tris-cl pH 8.0, 5% glycerol). I repeated replacement three times. The sample was finally concentrated to 500-300 µl final volume. The concentrated proteins were aliquoted and stored at -80°C.

2.3.3 Purified recombinant GST-eIF4A interaction with purified His-PDCD4 protein

One µg of GST-protein (GST-eIF4AII, GST-eIF4AIII or GST-eIF4AIII$_{P67L}$) and His-protein were incubated with 20 µl of equilibrated glutathione beads (GE Healthcare) per reaction for 2 hours at 4°C in 300 µl of total binding buffer (20 mM HEPES pH 7.6, 100 mM KCl, 0.5 mM EDTA, 20% glycerol, 0.5 TX-100, 10 µg/ml leupeptin and aprotinin and 400 µM PMSF). The protein bound beads were washed three times in 1 ml binding buffer (inverted tube 10 times/wash) to remove any residual binding proteins. To elute protein complexes from the beads, the samples were resuspended in 100 µl of sample buffer and heated 3-10 minutes at 98°C. Twenty µl of each reaction was loaded per well on a 10% acrylamide gel and proteins were separated by PAGE. For controls, 0.05 µg of each protein was loaded. To visualize proteins, 2 µl of each reaction were loaded per well and detected by anti-GST or penta-His immunoblot or membranes were stained with Coomassie.

2.3.4 GST-PDCD4 interactions with exogenously expressed V5-eIF4A

V5-constructs V5-eIF4AII, V5-eIF4AIII and V5-eIF4AIII$_{P67L}$ were transfected into HEK293 cells at 1 µg/ml using Lipofectamine LTX (Invitrogen) by manufacturer's

recommendations. Cells were harvested 16 hours after transfection into 1 ml binding buffer (20 mM HEPES pH 7.6, 100 mM KCl, 0.5 mM EDTA, 0.25% Triton X-100, 20% glycerol, 2 µg/µl aprotinin and leupeptin, 400 µM PMSF) per 10 cm dish and dounced to lyse. Lysates were clarified by centrifugation at 20,000 x g for 30 minutes at 4°C. Clarified lysates were assayed for protein concentration by Bradford and 65 µg of each lysate was diluted in 200 µl of binding buffer. One µg of GST-PDCD4 or GST bound to glutathione beads (GE Healthcare) was added to the diluted lysates and incubated 1 hour at room temperature. Beads with bound proteins were washed three times in binding buffer and interacting protein complexes were eluted with sample buffer at 98°C for 3 minutes. Samples were loaded onto a 10% acrylamide gel and proteins were separated by PAGE. Immunoblots were probed for V5-eIF4AII, V5-eIF4AIII and V5-eIF4AIII$_{P67L}$ with monoclonal antibody against V5. Immunoblots were stained with Coomassie to visualize GST-PDCD4 and GST proteins.

2.3.5 GST-eIF4AIII and GST-eIF4AII interactions with endogenous PDCD4

HEK293 lysates were prepared by pipetting cells from a 10 cm dish into 1 ml buffer. Cells were harvested into either Buffer A (20 mM HEPES pH 7.6, 100 mM KCl, 0.5 mM EDTA, 0.25% Triton X-100, 20% glycerol, 1 x protease inhibitor (Roche)) or Buffer B which was the same as Buffer A but with 0.1% Triton X-100. Cells were briefly spun in low speed bench top microfuge in 1.7 ml tubes and dounced with micro douncer. Lysates were further processed by passing through a 27.5 gauge needle. Lysates were clarified by centrifugation at 20,000 x g at 4°C for 30 minutes. Fifty µl of clarified

lysate were brought up to 200 µl with either buffer A or buffer B. Four µg of GST proteins bound to 15 µl of glutathione beads equilibrated in Buffer A or Buffer B were added to diluted lysates and incubated 2 hours at room temperature. Protein complexes bound to glutathione beads were washed three times with appropriate buffer A or B. These complexes were eluted at 98°C, 3 minutes in sample buffer. Fifty percent of each reaction (the equivalent of 25 µl of lysate) was loaded on a 10% acrylamide gel and proteins were separated by PAGE. 2.5 µl lysate was loaded for input.

2.3.6 Interphase and Ultra-S *Xenopus* egg extract preparation

Eggs were collected from frogs primed with injection of gonadotropin 15 hours prior to harvest. Eggs were dejellied in 2% cystein for 5 minutes. Eggs were washed three times in 0.25 x Modified Ringer's Solution (MMR) and one time in 1 x MMR (100 mM NaCl, 2 mM KCl, 1 mM $MgSO_4$, 2.5 mM $CaCl_2$, 0.5 mM HEPES pH 7.8, 0.8 mM EDTA). Eggs were rinsed two times in egg lysis buffer (ELB) (2.5 mM $MgCl_2$, 500 mM KCl, 100 mM HEPES pH 7.6, 250 mM sucrose) and once in ELB with 1 mM DTT and 0.5 mg/ml CHX. Washed eggs were packed into tubes by centrifugation 15 seconds at 800 RPMs in the clinical bench top centrifuge. Aprotinin, leupeptin and cytochalasin B were added on top of eggs at 5 µg/ml. Eggs were lysed by centrifugation at 10,000 RPM 15 minutes at 4°C in Beckman JS 13.1 rotor. Crude lysate was collected (S fraction) using an 18 gauge needle and glycerol was added to a concentration of 5%. Sixty µl aliquots were flash frozn in liquid nitrogen and stored at -80°C.

Ultra-S egg extract was prepared the same as interphase extract accept that the S-phase was further centrifuged at 250,000 x g for 70 minutes in Beckman TLS-100 rotor

at 4°C. The resulting supernatant was further centrifuged at 250,000 x g for 25 minutes at 4°C. The supernatant was aliquoted and flash frozen in liquid nitrogen and stored at -80°C.

2.3.7 Mitotic *Xenopus* egg extract preparation

Preparation of mitotic egg extract was performed like interphase egg extracts with the exception of using Mitotic Buffer (240 mM β-glycerophophate pH 7.3, 60 mM EGTA pH 8.0, 45 mM $MgCl_2$, 100 μM DTT-final pH 7.3) in place of ELB.

2.3.8 CSF *Xenopus* egg extract preparation

Preparation of CSF egg extract was performed like interphase egg extracts except after 0.25 x MMR wash, eggs were washed three times in fresh XB buffer (50 mM sucrose, 100 mM KCl, 0.1 mM $CaCl_2$, 1 mM $MgCl_2$, 10mM HEPES, pH 7.7). This was followed by three washes of XB buffer containing 5 mM EGTA and an additional 1 mM $MgCl_2$. Eggs were packed and lysed in this last XB buffer and the protocol was followed as in interphase egg extract preparation.

2.3.9 GST-eIF4AIII interaction with PDCD4 from nocodazole treated and serum starved HeLa cells

HeLa cells were treated with 100 ng/ml nocodazole for 15 hrs or deprived of serum for 72 hours. Lysates were prepared using Buffer A as in step 2.3.5. Sixty-four μg of each lysate were added to 5 μg of GST-eIF4AIII, GST-eIF4AII or GST bound to 15 μl of glutathione beads and brought up to 200 μl with Buffer A. Reactions were incubated 1

hour at room temperature and washed three times in binding buffer. Reactions were run on 10% acrylamide gels and proteins were separated by PAGE. Lysate equivalent to 10% of reactions were loaded in input lane. PDCD4 was probed by immunoblotting (antibody 51495 from AbCam at 1:1000). GST-proteins were visualized by subsequent Coomassie staining of immunoblot.

2.3.10 GST-PDCD4 binding reaction in Ultra-S egg extracts

Fifty µg of GST-PDCD4 or GST were bound to 20 µl of glutathione beads equilibrated in binding buffer (50 mM HEPES pH 7.8, 200 mM NaCl, 5 mM $MgCl_2$, 0.05% Triton X-100, 2 µg/ml leupeptin and aprotinin, 400 µM PMSF) by incubating together 1 hour at room temperature in 200 µl of binding buffer. GST-protein bound beads were washed three times with 1 ml binding buffer. Fifty µl of Ultra-S were added to each bead pellet and brought up to 200 µl with binding buffer. GST-proteins were incubated with Ultra-S at room temperature 2 hours. Protein complexes were washed in binding buffer four times. Protein complexes were eluted from the glutathione beads in 20 µl sample buffer at 98°C for 3 minutes. Fifty percent of each reaction was loaded on a 6% acrylamide gel and proteins were separated by PAGE. In the input lane, 0.2 µl of Ultra-S was loaded. Immunoblots were probed for Nup214, Nup153, Nup62, Nup98, β-COP or Tubulin. A separate gel was loaded with 1 µg or GST-PDCD4 and GST as a loading control and Coomassie stained.

2.3.11 GST-PDCD4 interacting proteins in mitotic and interphase egg extract for mass spectrometry analysis

Fifty µg of GST-PDCD4 or GST were incubated with 20 µl of glutathione beads (GE Healthcare) 1 hour in 500 µl of binding buffer (50 mM HEPES pH 7.5, 200 mM NaCl, 5 mM $MgCl_2$, 0.5% Triton X-100). Beads were washed three times in binding buffer. To the beads, 100 µl of mitotic or interphase egg extracts were added with an additional 400 µl of binding buffer. The protein bound beads were incubated with egg extract for 1.5 hour at room temperature. Samples were washed briefly two times with 500 µl of binding buffer. Beads were resuspended in 40 µl sample buffer and heated 98°C for 3 minutes to elute protein complexes. All 40 µl of each sample were loaded onto a 12% acrylamide gel and separated by electrophoresis. The resulting gel was subsequently stained with Coomassie to visualize interacting proteins. A 72 kD band in the interaphase extract lane and a 30 kD band in the mitotic lane were excised and sent for mass spectrometry analysis. All buffers were made with new reagents and fresh nano-water. Gel boxes and tubes used for samples were washed three times in methanol and then three times with nano-water before use to prevent environmental contamination. Gloves were used at all times.

2.3.12 GST-PDCD4 interactions in CSF and interphase egg extract supplemented with cyclinB

Twenty-five µg of GST-PDCD4 or GST were bound to 20 µl of glutathione beads (GE Healthcare) 1 hour at room temperature in 200 µl of binding buffer (50 mM HEPES pH 7.5, 200 mM NaCl, 5 mM $MgCl_2$, 0.5% Triton X-100). The interphase egg extract

was cycled into a mitosis state by adding Cyclin B and Creatine Kinase, Phosphocreatine, and ATP and incubating for 75 minutes at room temperature. To each 20 µl of protein bound beads, 60 µl of either interphase extract, interphase extract with cyclinB, mitotic extract or two preparations of CSF extract with or without phosphatase inhibitors (phosphatase inhibitors: 4 mM imidizole, 50 mM NaF, 2 mM NaOrthovanadate, 20 mM NaPyrophosphate, 10 mM β-glycerolphosphate) were added. Extracts were incubated with GST proteins 1.5 hours at room temperature. Complexes were eluted at 98°C for 3 minutes in sample buffer and run on 12% acrylimide gels. PRMT5 and Nup214 and Nup153 were assessed by immunoblot. GST protein capture was assessed by subsequent staining of the immunoblot.

2.3.13 In-gel protein digestion and mass-spectrometry

An SDS-PAGE gel slice with the band of interest was destained in 50% methanol, sliced into small pieces, and then dehydrated in acetonitrile. Samples were taken to our core facility and analyzed as follows: TPCK-modified trypsin (Promega ; 20µl of 10ng/µl in 50 mM ammonium bicarbonate) was added to the gel pieces and incubated for 2 to 4 hours at 37ºC. LC/MS/MS analysis was then performed using a LTQ-FT hybrid mass spectrometer (ThermoElectron Corp). Primary mass spectra were acquired with the FT-ICR; MS/MS fragmentation spectra were acquired in the ion trap. Digested samples were introduced by nanoLC (2D-Ultra, Eksigent, Inc.) with nano-electrospray ionization (ThermoElectron Corp). NanoLC chromatography was performed using a homemade C18 nanobore column (75 um ID x 10 cm; Atlantis C18, 3 um particle (C18 material from Waters Corp)). Peptides were eluted during a 50-minute linear gradient from 4%

acetonitrile (with 0.1% formic acid) to 60% acetonitrile (with 0.1% formic acid) with a flow rate of 350 nl/min. Peptide molecular masses were measured by FT-ICR yielding primary mass spectra of peptides with mass errors less than 2 ppm. Peptide sequencing was performed by collision-induced dissociation (CID) in the linear ion trap, yielding fragment ions with mass errors typically less than 0.2 Da. All identified peptides from protein digests were assigned from protein database searches, using in-house processing with MASCOT search engine (in-house licensed, ver. 2.2.1, Matrix Science, Inc.).

2.3.14 Nocodazole treatment and GST-PDCD4 pull-down

HEK293 and HT29 cells were cultured in DMEM supplemented with 10% FBS. HEK293 and HT29 cells were treated with Nocodazole at 100 ng/ml for 17 hours. Cells were harvested by using a tissue scraper with egg extract binding buffer (EEBB) (20 mM Hepes pH 7.6, 200 mM NaCl, 5 mM $MgCl_2$, 0.5% Triton X-100, 2 µg/ml leupeptin and aprotainin and 400 µM PMSF) and dounced to lyse cells. Lysates were centrifuged 20,000 x g for 30 minutes at 4°C to pellet insoluble debris. In each binding reaction, 400 µg of supernatant were used along with 25 µg of GST-PDCD4 or GST bound to glutathione beads. Samples were incubated at room temperature 2 hours rotating. Beads were washed three times with 500 µl of EEBB and proteins were eluted with SDS-sample buffer 2 minutes at 95°C. Reactions were run on a 10% acrylamide SDS gels and separated by PAGE. Immunoblots were probed with PRMT5 and phospho-histone H3 antibodies.

2.3.15 Antibodies

PDCD4 and PRMT5 antibodies were acquired from Abcam. For immunoblots, α-PDCD4 antibody was used at 1:1000-2000 while α-PRMT5 antibody was used at 1:1000. Lysates were loaded between 2-10 μg for immunoblots. Anti-V5 antibody (2F11F7 Invitrogen) was used at 1:1000, anti-tubulin (YL1/2, Accurate chemical and Scientific Corp.) at 1:2000 and anti-β-COP (Affinity Bioreagents) at 1:2000 for immunoblots. 414 antibody (Covance) was used at 1:1000 and phospho-H3 antibody (Millipore) was used at 1:1000. Anti-penta-His (Invitrogen) antibody was used at 1:2000. Rabbit anti-GST antisera was prepared in our lab and used at a concentration of 1:5000.

2.4 Results

2.4.1 Recombinant PDCD4 interacts with eIF4AIII produced recombinantly but not derived from a mammalian cell lysates

PDCD4 is involved in translation regulation by interacting with the translation initiation factors eIF4AI and II, interfering with their RNA helicase function (4). eIF4AI and eIF4AII are differentially expressed in various tissues, with eIF4AII highly expressed in the liver and brain (12). eIF4AI and II, which are 89% identical, are functionally interchangeable molecules and are often referred to collectively as eIF4A (13). The ability of PDCD4 to block eIF4A helicase function is thought to occur primarily in the cytoplasm (4), although PDCD4 is localized primarily in the nucleus in many cells (6, 8, 9). A closely related protein to eIF4AI and II, eIF4AIII, is an integral core molecule of the exon junction complex (EJC) and is found primarily in the nucleus (14, 15). The EJC is deposited during splicing of pre-mRNAs, marking exon-exon boundaries. This

complex promotes efficient transport of mRNAs from the nucleus to the cytoplasm (16, 17) and can impact downstream fates of mRNA, such as translation efficiency, localization and stability (18-20). For instance, persistence of the EJC on mis-spliced RNAs targets these species for degradation, termed nonsense mediated decay (21). Alignment of eIF4A to eIF4AIII shows 72% identity over a 378 residue overlap (Figure 2.1). The regions surrounding residues known to be involved in PDCD4 binding are conserved (Figure 2.1 regions in yellow). Although PDCD4 interaction with eIF4AI and eIF4AII (eIF4A) has been extensively studied, a novel interaction with eIF4AIII has not been explored. This interaction could alter known functions of the EJC: changing the ratio of nuclear and cytoplasmic mRNAs, exon utilization and the efficiency of translation or nonsense mediated decay, any of which might contribute to suppression of cell growth and transformation. Since eIF4AIII is closely related to the known PDCD4 binding partners eIF4AI and eIF4AII and both PDCD4 and eIF4AIII are localized in the nucleus of human cells, we hypothesized that PDCD4 could also interact with eIF4AIII and that this interaction could contribute in a novel way to the tumor suppressor function of PDCD4.

To determine if PDCD4 and eIF4AIII directly interact, both molecules were bacterially expressed as recombinant proteins. Glutathione-S-Transferase (GST)-tagged eIF4AIII and GST-tagged eIF4AII were incubated with His-tagged PDCD4. Glutathione resin capture of GST-eIF4AIII or GST-eIF4AII also co-isolated His-PDCD4 from the protein mixture (Figure 2.2, lane 1), whereas GST alone did not (Figure 2.2, lane 7). To further determine the specificity of this interaction, we mutated eIF4AIII at proline 67 to a leucine. The analogous mutation (proline 56 to leucine) in eIF4AII is reported to cause

loss of PDCD4 binding (22). When this eIF4AIII mutant was expressed as a recombinant protein, it displayed reduced binding to PDCD4 (Figure 2.2, lane 3). In this and other experiments, wild-type eIF4AIII had reduced binding compared to the positive wild-type eIF4AII control (Figure 2.2, lane 5 compare to lane 1). Overall, these results demonstrate that eIF4AIII can also directly interact with PDCD4 and that the proline analogous to that in the known binding partner eIF4AII is necessary for interaction with eIF4AIII. Despite the high similarity between protein sequences, eIF4AIII appears to have a lower affinity for PDCD4 than eIF4AII. This could be a result of the divergent sequence in other amino acids necessary for binding or it could be due to allosteric hindrance.

In this *in vitro* protein/protein binding assay, neither PDCD4 nor eIF4AIII contain native cellular interacting partners or post-translational modifications. To further characterize the PDCD4/eIF4AIII interaction I chose to isolate transfected V5-eIF4AIII and V5-eIF4AIII$_{P67L}$ from cell lysates using recombinant purified GST-PDCD4. In this context, PDCD4 interacted with V5-eIF4AIII but at a low level (Figure 2.3, lane 1). To our surprise, PDCD4 reproducibly interacted with V5-eIF4AIII$_{P67L}$ to a greater extent than to wild-type (Figure 2.3, lane 2 versus 1). This indicates that there may be interacting partners of wild-type eIF4AIII that inhibit PDCD4 binding while eIF4AIII$_{P67L}$ has lost these interactions allowing for residual binding of PDCD4. eIF4AIII is known to bind Y14 and MAGO tightly in the context of the EJC. It would be interesting if eIF4AIII$_{P67L}$ has lost the ability to interact with these proteins.

To further characterize conditions that alter PDCD4/eIF4AIII binding, I performed the reciprocal experiment where bacterially expressed GST-eIF4AIII was

tested for interaction with endogenous PDCD4 in a cell lysate context. GST-eIF4AIII did not interact with endogenous PDCD4 under two different buffer conditions (Figure 2.4, lane 1 and 4) in contrast to robust interaction with GST-eIF4AII (Figure 2.4, lanes 2 and 5).

The inability of eIF4AIII to interact with endogenous PDCD4 indicates that binding partners or posttranslational modification of PDCD4 may inhibit this interaction. PDCD4 levels, and potentially binding partners and post-translational modifications, could be altered under cell stress conditions or at different cell cycle phases. The ability of eIF4AIII to interact with endogenous PDCD4 could also be enhanced under different cell growth conditions. To further determine if changes in cell growth conditions influence GST-eIF4AIII binding to PDCD4, lysates from serum starved or mitotically enriched cells were prepared. Purified eIF4AIII failed to recover endogenous PDCD4 under any of these conditions (Figure 2.5, lane 1). To verify the results that $eIF4AIII_{P67L}$ interacts with PDCD4 to a greater extent in the cell lysate context, it would be interesting to see if purified GST-$eIF4AIII_{P67L}$ associates with endogenous PDCD4 in cell lysates.

It is interesting that PDCD4 can bind to eIF4AIII when both are recombinant but is unable to interact using material from transformed cells. Partnerships taking place in the cell could be interfering with binding. Alternatively, the ability of PDCD4 to interact with eIF4AIII could be changed by post-translational alterations, such as methylation, sumoylation, and phosphorylation, that do not occur when these proteins are expressed in prokaryotes. Protein partners or posttranslational modifications could be altered by the cell cycle, transformed status, or the differentiated state of a cell. Although my studies did not fully elucidate whether there is a physiological connection between PDCD4 and

eIF4AIII, it remains interesting to consider whether disruption of, or forced interaction between PDCD4 and eIF4AIII, alters EJC-dependent aspects of mRNA biogenesis and contributes to a pro-tumor growth phenotype.

2.4.2 Recombinant PDCD4 interacts with Nup153 and Nup62

Data from a yeast two-hybrid screen performed by Prolexys indicated that PDCD4 interacts with a number of nuclear pore complex proteins. To validate these findings, purified GST-PDCD4 was immobilized on glutathione resin and incubated in *Xenopus* egg extract. Enriched proteins were eluted and separated by PAGE and immunoblots probed for nuclear pore proteins using the 414 monoclonal antibody that recognizes multiple Nups. Both Nup153 and Nup62 were enriched with GST-PDCD4 while Nup214 was not (Figure 2.6, lanes 1). In an attempt to find negative binding controls, we probed pull-downs for Nup98, β-COP and Tubulin. β-COP and Tubulin showed a positive interaction with PDCD4 whereas Nup98 turned out to be a good negative control (Figure 2.7, lane 1). We also tested ARF1 and α-COP, both of which did not interact (data not shown). To determine if PDCD4 interacts with Nup153 and Nup62 from mammalian cells, GST-PDCD4 was immobilized on glutathione resin and incubated in HEK293 cell lysates. Nup153 interacted with PDCD4 whereas Nup62 did not (Figure 2.8, top panel, lane 1). As in *Xenopus* extract, Nup98 from mammalian cells did not interact with PDCD4 (Figure 8, middle panel, lane 1). We have yet to confirm if Tubulin and β-COP bind to PDCD4 in mammalian cell lysates.

The ability to interact with the translation initiation complex and bind to RNA points to a potential role for PDCD4 in mRNA biogenesis. Many of the translation

initiation factors are thought to be loaded onto mRNAs in the nucleus for the pioneer round of translation and may be transported to the cytoplasm through the nuclear pore complex (23, 24). The efficiency of these mRNPs to transit between subcellular compartments is an important step in efficient translation since polyribosome loading occurs in the cytoplasm. It is interesting, in this light, that a translation inhibitor, PDCD4, interacts with nuclear pore components Nup153 and possibly Nup62. In non-cancerous cells, PDCD4 is often found primarily in the nucleus (6, 8, 9). PDCD4 may dock at the nuclear pore in the context of mRNPs and travel transiently to the cytoplasm to inhibit translation of susceptible mRNAs. It is also possible that PDCD4 functions as a molecule that sorts transiting mRNPs, inhibiting or facilitating the export of mRNA-protein complexes. PDCD4 could also negatively impact translation by forcing the retention of mRNAs in nucleus. It would be interesting to determine if the subcellular localization of a class of mRNAs, such as those with specific sequences or structures, was altered in PDCD4 overexpressing cells by assessing mRNAs from nuclear and cytoplasmic cell fractions by microarray.

2.4.3 PDCD4 binds proteins differentially in interphase versus mitotic egg extract

Overexpression of nondegradable PDCD4 causes delays in G1-S phase transition (25) and altering the levels of PDCD4 causes changes in $p21^{waf1/cip1}$ expression (26). It is unclear exactly what role PDCD4 plays during the cell cycle but its ability to act as a tumor suppressor may be due, in part, to a role in cell cycle control perhaps independent of a function in translation regulation. Determining PDCD4 interactions that occur

differentially during alternate phases of the cell cycle could illuminate novel roles PDCD4 plays during the cell cycle. Toward this end, I probed interphase versus mitotic *Xenopus* egg extract for novel interacting partners of PDCD4.

GST-PDCD4 was immobilized on glutathione resin and incubated with either interphase or mitotic egg extracts. Interacting proteins were separated by PAGE and were visualized by Coomassie staining. We found two prominent bands that bound exclusively to interphase or mitotic extracts. The first band of interest was at 72 kD and appeared only when interphase extract was used (Figure 2.9 lane 1), whereas a 30kD band was observed only with mitotic material (Figure 2.9, lane 2). Neither 72 kD or 30 kD band bound to GST (Figure 2.9, lanes 3-4). These bands were excised and processed for mass spectrometry analysis.

I was particularly interested in the number of ribosomal subunits that were identified in the mitotic egg extract (Table 2.1). To follow up on this line of experiments, isolation of ribosomes out of mitotic egg extracts was performed using GST-PDCD4, but with variable results. A recent paper describes an interaction between PDCD4 and the ribosomes confirming these mass spectrometry results (27). Further experimentation is needed to determine which of these subunits interact with PDCD4 and whether this is bridged by mRNA and/or the eIF4F complex. Furthermore, determining if a PDCD4 interaction with ribosomes is cell cycle regulated in mammalian cells is of interest.

The first two proteins identified in the interphase extract were two alleles of protein arginine methyltransferase 5 (PRMT5) (Table 2.2). In humans, there is only one allele while *Xenopus laevis* expresses both xPRMT5 (a hypothetical protein that I have shown is expressed) and Hsl7 (an alternate name for PRMT5 based on yeast

nomenclature). This interaction is explored in greater detail in the following section and Chapter 3 (see Figure 3.3).

2.4.4 PRMT5 differentially binds to PDCD4 in interphase versus mitotic *Xenopus* egg extract

Analysis of the 72 kD protein in the interphase extract by mass spectrometry yielded mostly peptides from the protein PRMT5, also known as Hsl7. I confirmed that PDCD4 binds to PRMT5 in interphase egg extract by immunoblot (Figure 2.10, lane 1). To rule out that changes of buffer conditions between interphase and mitotic extracts contributed to PRMT5 binding to PDCD4, cyclin B was added to shift interphase extract into a mitotic state. The cell cycle state of the egg extract was confirmed by monitoring hyperphosphorylation of Nup153 in mitotic extract versus hypophosphorylation in interphase state with resulting molecular weight shift (Figure 2.11 bottom panel lanes 1-7). With addition of cyclin B, PRMT5 no longer interacted with PDCD4 (Figure 2.11, top panel, lane 7). To further determine substantiate this cell cycle binding preference, CSF egg extract (CSF is an egg extract that has been arrested in mitosis by cytostatic factor) was used. CSF extract progresses from mitosis to interphase if phosphatase inhibitors (PI) are omitted. In CSF treated with PI, GST-PDCD4 bound to PRMT5 to a much lower extent (Figure 2.11 lanes 2 and 4), comparable to regular mitotic extract or interphase extract with the addition of cyclinB (Figure 2.11, lanes 6-7). When CSF was allowed to cycle out of a mitotic state, GST-PDCD4 was able to interact with PRMT5 at an elevated level (Figure 2.11, lanes 1 and 3) comparable to interphase extract (Figure

2.11, lane 5) showing that this interaction is preferential in *Xenopus* egg extract only in the interphase but not mitotic state.

To determine if similar cell cycle regulation of the PDCD4-PRMT5 partnership occurs in mammalian cells, unsynchronized lysate and lysates enriched in prometaphase by nocodazole treatment were incubated with recombinant PDCD4. Interacting proteins were separated by PAGE and interrogated for PRMT5 by immunoblotting. PRMT5 bound equally as well in asynchronous and mitotic enriched lysates from both HEK293 and HT29 cells (Figure 2.12, lanes 1-4). The mitotic state of the lysates was assessed by phospho-histone H3 levels (Figure 2.12, lanes 9-12).

The ability of PDCD4 to interact with PRMT5 only in interphase but not mitotic *Xenopus laevis* egg extract indicates that this interaction may be cell cycle regulated within this context. This regulation does not appear to happen in mammalian cells tested. This indicates the lack of such regulation in transformed tissue culture cells, but does not rule it out in normal mammalian cells. Furthermore, the *Xenopus* egg extract represents an early undifferentiated cell environment, leaving open the question of whether PDCD4 and PRMT5 are regulated in development (both frog and mammalian). It would be interesting to determine whether mis-regulation of PDCD4 and PRMT5 interaction has a developmental phenotype.

2.5 Discussion

Discovery of new PDCD4 interacting factors indicates the possibility that PDCD4 plays multiple roles in the cell. These roles could be complementary or independent of the role PDCD4 plays in translation regulation. It is intriguing that these new interacting

proteins all have roles in RNA biogenesis. eIF4AIII is a critical component of the exon junction complex that regulates mRNA stability and transit to the cytoplasm from the nucleus. If PDCD4 interacts with cellular eIF4AIII it could regulate either of these functions. The ability of PDCD4 to bind to Nup153 and possibly Nup62 may connect PDCD4 to the site of mRNA trafficking, the nuclear pore complex. This could indicate a sorting function or a jumping off point for PDCD4 as it transits to the cytoplasm to presumably function in translation regulation. Finally, the ability of PDCD4 to bind to PRMT5 points to a potential modulatory role in stable spliceosome assembly since PRMT5 is a methyltransferase that targets Sm proteins to enhance their incorporation into snRNPS (28, 29). The interaction of PDCD4 with PRMT5 will be explored further in Chapter 3.

2.6 References

1. Kolch W, Pitt A. Functional proteomics to dissect tyrosine kinase signalling pathways in cancer. Nat Rev Cancer 2010;10(9):618-29.

2. Pan C, Olsen JV, Daub H, Mann M. Global effects of kinase inhibitors on signaling networks revealed by quantitative phosphoproteomics. Mol Cell Proteomics 2009;8(12):2796-808.

3. Gavin AC, Aloy P, Grandi P, *et al.* Proteome survey reveals modularity of the yeast cell machinery. Nature 2006;440(7084):631-6.

4. Yang HS, Jansen AP, Komar AA, *et al.* The transformation suppressor Pdcd4 is a novel eukaryotic translation initiation factor 4A binding protein that inhibits translation. Mol Cell Biol 2003;23(1):26-37.

5. Yang HS, Cho MH, Zakowicz H, Hegamyer G, Sonenberg N, Colburn NH. A novel function of the MA-3 domains in transformation and translation suppressor Pdcd4 is essential for its binding to eukaryotic translation initiation factor 4A. Mol Cell Biol 2004;24(9):3894-906.

6. Chen Y, Knosel T, Kristiansen G, *et al.* Loss of PDCD4 expression in human lung cancer correlates with tumour progression and prognosis. J Pathol 2003;200(5):640-6.

7. Fassan M, Cagol M, Pennelli G, *et al.* Programmed cell death 4 protein in esophageal cancer. Oncol Rep 2010;24(1):135-9.

8. Mudduluru G, Medved F, Grobholz R, *et al.* Loss of programmed cell death 4 expression marks adenoma-carcinoma transition, correlates inversely with phosphorylated protein kinase B, and is an independent prognostic factor in resected colorectal cancer. Cancer 2007;110(8):1697-707.

9. Wei NA, Liu SS, Leung TH, *et al.* Loss of Programmed cell death 4 (Pdcd4) associates with the progression of ovarian cancer. Mol Cancer 2009;8:70.
10. Wei ZT, Zhang X, Wang XY, *et al.* PDCD4 inhibits the malignant phenotype of ovarian cancer cells. Cancer Sci 2009;100(8):1408-13.

11. Bohm M, Sawicka K, Siebrasse JP, Brehmer-Fastnacht A, Peters R, Klempnauer KH. The transformation suppressor protein Pdcd4 shuttles between nucleus and cytoplasm and binds RNA. Oncogene 2003;22(31):4905-10.

12. Nielsen PJ, Trachsel H. The mouse protein synthesis initiation factor 4A gene family includes two related functional genes which are differentially expressed. Embo J 1988;7(7):2097-105.

13. Yoder-Hill J, Pause A, Sonenberg N, Merrick WC. The p46 subunit of eukaryotic initiation factor (eIF)-4F exchanges with eIF-4A. J Biol Chem 1993;268(8):5566-73.

14. Chan CC, Dostie J, Diem MD, *et al.* eIF4A3 is a novel component of the exon junction complex. Rna 2004;10(2):200-9.

15. Ferraiuolo MA, Lee CS, Ler LW, *et al.* A nuclear translation-like factor eIF4AIII is recruited to the mRNA during splicing and functions in nonsense-mediated decay. Proc Natl Acad Sci U S A 2004;101(12):4118-23.

16. Luo MJ, Reed R. Splicing is required for rapid and efficient mRNA export in metazoans. Proc Natl Acad Sci U S A 1999;96(26):14937-42.

17. Le Hir H, Gatfield D, Izaurralde E, Moore MJ. The exon-exon junction complex provides a binding platform for factors involved in mRNA export and nonsense-mediated mRNA decay. Embo J 2001;20(17):4987-97.

18. Le Hir H, Gatfield D, Braun IC, Forler D, Izaurralde E. The protein Mago provides a link between splicing and mRNA localization. EMBO Rep 2001;2(12):1119-24.

19. Gatfield D, Unterholzner L, Ciccarelli FD, Bork P, Izaurralde E. Nonsense-mediated mRNA decay in Drosophila: at the intersection of the yeast and mammalian pathways. Embo J 2003;22(15):3960-70.

20. Wiegand HL, Lu S, Cullen BR. Exon junction complexes mediate the enhancing effect of splicing on mRNA expression. Proc Natl Acad Sci U S A 2003;100(20):11327-32.

21. Cheng J, Belgrader P, Zhou X, Maquat LE. Introns are cis effectors of the nonsense-codon-mediated reduction in nuclear mRNA abundance. Mol Cell Biol 1994;14(9):6317-25.

22. Zakowicz H, Yang HS, Stark C, Wlodawer A, Laronde-Leblanc N, Colburn NH. Mutational analysis of the DEAD-box RNA helicase eIF4AII characterizes its interaction with transformation suppressor Pdcd4 and eIF4GI. Rna 2005;11(3):261-74.

23. Ishigaki Y, Li X, Serin G, Maquat LE. Evidence for a pioneer round of mRNA translation: mRNAs subject to nonsense-mediated decay in mammalian cells are bound by CBP80 and CBP20. Cell 2001;106(5):607-17.

24. McKendrick L, Thompson E, Ferreira J, Morley SJ, Lewis JD. Interaction of eukaryotic translation initiation factor 4G with the nuclear cap-binding complex provides a link between nuclear and cytoplasmic functions of the m(7) guanosine cap. Mol Cell Biol 2001;21(11):3632-41.

25. Dorrello NV, Peschiaroli A, Guardavaccaro D, Colburn NH, Sherman NE, Pagano M. S6K1- and betaTRCP-mediated degradation of PDCD4 promotes protein translation and cell growth. Science 2006;314(5798):467-71.

26. Bitomsky N, Wethkamp N, Marikkannu R, Klempnauer KH. siRNA-mediated knockdown of Pdcd4 expression causes upregulation of p21(Waf1/Cip1) expression. Oncogene 2008;27(35):4820-9.

27. Wedeken L, Ohnheiser J, Hirschi B, Wethkamp N, Klempnauer KH. Association of Tumor Suppressor Protein Pdcd4 With Ribosomes Is Mediated by Protein-Protein and Protein-RNA Interactions. Genes & Cancer 2010;1(3):293-31.

28. Meister G, Fischer U. Assisted RNP assembly: SMN and PRMT5 complexes cooperate in the formation of spliceosomal UsnRNPs. Embo J 2002;21(21):5853-63.

29. Meister G, Eggert C, Buhler D, Brahms H, Kambach C, Fischer U. Methylation of Sm proteins by a complex containing PRMT5 and the putative U snRNP assembly factor pICln. Curr Biol 2001;11(24):1990-4.

Figure 2.1 eIF4AIII and II share conserved amino acids known to contact PDCD4. Alignment of eIF4AIII with the known PDCD4 interacting partner eIF4AII shows greater than 60% identity. Asterisks represent identical amino acids. Amino acids known to directly be involved with PDCD4 binding are shown in red type with the surrounding conserved amino acids highlighted in yellow.

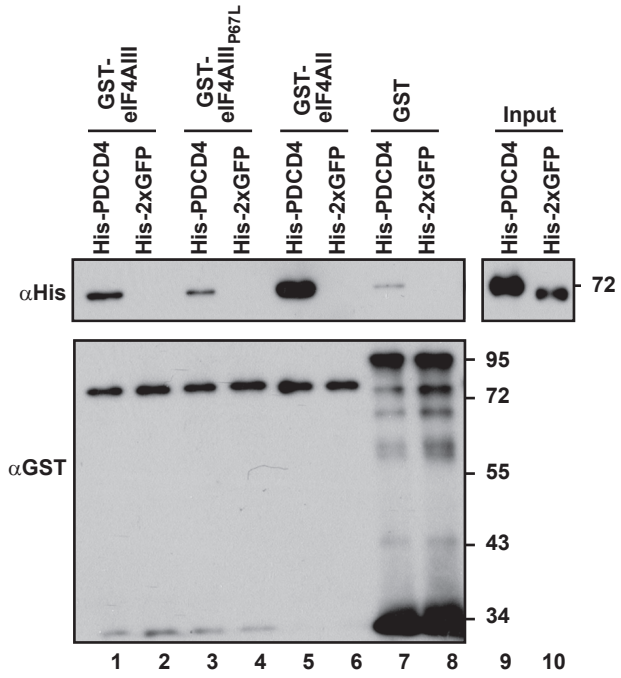

Figure 2.2 Recombinant PDCD4 and eIF4AIII interact *in vitro* in a manner dependent on proline 67 of eIF4AIII. Purified His-tagged recombinant PDCD4 interacts with purified GST-tagged recombinant eIF4AIII (top panel, lane 1). The eIF4AIII$_{P67L}$ mutant has reduced binding to PDCD4 (top panel, lane 3). His-tagged tandem GFP was used as a negative control (top panel, lanes 2, 4, 6, and 8). Recombinant GST-tagged eIF4AII interacts with His-PDCD4 (top panel, lane 5). Recovery of GST-tagged proteins was tracked by immunoblotting with GST-specific antibody (bottom panel, lanes 1-8). 25% of protein concentrations used in reactions were loaded in input lanes (lanes 9-10).

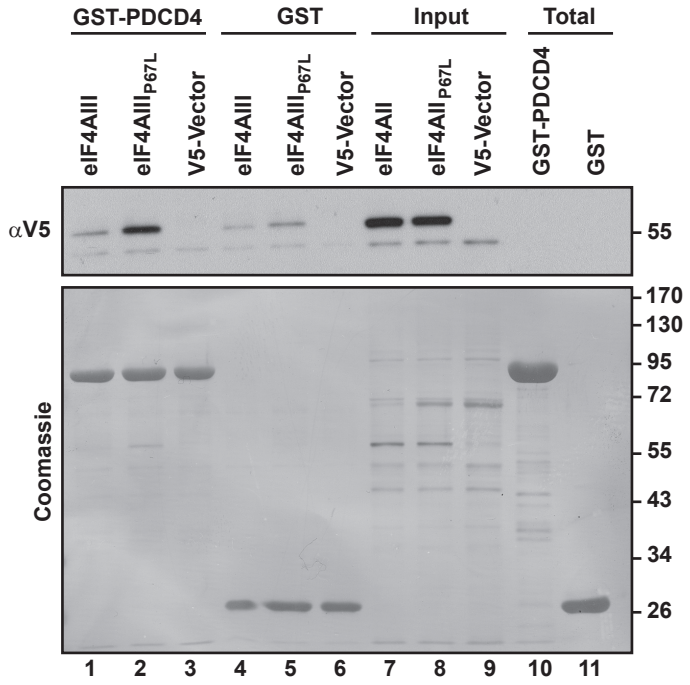

Figure 2.3 GST-PDCD4 recovers eIF4AIII$_{P61L}$ to a greater extent than wild-type eIF4AIII from cell lysates. Lysates from HEK293 cells transfected with V5-tagged eIF4AIII, V5-eIF4AIII$_{P67L}$, or parental vector (see Input, top panel, lanes 7-9) were incubated with purified GST-PDCD4. Input and bound material was subjected to immunoblotting to detect V5-tagged proteins (upper panel) and the membrane was subsequently stained with Coomassie to assess GST recovery (bottom panel). Wild-type eIF4AIII associated to a lower extent than eIF4AIII$_{P67L}$ with GST-PDCD4 (top panel, lane 1 and 2).

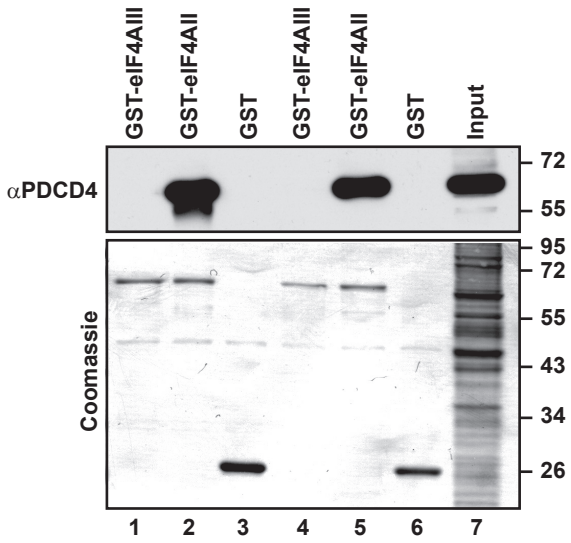

Figure 2.4 GST-eIF4AIII is unable to interact with endogenous PDCD4 from cell lysates. Purified GST-eIF4AIII cannot interact with endogenous PDCD4 from HEK293 lysates (top panel, lane 1). GST-eIF4AII efficiently pulls down endogenous PDCD4 from HEK293 lysates (top panel, lane 2). GST recombinant proteins were visualized by subsequent Coomassie staining of the immunoblot (bottom panel, lanes 1-6). The binding buffer used in lanes 1-3 contianed 0.25% Triton-X. 10% of lysate was loaded in input lane 7.

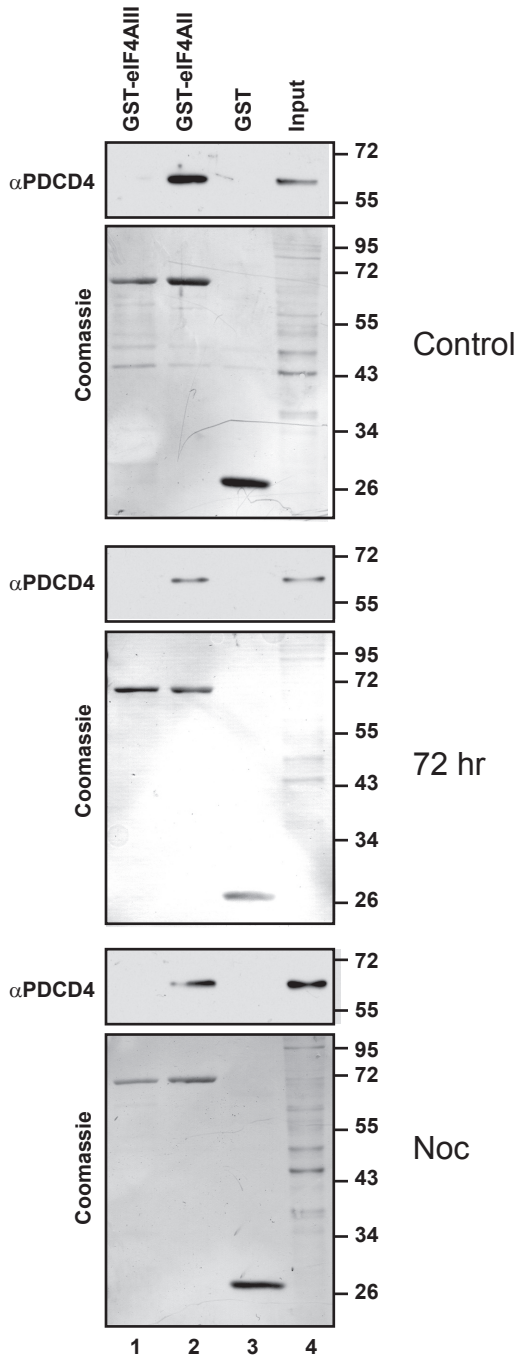

Figure 2.5 Changing cell growth status does not stimulate interactions between PDCD4 and recombinant eIF4AIII. GST-eIF4AIII does not interact with endogenous PDCD4 from lysates of HeLa cells grown under normal culture conditions (top immunoblot, lane 1) or serum starved (middle immunoblot, lane 1) or treated with nocodazole to trap in mitosis (bottom immunoblot, lane 1). GST-eIF4II interacted with PDCD4 under all cell culture interactions (all immunoblots, lane 2). Recovery of GST recombinant proteins for all conditions were visualized by subsequent Coomassie staining of immunoblot membranes (see three Coomassie panels). Lysates loaded at 10% of reaction were ran in input lane (lane 4).

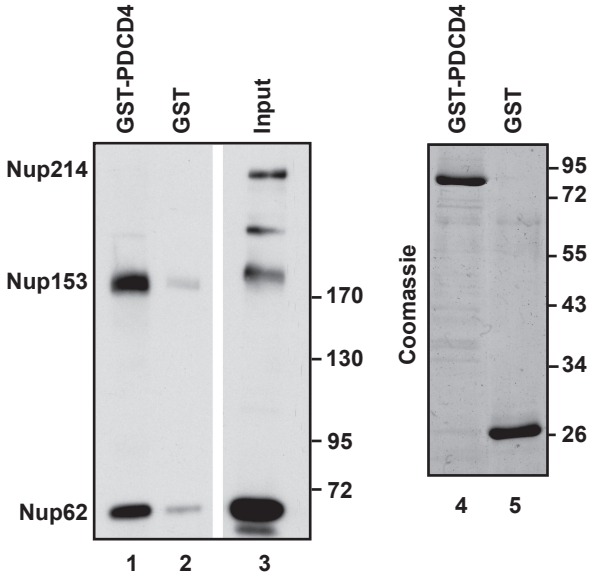

Figure 2.6 GST-PDCD4 interacts with Nup153 and Nup62 in ultra-S egg extracts. Purified GST-PDCD4 or GST was incubated with *Xenopus* ultra-S egg extract and interacting proteins were separated by PAGE and probed for Nups using the 414 antibody. PDCD4 interacts with Nup153 and Nup62 but not Nup214 (lane 1). Loading controls were visualized by Coomassie staining of a gel with 1 ug of GST-PDCD4 or GST loaded (lanes 4-5).

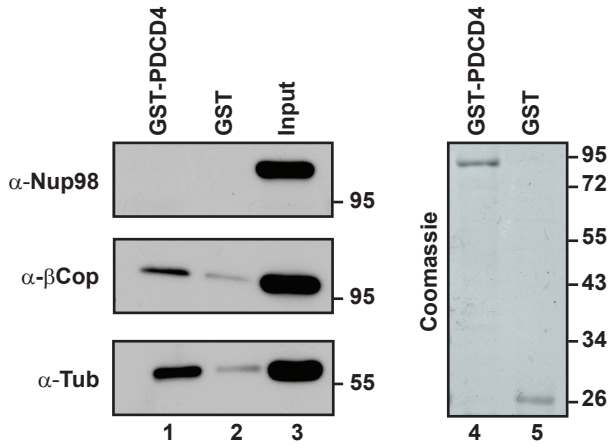

Figure 2.7 GST-PDCD4 interacts with β-COP and Tubulin, but not with Nup98. Purified GST-PDCD4 or GST was incubated with *Xenopus* egg extract and interacting proteins were separated by PAGE and probed for interacting partners by immunoblotting. PDCD4 fails to interact with Nup98 (top panel, lane 1) but does interact with β-COP (middle panel, lane 1) and Tubulin (bottom panel, lane 1). Loading controls were visualized by Coomassie staining of a gel with 1 ug of GST-PDCD4 or GST loaded (lanes 4-5).

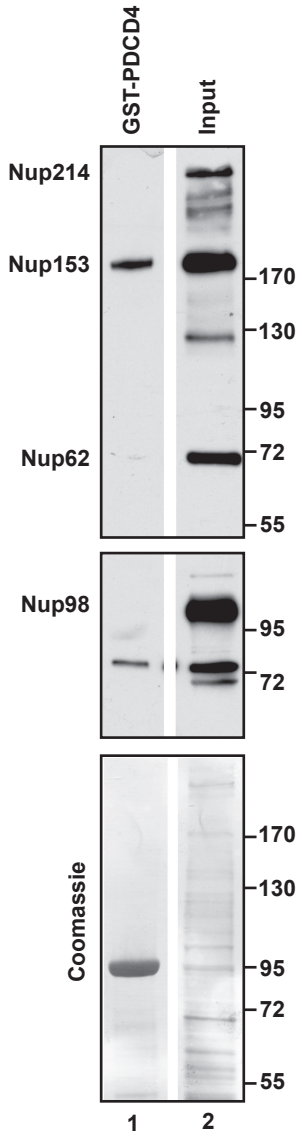

Figure 2.8 GST-PDCD4 interacts with Nup153 but not Nup62 or Nup98 in HEK293 cell lysates. Purified GST-PDCD4 was incubated with HEK293 lysates and interacting proteins were separated by PAGE and probed for interacting partners by immunoblotting with mAb414. PDCD4 interacts with Nup153 but not Nup62 in mammalian cell lysates (top panel, lane 1). PDCD4 fails to interact with Nup98 (middle panel, lane 1). Recovery of GST-PDCD4 was visualized by subsequent Coomassie staining of immunoblot (bottom panel, lane 1).

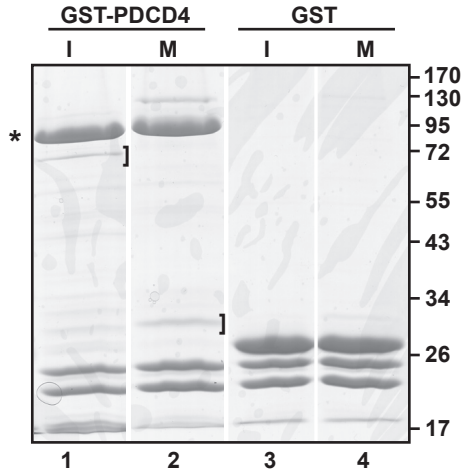

Figure 2.9 Differential binding partners of GST-PDCD4 in interphase and mitotic *Xenopus* egg extract. GST-PDCD4 was incubated with interphase or mitotic *Xenopus* egg extract and interacting proteins were separated by PAGE visualized by Coomassie staining. A specific 72 kD protein interacted with PDCD4 in interphase extracts and was excised for mass spec analysis (lane 1, bracket). A 30 kD species interacted with PDCD4 in mitotic egg extract and was also excised and subjected to mass spec analysis (lane 2, bracket). Asterisk indicates GST-PDCD4 band. Part of this gel was used in Figure 3.2 , Chapter 3 (Powers et al., submitted).

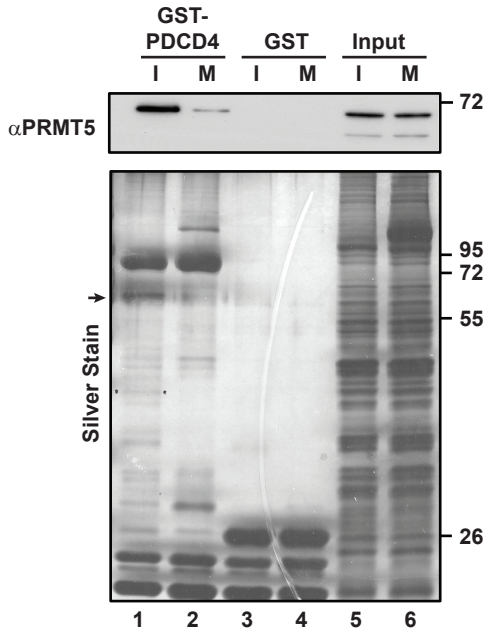

Figure 2.10 PRMT5 interacts with PDCD4 in *Xenopus* egg extract and this interaction is cell cycle regulated. Purified GST-PDCD4 was incubated with interphase and mitotic *Xenopus* egg extract and interacting proteins were separated by PAGE. Interacting species were detected by immunoblot using PRMT5 antibody (top panel) and by silver staining (bottom panel). The mass spec indentified interaction of PRMT5 with PDCD4 was confirmed (top panel, lane 1) and this interaction was more robust in interphase than mitotic egg extract (top panel, lane 1 versus lane 2). Arrow shows robust 72 kD band by silver stain in interphase egg extract (bottom panel, lane 1).

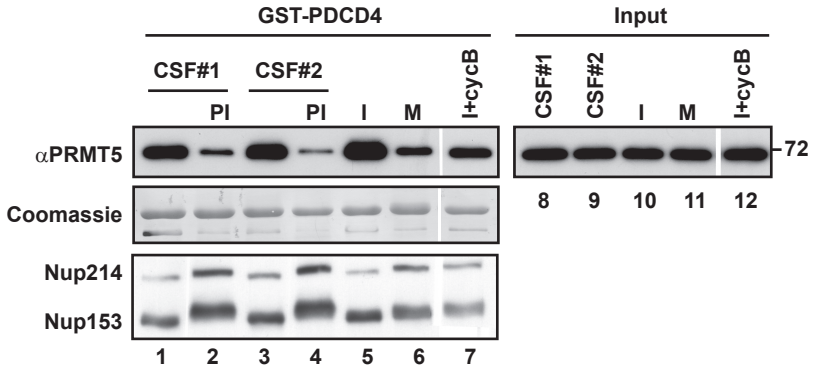

Figure 2.11 Mitotic state, not buffer conditions, regulates interaction of PDCD4 with PRMT5. GST-PDCD4 was incubated in two different preparations of CSF *Xenopus* egg extract either without (lanes 1 and 3) or with phosphatase inhibitors (lanes 2 and 4). PDCD4 interacts to a greater extent with PRMT5 in CSF egg extract in an interphase state (top panel, lanes 1 and 3) than in a mitotic state maintained with inhibitors (top panel, lanes 2 and 4). These interactions are comparable to that seen in normal interphase and mitotic egg extracts (top panel, lanes 5 and 6). Interphase extract incubated with cyclinB to induce transition to mitotic state has lowered PRMT5 binding than interphase extract alone (lane 7 versus 5). Recovery of GST-PDCD4 loading was visualized by subsequent Coomassie staining of immunoblot membrane (middle panel, lanes 1-7). Interphase and mitotic state of extracts was assessed by immunoblot with mAb414 to detect hypophosphorylation of Nup214 and Nup153 (interphase state, bottom panel, lanes 1, 3, and 5) versus hyperphosphorylation (mitotic state, bottom panel, lanes 2, 4, 6-7). Input levels of PRMT5 were assessed by immunoblot (lanes 8-12).

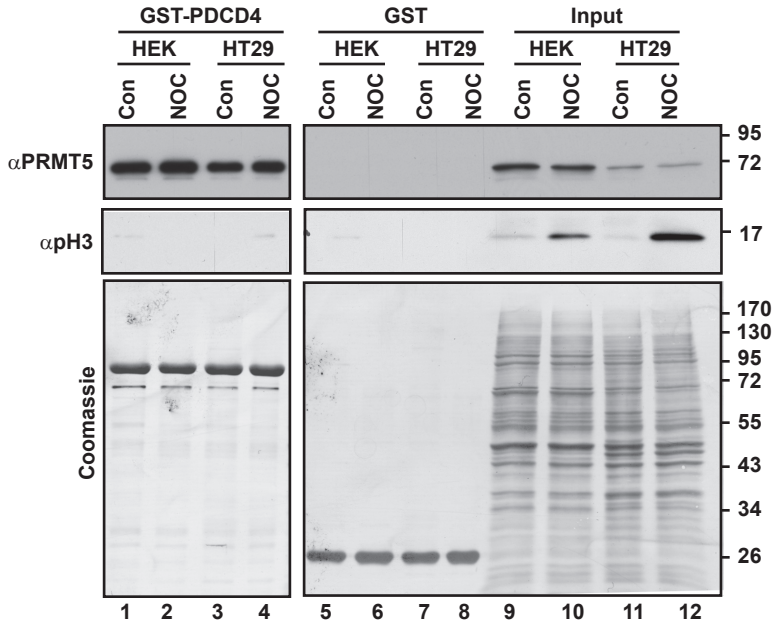

Figure 2.12 PDCD4 binds to PRMT5 equally well in asynchronous and prometaphase enriched human cell lysates. GST-PDCD4 was incubated in asynchronous and nocodazole treated lysates from HEK293 (lanes 1-2) or HT29 (lanes 3-4) cells. PRMT5 is efficiently recovered with GST-PDCD4 from all lysates and cell cycle conditions (top panel, lanes 1-4). The mitotic state of the lysates was assessed using phospho-histone 3 antibody (middle panel, lanes 9-12). PRMT5 did not interact with GST alone (top panel, lanes 5-8). Recovery of GST-PDCD4 and GST was visualized by subsequent Coomassie staining of immunoblots (bottom panel, lanes1-8).

Table 2.1 Mitotic interacting partners of PDCD4 identified by mass spectrometry

(Run-Rank)	Name Xenopus/Human	Accession #	MW kD	Peptide Hits	Known Function
Ribosomal subunits					
(1-3) (2-3)	40S ribosomal protein S4/ 40S ribosomal protein S4, X isoform	**Q6NRW9**	29.6	627	Belongs to the ribosomal protein S4E family.
(1-9)	40S ribosomal protein S3a/ 40S ribosomal protein S3?	**R3XL3A**	27	334	Belongs to the ribosomal protein S3P family.
(1-11) (2-12)	Lamr1-prov protein/40S ribosomal protein SA	**Q7ZX07**	33.9	202	Small ribosomal subunit
(1-13)	60S acidic ribosomal protein P0/ 60S acidic ribosomal protein P0	**Q8AVI3**	34.1	124	Ribosomal protein
(1-15) (2-9)	Rps6-prov protein/ 40S ribosomal protein S6	**Q7ZYU0**	28.7	73	Ribosomal subunit
(1-16) (2-14)	Rps2e protein/ Ribosomal protein S2	**Q7T0R9**	30.2	72	Belongs to the ribosomal protein S5P family
(1-29)	MGC80804 protein/ 40S ribosomal protein S9	**Q5XHQ8** **Q6GNX6**	22.6	21	Belongs to the ribosomal protein S4P family
(2-11)	MGC130910 protein/ 60S ribosomal protein L7	**Q3B8I3**	50.4	88	Large ribosomal subunit,
Mitochondrial proteins					
(1-2) (2-5)	Adenine nucleotide translocase (Slc25a5-prov protein) / ADP/ATP translocase 3	**Q9I9M9**	32.9	684	Belongs to the mitochondrial carrier family
(1-8)	MGC79005 protein/ ADP/ATP translocase 1	**Q6IP28**	33.1	404	Belongs to the mitochondrial carrier family
(1-14)	MGC82600 protein/ Mitochondrial 2-oxoglutarate/malate carrier protein	**Q6INH3**	33.6	111	Belongs to the mitochondrial carrier family.
(1-17)	LOC495171 protein/ Peroxisomal membrane protein PMP34	**Q5XGP8**	34.5	63	Mitochondrial transport.

Table 2.1 continued

(Run-Rank)	Name Xenopus/Human	Accession #	MW kD	Peptide Hits	Known Function
(1-26)	MGC82285 protein/ Mitochondrial dicarboxylate carrier	**Q6NRR4**	31.6	23	Mitochondrial carrier family
(1-30)	Cytochrome P450/ Cytochrome P450, family 1, subfamily A, polypeptide 1 variant [Fragment]	**Q9YI89**	59.7	21	Belongs to the cytochrome P450 family
Metabolism					
(1-4) (2-1)	LOC496039 protein/ Carbonyl reductase [NADPH] 1	**Q5PPZ0**	30.2	530	Oxidoreductase activity
(1-24)	LOC495290 protein/ 5'-AMP-activated protein kinase catalytic subunit alpha-1	**Q5U5E3**	64	24	Belongs to the Ser/Thr protein kinase family.
Miscellaneous					
(1-1) (2-2)	vitellogenin A2 precursor/?	**S03124**	201.4	1234	Precursor-product relationship between vitellogenin and the yolk proteins as derived from the complete sequence of a Xenopus vitellogenin gene
(1-6) (2-6)	Vitellogenin B1/?	**Q7SZF6**	202.9	492	Lipid transporter activity
(1-19)	Ns:zf-e326 protein/ SPRY domain-containing SOCS box protein 1	**Q7ZX62**	30.8	45	Contains 1 SOCS box domain/intracellular signaling.
(1-22)	Guanine nucleotide-binding protein-like 3/ Guanine nucleotide-binding protein-like 3	**Q7ZX41**	60.8	30	GTP binding/regulation of cell proliferation
(1-28)	MGC82350 protein/ CDK5 regulatory subunit-associated protein 3	**Q6AZH9**	57.5	22	Regulator of CDK5 activity
(2-15)	Ubiqutin	**UQBO**	8.5	45	Protein modifier/degredation
(1-16)	?	**AAH70968**	?	36	?
(2-17)	Proteasome subunit alpha type/ Proteasome subunit alpha type-4	**Q3KPN6**	29.4	29	Proteasome core complex

Table 2.1 continued

(Run-Rank)	Name Xenopus/Human	Accession #	MW kD	Peptide Hits	Known Function
(2-18)	Mix-like endodermal regulator/ Mix1 homeobox-like protein 1	**O73867**	41.8	28	DNA binding transcription factor
(2-19)	MGC69081 protein/ VEZT protein	**Q6PCG6**	88.3	25	?
(2-20)	Myosin heavy chain	**A47297**	23	25	Myosin complex
(2-21)	N-acetyltransferase 11/N-acetyltransferase 11	**Q6NUH2**	27.1	22	Acetyltransferase family. GNAT subfamilyContains 1 N-acetyltransferase domain
(2-22)	Scc2-1B/Nipped-B-like protein: Delangin SCC2 homolog	**Q1XG44**	32.9	21	Chromatid cohesion
(2-23)	MGC115095 protein/ Myosin head domain containing 1 variant [Fragment]	**Q569U0**	11	20	Myosin complex
(2-24)	Sister chromatid cohesion protein PDS5 homolog A-B/ Sister chromatid cohesion protein PDS5 homolog A	**Q4KLU7**	14	20	Chromatid cohesion
(2-25)	Integrin alpha-4 [Precursor]/ Integrin alpha-4 [Precursor]	**AAA98673**	115	19	Fibronectin and V-CAM adhesion receptor
(2-26)	LOC496029 protein/ snRNA-activating protein complex subunit 2	**Q5PQ00**	45.5	19	DNA binding/ Part of the SNAPc
(2-27)	Ambp protein/ AMBP protein [Precursor]	**Q7SZ46**	38.5	18	Contains 2 BPTI/Kunitz inhibitor domains

Table 2.2 Interphase interacting partners of PDCD4 identified by mass spectrometry

Rank	Name Xenopus/Human	Accession #	MW kD	Peptide Hits	Known Function
PRMT5					
1	LOC495515/Protein arginine N-methyltransferase 5	**Q2VPH9**	72	1300	Arginine dimethyltransferase
2	Hsl7 protein/ Protein arginine N-methyltransferase 5	**Q6NUA1**	72.2	1022	Arginine dimethyltransferase
Mitochondrian					
3	MGC69168/ Mitochondrial aspartate-glutamate carrier protein	**Q6PCF1**	74.5	498	Mitochondrial carrier family
23	LOC733343 protein [Fragment]/ Mitochondrial inner membrane protein	**Q3KQ64**	**54.6**	21	Mitochondrion inner membrane protein
RNA metabolsim					
8	MGC85069 protein/ Pre-mRNA-splicing factor 18	**Q5EAV6**	**39.7**	39	RNA splicing
13	MGC114630 / CDNA FLJ10005 fis, clone HEMBA1000156. [Fragment]	**Q498L2**	**11.3**	29	RNA binding
17	LOC446275 protein / Serine-arginine repetitive matrix protein 2	**Q68F69**	101.3	27	RNA splicing
Metabolism					
10	MGC81848 protein/ Thioredoxin reductase 3 [Fragment]	**Q66J56**	65.7	33	Disulfide oxidoreductase
11	MGC79063 protein/ 6-phosphofructokinase, muscle type	**Q6DD69**	88.3	30	6-phosphofructokinase complex
22	LOC398437/ Procollagen-lysine,2-oxoglutarate 5-dioxygenase 1	**Q7ZXD7**	83.3	22	Procollagen-lysine 5-dioxygenase activity
24	MGC82842 protein/ Xylosyltransferase 1	**Q5XFZ9**	105.2	20	Acetylglucosaminyltransferase activity

Table 2.2 continued

Rank	Name Xenopus/Human	Accession #	MW kD	Peptide Hits	Known Function
29	MGC131193/ Phospholipase C, delta 4	**Q32NH8**	87.3	19	Phosphoinositide phospholipase C activity
30	Vitellogenin B1	**Q7SZF6**	202.3	18	Lipid transporter activity
Miscellaneous					
4	MGC53952 protein/ Heat shock cognate 71 kDa protein	**Q7ZTK6**	70.7	304	Heat shock protein 70 family/Chaperone.
6	XlZPA protein/ Zona pellucida sperm-binding protein 2	**Q6AX05**	77.2	62	The mammalian zona pellucida
12	MGC84421 protein/Angiopoietin-related protein 7	**Q6DJE9**	**32.9**	29	Signal transduction response to oxidative stress
15	LOC495293 protein/ Leucyl-cystinyl aminopeptidase	**Q5U5D5**	116.1	28	Membrane alanyl aminopeptidase activity Degrades peptide hormones
18	Xgly4 protein/ Glypican-4 (GPC4)	**Q5EAV3**	62.9	23	Lipid-anchor, GPI-anchor.
20	Chrna5-prov/ Neuronal acetylcholine receptor subunit alpha-5	**Q6DFE9**	**53**	22	Nicotinic acetylcholine-activated cation-selective channel activity
21	MGC131112/ ADP-ribosylation factor-like protein 4C	**Q2TAQ7**	**21.7**	22	ER to Golgi vesicle-mediated transporter
28	Annexin A2-A/ Annexin A2	**ANX2A**	**38.3**	19	Secreted, extracellular space, extracellular matrix, basement membrane.

CHAPTER 3

PRMT5 ACCELERATES TUMOR GROWTH BY ARGININE METHYLATION OF THE TUMOR SUPPRESSOR PDCD4

3.1 Abstract

Programmed Cell Death 4 (PDCD4) has been described as a tumor suppressor, with high expression correlating with better outcomes in a number of cancer types. Yet, subpopulations of cancer patients, despite high PDCD4 expression in tumors, have poor survival, suggesting oncogenic pathways may inhibit or change PDCD4 function. Here, we explore the significance of PDCD4 in the context of breast cancer and describe the discovery of Arginine Methyl Transferase 5 (PRMT5) as a cofactor that radically alters PDCD4 function. Specifically, we find that co-expression of PDCD4 and PRMT5 in an

---

This chapter is a modified version of a paper submitted to Cancer Research. This paper was co-first authored by Matthew A. Powers and Marta M. Fay. The following authors are Rachel E. Factor, Alana L. Welm and Katharine S. Ullman. Author contributions: MP: discovered interaction between PDCD4-PRMT5, oversaw truncation mutations of PDCD4, developed MCF7e cell lines and measured and analyzed tumor growth in mice and helped analyze clinical breast cancer data, wrote paper; MF: discovered PDCD4 methylation and performed all methylation reactions and discovered methylation site arginine 110 and made all methyl-mutants, analyzed data, edited paper;RF: assessed protein expression in clinical samples; AW: designed research and analyzed data, edited paper; KU: designed research and analyzed data; wrote paper.

orthotopic model of breast cancer causes accelerated tumor growth and that this growth phenotype is dependent on both the catalytic activity of PRMT5 and a site of methylationwithin the N-terminal region of PDCD4. In agreement with the xenograft model, elevated phenotype is dependent on both the catalytic activity of PRMT5 and a site of methylation within the N-terminal region of PDCD4. In agreement with the xenograft model, elevated PRMT5 expression correlates significantly with worse outcome within the cohort of breast cancer patients whose tumors contain higher levels of PDCD4. These results reveal a new cofactor for PDCD4 that alters tumor suppressor function and point to the utility of PDCD4/PRMT5 status as both a prognostic biomarker and a potential target for chemotherapy.

3.2 Introduction

Although an active area of research where significant advances have been achieved, breast cancer is a leading cause of mortality among women (2). Breast cancer is a heterogeneous disease that can be difficult to stratify into distinct categories with precise outcomes, especially as improved detection methods allow for diagnosis of early subclinical disease (3). The dilemma of unknown/unquantifiable risk assessments can lead to over-treatment, accompanied by unwanted side effects, or under-treatment, which risks increased recurrence (4). Increasingly, biomarkers, such as hormone receptors, are used to enhance outcome predictions and refine treatment plans. Expanding the arsenal of prognostic biomarkers will help reduce guesswork in treatment plans, leading to better overall survival and improved quality of life.

Programmed Cell Death 4 (PDCD4) is a promising biomarker that correlates with better outcomes in lung, colon, ovarian and esophageal cancer (5-8). PDCD4 is expressed at lower levels in invasive breast carcinoma compared with ductal carcinoma in situ or normal samples, indicating there may be loss of PDCD4 during disease progression (9). Experimental models substantiate a tumor suppressor role for PDCD4. In a mouse epithelial cell line, PDCD4 expression reduced phorbol ester-induced transformation (10) and, in transformed cells, PDCD4 expression suppressed anchorage-independent cell growth (11). Transgenic mice expressing epidermal PDCD4 were resistant to chemically induced skin tumors (12), while PDCD4 knockout mice developed B-cell lymphoma (13).

Here, we find that PDCD4 expression in breast cancer correlates with better survival. Yet, as with many biomarkers, there are limitations in using PDCD4 to predict outcome: subsets of patients whose tumors contain elevated PDCD4 mRNA still experienced poor clinical outcome, indicating the presence of mechanisms that abrogate or change PDCD4 function. Pursuing such a mechanism, we have found a novel PDCD4-interacting partner, PRMT5, which posttranslationally methylates PDCD4. Together, these proteins cause a pro-growth tumor phenotype in an orthotopic breast cancer model. Moreover, we have found that PRMT5 is a significant factor in determining long term survival in PDCD4-upregulated breast cancer. Discovery of this new pro-tumor growth pathway improves the utility of PDCD4 as a prognostic tool and reveals PRMT5 as a potential therapeutic target, whose inhibition may unmask the function of a tumor suppressor.

3.3 Experimental Procedures

3.3.1 Constructs

Open reading frames for human PDCD4, PRMT5 and the PDCD4 truncation mutants were PCR cloned with Gateway (Invitrogen) compatible ends and introduced into pDONR221. $PRMT5_{cd}$ was created by mutation of amino acids glycine 367 and arginine 368 to alanines (14). The pGEX-4T vector and the pMIG (Addgene plasmid 9044, William Hahn) vector were made Gateway compatible using the RFB and RFA oligos (Invitrogen) respectively. PDCD4, PDCD4 point mutants and truncation mutants were cloned into the pGEX-4T Gateway compatible vector. PRMT5 and $PRMT5_{cd}$ were cloned into the pcDNA3.1 nV5/DEST (Invitrogen). PDCD4 and $PDCD4_{mm}$ were cloned into the pMIG Gateway compatible vectors, while PRMT5 and $PRMT5_{cd}$ were cloned into pMSCVpuro (Clontech) vector using BglII and EcoRI cut sites.

3.3.2 Recombinant protein production

Cultures of BL21/RIL cells (Novagen) transduced with PDCD4-pGEX4T were induced using 0.1mM IPTG for 1-3 hours. Pellets were resuspended and sonicated in 1xPBS, 0.4mM PMSF, 5µg/ml leupeptin and aprotinin, 5% deoxycholate. Cleared supernatants were incubated with glutathione beads followed by TBS wash and elution in 100mM Tris pH 8.0, 150mM NaCl, 20mM glutathione. Purified protein was dialyzed into TBS and concentrated for storage; 10% glycerol was added prior to freezing in aliquots at -80°C.

3.3.3 Recombinant PDCD4 pull downs in human cell lysates

Ten μg of GST-proteins were incubated with glutathione resin (GE Healthcare) in binding buffer (20 mM Hepes pH7.6, 100 mM KCl, 0.5 mM EDTA, 0.25% Triton X-100, 20% glycerol) at room temperature for 1 hour. GST-glutathione conjugates were washed and incubated with 100-300 μg of cell lysate in a final volume of 200 μl binding buffer for 1 hour at room temperature. Proteins were eluted in SDS sample buffer 98°C for 3 minutes.

3.3.4 Preparation of ecotropic retrovirus and MCF7e infections

To prepare virus, HEK293T cells were cotransfected with pCL-Eco plasmid and pMIG or pMSCVpuro retroviral vectors in a 1:3 ratio. One day after transfection, the medium was exchanged with fresh media. Virus containing medium was collected 48 hours after transfection and filtered through a 0.45 micron filter. Virus was diluted 1:4 into MCF7 media (DME:F12 1:1, 10% FBS, 10 mg/L insulin) and mixed with polybrene (to 8 μg/ml) . This virus mixture was overlaid on 20-50% confluent MCF7e cells, which stably express an ecotropic receptor. Virus media was exchanged for MCF7 media at 24 hours. Cells were maintained for ~1 week prior to selection. pMIG-transduced cells were selected by FACS for GFP-positive cells and pMSCVpuro-transduced cells were selected for 2 weeks with 2 μg/ml puromycin.

3.3.5 Transplantation of transduced MCF7e cells and tumor growth

One-million cells were diluted into 10 μL of matrigel (BD bioscience) and kept on ice. Three-week-old recipient NOD/SCID mice were anesthetized with vaporized

isoflurane and then injected with the cell suspension into the cleared inguinal fat pads as described (15). Tumors were physically measured using calipers at 14-21 day intervals throughout duration of growth. Mice were sacrificed by CO_2 asphyxiation and visible tumors collected. Upon sacrifice of mice, lungs, spleen and liver were dissected and visually inspected for macro-metastases. Micro-metastases were assessed by detection of GFP positive cells in tissues using an Olympus MVX10 dissecting scope with a UV light source.

3.3.6 V5-Immunoprecipitation

HEK293 cells were transiently transfected with catalytically active or dead PRMT5 pcDNA3.1 nV5/EXP vectors. Cells were lysed in methylation buffer (1mM DTT, 0.25% Triton X-100, 5% glycerol in 1 x PBS) 18-24 hours after transfection and incubated with V5 antibody (Invitrogen) conjugated to protein A beads. One mg of lysate was incubated with prebound beads for a minimum of 2 hours at 4ºC. IPs were washed three times with methylation buffer prior to use in further reactions

3.3.7 Methyltransferase reactions

One to five μg of GST tagged protein was incubated with HEK293 cell lysate or immunoprecipitated V5-PRMT5 in methyl buffer and supplemented with 0.5-2 μCi ^{3}H-SAM (Perkin Elmer). Reactions were incubated at 30°C for 1 hour and terminated by addition of SDS sample buffer. Tritiated proteins were separated by SDS-PAGE, and transferred to PVDF. For autoradiography, blots were treated with Enhance Spray (Perkin

Elmer) according to manufacturer's recommendations and exposed to film at -80°C for 6 hours-5 days.

3.3.8 Antibodies

PDCD4 and PRMT5 antibodies were acquired from Abcam. For immunoblots, α-PDCD4 antibody was used at 1:2000 while α-PRMT5 antibody was used at 1:1000 and cell lysates were loaded at 2.5-5 µg per lane. Anti-V5 antibody (2F11F7 Invitrogen) was used at 1:1000, anti-tubulin (YL1/2, Accurate chemical and Scientific Corp.) at 1:2000 and anti-β-actin (AC-74, Sigma) at 1:2000 for immunoblots.

3.3.9 Gene expression and statistical analysis

Gene expression and clinical outcome information were obtained from two independent publicly available datasets (1, 16, 17). Clinical outcomes from the Pawitan study (17) was obtained from data published in the Ivshina study (1). Data for *PRMT5* and *PDCD4* were extracted from normalized expression data for each breast tumor sample, and patients were divided into groups based on expression of the two genes. Each dataset was analyzed separately. For the data from the van de Vijver study, distant metastasis was analyzed as first event only. If a patient developed a local recurrence, axillary recurrence, contra-lateral breast cancer, or a second primary cancer (except for non-melanoma skin cancer), she was censored at that time. Any distant metastasis after the first event was not analyzed, based on the theoretical possibility that the secondary cancers could be a source for distant metastases. An ipsalateral supra-clavicular recurrence was considered as first clinical evidence for metastatic disease for this

analysis. Therefore, patients with ipsalateral supra-clavicular recurrence were not censored. Patients were censored at last follow-up. Kaplan-Meier survival curves were generated using the software WINSTAT FOR EXCEL (R. Fitch Software, Staufen, Germany), and p values were calculated by log-rank analysis. p values <0.05 were considered significant.

All tissue samples used for this study were obtained from informed and consented patients under an approved IRB protocol. All animal experiments were reviewed and approved by the U of U IACUC prior to conducting the experiments.

3.4 Results

3.4.1 Analysis of PDCD4 as a prognostic marker in breast cancer

To determine the relationship between PDCD4 transcript expression in breast cancer and patient survival, we evaluated a previously published microarray dataset. This dataset was obtained from tumors less than 5cm deposited at the Netherlands Cancer Institute from 295 breast cancer patients under the age of 55 (16). We stratified this dataset into two groups based on PDCD4 transcript levels, with the "high" group representing those above the median. High expression significantly correlated with better probability of survival ($p=0.0014$) (Figure 3.1). Nevertheless, a significant fraction of patients within the high *PDCD4* cohort (~35%, which extrapolates to over 38,000 new patients this year in the U.S. alone (2)) did not appear to gain benefit from this elevated expression. One explanation for this could be the presence of interacting partners of PDCD4 that inactivate or change its role as a tumor suppressor.

3.4.2 A novel interaction between PDCD4 and PRMT5

To look for potential new regulatory factors of PDCD4, we took a biochemical approach to identify binding partners. We used *Xenopus laevis* egg extract, which has the advantage of limited manipulation to disrupt protein complexes and retains a very high concentration of proteins. A 72 kD protein was consistently recovered from egg extract with recombinant PDCD4 (Figure 3.2A). When analyzed by mass spectrometry, this protein was identified as Protein Arginine Methyltransferase 5 (Figure 3.3). To confirm that PDCD4 also interacts with human PRMT5, lysates were made from HEK293 and three breast cancer cell lines, and interacting proteins were similarly isolated using GST-PDCD4, this time on an analytical scale. Immunoblotting the proteins retained with recombinant PDCD4 confirmed the interaction with human PRMT5 and indicated that this is an interaction to consider in the context of breast cancer (Figure 3.2B).

PRMT5 is a type II methyltransferase and catalyzes addition of a methyl group to both terminal nitrogens of arginine residues (18). Like other posttranslational modifications, methylation can alter protein function, localization and/or binding partners (18). To assess whether PRMT5 has the potential to be a regulatory factor in the context of breast cancer, we examined a set of clinical biopsies for protein expression. This survey found that PRMT5 is expressed in breast cancer and can vary in level as well as whether it is co-expressed with PDCD4 (Figure 3.4).

3.4.3 PDCD4 and PRMT5 synergistically enhance tumor growth

Over-expression of PRMT5 transforms NIH3T3 cells and has been found to be upregulated in leukemia, lymphoma and gastric cancer (14, 19, 20). The presence of PRMT5 in breast cancer, its potential to modulate protein activity, and its reported attributes as a pro-tumor factor prompted us to test whether PRMT5 influences the role of PDCD4 in a tumor context. To do so, MCF7 breast cancer cells were engineered to express elevated levels of either protein alone or in concert. PDCD4 and PRMT5 expression levels were confirmed by immunoblot analysis (Figure 3.5A). There were no gross phenotypic changes as a result of increased expression of these proteins and all four cell lines had similar doubling times under normal tissue culture conditions (Figure 3.5B).

To assess tumor growth, cells were transplanted orthotopically into NOD/SCID mice. Increasing levels of either PDCD4 or PRMT5 alone in the context of MCF7e cells did not significantly alter the growth rate of the tumor (Figure 3.5C). However, the PDCD4-PRMT5 co-expressing cells exhibited significantly faster growth as tumors than singly-expressing PDCD4, PRMT5 or control cell lines (Figure 3.5C). Immunohistochemical analysis of harvested tumors showed the expected elevated levels of PDCD4 and PRMT5 expression (Figure 3.6). Analysis of lungs, spleen, and liver showed no significant difference in metastasis between cell lines.

3.4.4 PDCD4 is methylated in the N-terminal domain at R110 and is a target of PRMT5

To determine if PDCD4 can be methylated and possible regions of modification, we fragmented PDCD4 into two domains. We noted that the N-terminal region contains

an arginine rich (RR) subdomain (Figure 3.7A). The second region contains the MA3 domains responsible for eIF4A binding (Figure 3.7A) (21-23). Purified GST-fusion proteins of full-length and both truncation mutants were incubated with cell lysate as an enzyme source and supplemented with tritiated S-adenosylmethionine (SAM) as the methyl donor. Only full-length protein and the N-terminal fragment were labeled (Figure 3.7B). To further map the methylation site of PDCD4, we took a candidate approach. Within the arginine-rich region of PDCD4, R73 and R110 are flanked by glycines, resembling canonical methylation sites (Figure 3.7A). These arginines were mutated to lysine, conserving the amino acid charge but disrupting potential methyl acceptor sites. Mutation of R73 had no effect, whereas mutation of R110 abolished methylation (Figure 3.7C, lanes 2 and 4). Arginine 110 is therefore the major methyl acceptor site within PDCD4.

To determine if PRMT5 itself methylates PDCD4, wild-type or catalytically dead PRMT5 ($PRMT5_{cd}$) were transiently expressed and then immuno-isolated (Figure 3.7D). These enzyme sources were incubated with purified GST-PDCD4 and ^{3}H-SAM. Labeled GST-PDCD4 was detected in reactions using wild-type PRMT5 (Figure 3.7D, lane 4), demonstrating that PDCD4 can be targeted for methylation by PRMT5. PDCD4 was labeled at greatly reduced levels in reactions using $PRMT5_{cd}$; this residual activity is likely due to the ability of mutant PRMT5 to homo-oligomerize with its endogenous counterpart (24). Mutation of R110 again resulted in the absence of methylation (Figure 3.7D, lane 7), confirming that this is the acceptor site for methylation by PRMT5.

3.4.5 The catalytic activity of PRMT5 and PDCD4-R110 are necessary for enhanced tumor growth

The ability of PRMT5 to function as a pro-cancer factor in leukemia/lymphoma cells is dependent on its methyltransferase activity (20). However, PRMT5 overrides a G2/M phase checkpoint independent of enzymatic activity (25). To determine if PRMT5 enzymatic activity is necessary to promote tumor growth in our breast cancer model system, MCF7e cell lines were generated expressing $PRMT5_{cd}$ alone or in conjunction with wild-type PDCD4 (Figure 3.8A). These cells were transplanted orthotopically and assessed for tumor growth over a 22 week period. As controls, vector only and wild-type PDCD4-PRMT5 cells were also re-transplanted. The new injection of the PDCD4-PRMT5 cell line tracked well with the previous PDCD4-PRMT5 tumor growth rate, underscoring their synergistic effect (Figure 3.8B). However, the $PRMT5_{cd}$-PDCD4 cells did not show an accelerated growth rate (Figure 3.8B, C), indicating that the enzymatic activity of PRMT5 is necessary for enhanced tumor growth due to co-expression with PDCD4.

To determine whether PDCD4 is the relevant target of PRMT5 in this context or whether PRMT5 is working through a parallel pathway. MCF7e cell lines were generated expressing the methyl mutant $PDCD4_{mm}$ (PDCD4 with R110K mutation) with or without wild type PRMT5 and then assessed for tumor growth (Figure 3.8A). Tumor growth of $PDCD4_{mm}$ with PRMT5 was not significantly different from the control cell line (Figure 3.8C). This indicates that methylation of PDCD4, and R110 in particular, is necessary for the enhanced tumor growth observed with co-expression of both wild type PDCD4 and PRMT5.

3.4.6 Clinical data indicate that PRMT5 levels impact the probability of survival when tumors express PDCD4

Our observations that simultaneous expression of elevated PDCD4 and PRMT5 causes accelerated tumor growth in an orthotopic mouse model raised the question of whether this combination of markers would be useful in a clinical setting. To address this, we stratified patients with high tumor levels of *PDCD4* into quartiles based on *PRMT5* expression. Each one of these cohorts can be extrapolated to approximately 25,000 patients a year in the U.S. alone (2). We found that the top quartile –in which tumors highly express both *PDCD4* and *PRMT5*– had poor outcomes, similar to the low *PDCD4* cohort. In contrast, with decreases in *PRMT5* expression, the probability of survival increased significantly (p=0.0016) The bottom quartile –high for *PDCD4* and low for *PRMT5*– had remarkably better outcome than the top quartile (Figure 3.9A), with a 20-year survival of 80% vs 43%. Similar quartile analysis of *PRMT5* alone showed a trend in improved probability of survival with decreasing *PRMT5*, but was not significant (Figure 3.9B). This suggests that the combination of *PRMT5* and *PDCD4* as biomarkers for outcome is potentially useful: high levels of *PDCD4* are protective, unless *PRMT5* is also highly expressed.

To test the reproducibility of these observations, we used another, independent breast cancer dataset (1). We selected patients from this cohort based on availability of both clinical follow-up and gene expression data. This resulted in a set of 224 tumors, which we then stratified for *PDCD4* expression, with "high" defined as those in the top third of expression levels. Patients in this high expression group also had a significantly higher probability of longer disease-free survival (p= 0.0066) (Figure 3.10A). Yet, within the high *PDCD4* expression group there was still a >25% probability of relapse. We then further stratified the *PDCD4* high group by *PRMT5* levels (each sub-group extrapolates

to greater than 15,000 patients a year in the U.S. alone (2)) and, again, lower levels of *PRMT5* proved to correspond to better outcome in this context (p=0.0203; Figure 3.10B), whereas quartile analysis of *PRMT5* alone did not show a correspondence to outcome (Figure 3.10C). This data confirms that considering *PRMT5* levels in the context of *PDCD4* could be an effective strategy toward an improved prognostic tool in breast cancer.

3.5 Discussion

PDCD4 shows promise as a biomarker, with prognostic attributes in a number of cancers (5-8). Here, we further find that *PDCD4* expression is informative with regard to survival of breast cancer patients, where increased levels correlate with better outcome in two large scale clinical evaluations. *PDCD4* expression alone, however, has limitations in stratifying cancer patient outcomes as ~30% of patients with tumors expressing relatively high PDCD4 mRNA levels have poor survival. This could be due to a potential discrepancy between mRNA and protein levels (26, 27), to environmental factors, or to interacting regulatory pathways.

The discovery here of PRMT5 as an interacting partner opened a new level of regulation to consider. Neither PDCD4 nor PRMT5 affected tumor cell growth when expressed alone in our model system. Although this was somewhat surprising, it may indicate that in a particularly aggressive or advanced tumor context, elevated expression of either protein alone is insufficient to alter tumor properties. In the case of PDCD4, this may be due at least in part to endogenous levels of PRMT5. Importantly, the orthotopic tumor model revealed that, together, elevated PDCD4 and PRMT5 expression

significantly enhanced tumor growth. This result suggests that PRMT5 does not just negate a PDCD4 tumor suppressor function, but works synergistically to promote tumor growth. This pro-growth effect occurred only in the tumor context, not in tissue culture, hinting that the combination of proteins activates a pathway that enhances the ability to establish a productive tumor microenvironment. A dual role for a tumor suppressor as a contributor to oncogenesis is not unprecedented. For instance, p27 is considered a tumor suppressor via blocking cyclin activation, but has cyclin-independent roles that promote oncogenesis (28).

The change in PDCD4 function that occurs in the presence of elevated PRMT5 pointed to a role for post-translational modification. We found that indeed PDCD4 is methylated and is a target of PRMT5 at R110. Furthermore, the PDCD4 methyl mutant expressed with wild type PRMT5 or the catalytically dead PRMT5 expressed with wild type PDCD4 failed to promote tumor growth. This demonstrates that methylation of PDCD4 by PRMT5 is critical for enhanced tumor growth. The methylation target residue, R110, lies near a S6 Kinase 1 site (S67) reported to regulate PDCD4 stability (27, 29). While levels of ectopic expression of PDCD4 did not appear to be influenced by the presence of PRMT5 or mutation of R110 (Figure 3.5 and 3.8), whether there is cross-talk between these post-translational modifications requires further investigation.

PDCD4 is thought to exert its tumor suppressor role by regulating translation (21, 30), fitting with a growing theme of translation initiation as a node of regulation in cancer (31). More specifically, the ability of PDCD4 to function as an inhibitor of transformation and anchorage-independent cell growth relies on its ability to bind to the translation initiation factor eIF4A (21, 30, 32). Interestingly, PRMT5 has been shown to

influence eIF4E levels (33) and was recently shown to interact with the ribosomal subunit RPS10 and, through methylation, influence ribosomal stability (34). Although methylation of PDCD4 may impact its role in translation regulation, we cannot rule out that, conversely, methylated PDCD4 changes PRMT5 function or specificity. In addition to the recent connection to translation, PRMT5 is known to be involved in transcription (14, 20, 35), in efficient assembly of the spliceosome (36), and in modulation of p53-dependent cell cycle arrest (33, 37). Methylated PDCD4 could interact with PRMT5 and accelerate tumor growth by altering these or other functions downstream of PRMT5 (33, 37).

By integrating biochemical and tumor model data, we have found that an elevated level of PRMT5 in conjunction with PDCD4 reverses the tumor suppressive properties of PDCD4. Chemical inhibition of PRMT5 methyltransferase activity could abrogate the synergism between PDCD4 and PRMT5, potentially unmasking PDCD4 tumor suppressor function in cancers that express both proteins. The finding that combined expression analysis of *PDCD4* and *PRMT5* is a powerful prognostic indicator for outcome in breast cancer suggests that these factors could be used as rational, activity-based biomarkers to aide in decisions about how aggressively to treat a breast cancer patient. Finally, although our focus here has been on breast cancer, PDCD4 plays a tumor suppressor role in a wide spectrum of cancers (5-7), raising the possibility that its connection to PRMT5 will be of broad prognostic, and perhaps therapeutic, value.

3.6 References

1. Ivshina AV, George J, Senko O*, et al.* Genetic reclassification of histologic grade delineates new clinical subtypes of breast cancer. Cancer Res 2006;66(21):10292-301.

2. Jemal A, Siegel R, Xu J, Ward E. Cancer Statistics, 2010. CA Cancer J Clin 2010;60 (5):277-300.

3. Burke HB. Outcome prediction and the future of the TNM staging system. J Natl Cancer Inst 2004;96(19):1408-9.

4. Duffy MJ, Crown J. A personalized approach to cancer treatment: how biomarkers can help. Clin Chem 2008;54(11):1770-9.

5. Chen Y, Knosel T, Kristiansen G*, et al.* Loss of PDCD4 expression in human lung cancer correlates with tumour progression and prognosis. J Pathol 2003;200(5):640-6.

6. Fassan M, Cagol M, Pennelli G*, et al.* Programmed cell death 4 protein in esophageal cancer. Oncol Rep 2010;24(1):135-9.

7. Mudduluru G, Medved F, Grobholz R*, et al.* Loss of programmed cell death 4 expression marks adenoma-carcinoma transition, correlates inversely with phosphorylated protein kinase B, and is an independent prognostic factor in resected colorectal cancer. Cancer 2007;110(8):1697-707.

8. Wei NA, Liu SS, Leung TH*, et al.* Loss of Programmed cell death 4 (Pdcd4) associates with the progression of ovarian cancer. Mol Cancer 2009;8:70.

9. Wen YH, Shi X, Chiriboga L, Matsahashi S, Yee H, Afonja O. Alterations in the expression of PDCD4 in ductal carcinoma of the breast. Oncol Rep 2007;18(6):1387-93.

10. Yang HS, Jansen AP, Nair R*, et al.* A novel transformation suppressor, Pdcd4, inhibits AP-1 transactivation but not NF-kappaB or ODC transactivation. Oncogene 2001;20(6):669-76.

11. Yang HS, Knies JL, Stark C, Colburn NH. Pdcd4 suppresses tumor phenotype in JB6 cells by inhibiting AP-1 transactivation. Oncogene 2003;22(24):3712-20.

12. Jansen AP, Camalier CE, Colburn NH. Epidermal expression of the translation inhibitor programmed cell death 4 suppresses tumorigenesis. Cancer Res 2005;65(14):6034-41.

13. Hilliard A, Hilliard B, Zheng SJ*, et al.* Translational regulation of autoimmune inflammation and lymphoma genesis by programmed cell death 4. J Immunol 2006;177(11):8095-102.

14. Pal S, Vishwanath SN, Erdjument-Bromage H, Tempst P, Sif S. Human SWI/SNF-associated PRMT5 methylates histone H3 arginine 8 and negatively regulates expression of ST7 and NM23 tumor suppressor genes. Mol Cell Biol 2004;24(21):9630-45.

15. Rijnkels M, Rosen JM. Adenovirus-Cre-mediated recombination in mammary epithelial early progenitor cells. J Cell Sci 2001;114(Pt 17):3147-53.

16. van de Vijver MJ, He YD, van't Veer LJ*, et al.* A gene-expression signature as a predictor of survival in breast cancer. N Engl J Med 2002;347(25):1999-2009.

17. Pawitan Y, Bjohle J, Amler L*, et al.* Gene expression profiling spares early breast cancer patients from adjuvant therapy: derived and validated in two population-based cohorts. Breast Cancer Res 2005;7(6):R953-64.

18. Bedford MT, Clarke SG. Protein arginine methylation in mammals: who, what, and why. Mol Cell 2009;33(1):1-13.

19. Kim JM, Sohn HY, Yoon SY*, et al.* Identification of gastric cancer-related genes using a cDNA microarray containing novel expressed sequence tags expressed in gastric cancer cells. Clin Cancer Res 2005;11(2 Pt 1):473-82.

20. Pal S, Baiocchi RA, Byrd JC, Grever MR, Jacob ST, Sif S. Low levels of miR-92b/96 induce PRMT5 translation and H3R8/H4R3 methylation in mantle cell lymphoma. Embo J 2007;26(15):3558-69.

21. Yang HS, Cho MH, Zakowicz H, Hegamyer G, Sonenberg N, Colburn NH. A novel function of the MA-3 domains in transformation and translation suppressor Pdcd4 is essential for its binding to eukaryotic translation initiation factor 4A. Mol Cell Biol 2004;24(9):3894-906.

22. Chang JH, Cho YH, Sohn SY*, et al.* Crystal structure of the eIF4A-PDCD4 complex. Proc Natl Acad Sci U S A 2009;106(9):3148-53.

23. Loh PG, Yang HS, Walsh MA*, et al.* Structural basis for translational inhibition by the tumour suppressor Pdcd4. Embo J 2009;28(3):274-85.

24. Rho J, Choi S, Seong YR, Cho WK, Kim SH, Im DS. Prmt5, which forms distinct homo-oligomers, is a member of the protein-arginine methyltransferase family. J Biol Chem 2001;276(14):11393-401.

25. Yamada A, Duffy B, Perry JA, Kornbluth S. DNA replication checkpoint control of Wee1 stability by vertebrate Hsl7. J Cell Biol 2004;167(5):841-9.

26. Asangani IA, Rasheed SA, Nikolova DA, *et al.* MicroRNA-21 (miR-21) post-transcriptionally downregulates tumor suppressor Pdcd4 and stimulates invasion, intravasation and metastasis in colorectal cancer. Oncogene 2008;27(15):2128-36.

27. Dorrello NV, Peschiaroli A, Guardavaccaro D, Colburn NH, Sherman NE, Pagano M. S6K1- and betaTRCP-mediated degradation of PDCD4 promotes protein translation and cell growth. Science 2006;314(5798):467-71.

28. Besson A, Hwang HC, Cicero S, *et al.* Discovery of an oncogenic activity in p27Kip1 that causes stem cell expansion and a multiple tumor phenotype. Genes Dev 2007;21(14):1731-46.

29. Schmid T, Jansen AP, Baker AR, Hegamyer G, Hagan JP, Colburn NH. Translation inhibitor Pdcd4 is targeted for degradation during tumor promotion. Cancer Res 2008;68(5):1254-60.

30. Yang HS, Jansen AP, Komar AA, *et al.* The transformation suppressor Pdcd4 is a novel eukaryotic translation initiation factor 4A binding protein that inhibits translation. Mol Cell Biol 2003;23(1):26-37.

31. Silvera D, Formenti SC, Schneider RJ. Translational control in cancer. Nat Rev Cancer 2010;10(4):254-66.

32. Yang HS, Matthews CP, Clair T, *et al.* Tumorigenesis suppressor Pdcd4 down-regulates mitogen-activated protein kinase kinase kinase kinase 1 expression to suppress colon carcinoma cell invasion. Mol Cell Biol 2006;26(4):1297-306.

33. Scoumanne A, Zhang J, Chen X. PRMT5 is required for cell-cycle progression and p53 tumor suppressor function. Nucleic Acids Res 2009;37(15):4965-76.

34. Ren J, Wang Y, Liang Y, Zhang Y, Bao S, Xu Z. Methylation of ribosomal protein S10 by protein-arginine methyltransferase 5 regulates ribosome biogenesis. J Biol Chem 2010;285(17):12695-705.

35. Pal S, Yun R, Datta A, *et al.* mSin3A/histone deacetylase 2- and PRMT5-containing Brg1 complex is involved in transcriptional repression of the Myc target gene cad. Mol Cell Biol 2003;23(21):7475-87.

36. Meister G, Fischer U. Assisted RNP assembly: SMN and PRMT5 complexes cooperate in the formation of spliceosomal UsnRNPs. Embo J 2002;21(21):5853-63.

37. Jansson M, Durant ST, Cho EC, *et al.* Arginine methylation regulates the p53 response. Nat Cell Biol 2008;10(12):1431-9.

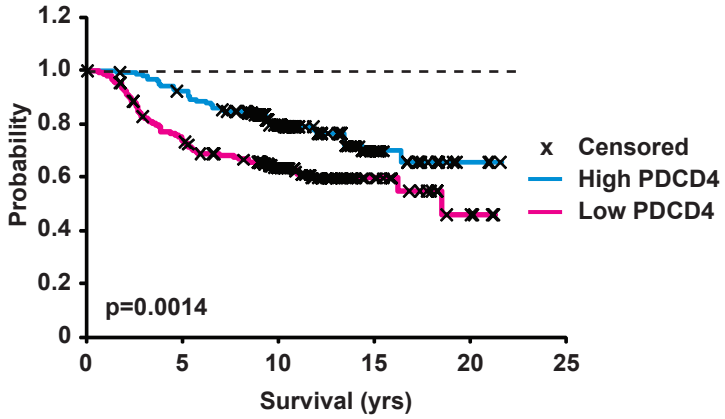

Figure 3.1 Analysis of PDCD4 as a prognostic marker in breast cancer. Microarray data from 295 tumors less than 5 cm collected from patients younger than 55 and stored at the Netherlands Cancer Institute (13) was analyzed with respect to PDCD4 expression. Patients with tumors expressing PDCD4 mRNA above the median ("high", shown in blue) had a significantly higher probability of survival than the other patients ("low", shown in pink).

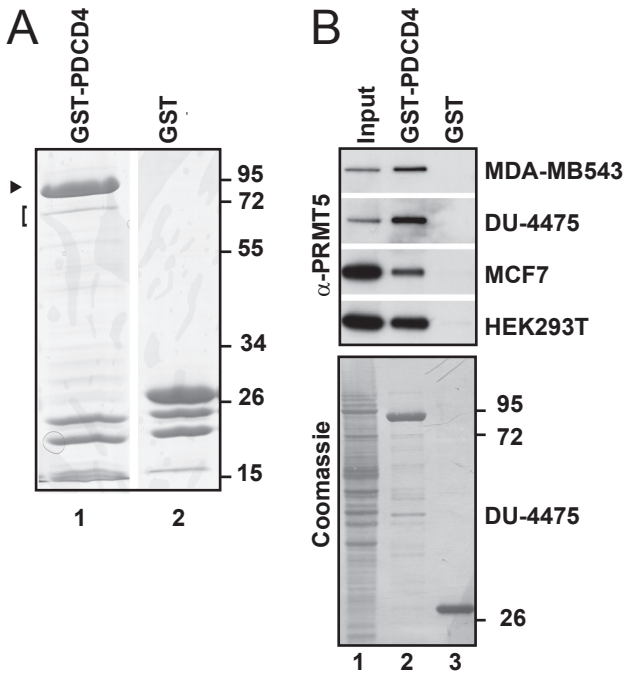

Figure 3.2 PRMT5 is a protein partner of PDCD4. (A) Coomassie-stained gel of proteins associated with GST-PDCD4 (lane 1; GST-PDCD4 indicated with arrowhead), compared to background levels of proteins that associate with GST (lane 2), following incubation with *Xenopus laevis* egg extract. The gel was sliced (bracket), to recover a 72 kD band. Analysis by mass spectrometry identified PRMT5 in this gel slice. **(B)** Upper panel: immunoblot to detect PRMT5 among proteins associated with GST-PDCD4 (lane 2) or GST (lane 3), following incubation with lysates from the human cell lines indicated. 8.5-17% of input material is shown in lane 1. Lower panel: Coomassie stain of western blot (DU-4475 samples), showing recovery of GST-tagged proteins (lanes 2, 3).

A

R.SYTIG.L, K.VYAVEK.N, K.QPISLR.E, K.GFPVLSK.V, K.GFPVLTK.V, K.LYNEVR.A, K.TDSEVSR.I, K.LYNEVR.A, R.WLGEPIK.A,
R.SDLLLSGR.D, R.VPLLAHNDLR.D, R.SDLLLSGR.D, K.SRPGPQTR.S, R.GPLVNASLR.A, K.IKVYAVEK.N, R.EFYKEPAK.S,
K.QEDNSNLSR.L, R.VPLMAPNDLR.D, K.REFYKEPAK.S, K.YSQYQQAVYK.C, R.TWIWWHNFR.S, K.NPNAVITLEGWR.Y
K.AAFLPTSIFLTNKK.G, K.AAFLPTSLFLTNKK.G, K.ETNIQVLMVLGAGR.G, K.LSDWIQTDSEVPQTR.K, K.DKDPEAQFEMPYVVR.L
R.VALAIEVGADLPSGHVIDR.W, R.YEEWGSQVTVVSGDMR.E, K.DRDPEAQFEMPYVVR.L, K.IALAIEIGADLPSGHVIDR.W,
R.EKDRDPEAQFEMPYVVR.L, R.EKDKDPEAQFEMPYVVR.L, K.EDGVSIPGEYTSFLAPISSSK.L, K.DDGVSIPGEYTSYLAPISSSK.L
R.LLINHILSGHHSTMFWMR.V, R.VPEEEKETNIQILMVLGAGR.G, R.VPEEEKETNIQVLMVLGAGR.G,
K.GYEDYLQSPLQPLMDNLESQTYEVFEKDPVK.Y

B

```
xPRMT5    1 MAAGGGGRVSSGRDLGCVTEVADTLGAVAKQGFDFLCMPIFHPRFKREFYKEPAKSRPGP
xHsl7     1 MAAGDGGRVSSGRDVACVTEVADTLGAMANQGFDFLCMPIFHPRFKREFYKEPAKSRPGP
            **** *********  *********** * ******************************

xPRMT5   61 QTRSDLLLSGRDWNTLIVGKLSDWIQTDSEVPQTRKTSEAALQQELHFSAYLGLPAFLIP
xHsl7    61 QTRSDLLLSGRDWNTLIVGKLSDWIKTDSEVSRIRKTSEAAMQQELNFSAYLGLPAFLIP
            ************************* *****   ******* **** **************

xPRMT5  121 LKQEDNSNLSRLLINHILSGHHSTMFWMRVPLLAHNDLRDDLIENEPFSPSEEDNSGEER
xHsl7   121 LKQEDNSNLSRLLINHIHVGHHSTMFWMRVPLMAPNDLRDDLIENEPISLSEEDNSGEER
            *****************  ************* * ************ * **********

xPRMT5  181 TWIWWHNFRSLCDYNKRVALAIEVGADLPSGHVIDRWLGEPIKAAFLPTSLFLTNKKGFP
xHsl7   181 TWIWWHNFRSLCDYNKKIALAIEIGADLPSGHVIDRWLGEPIKAAFLPTSIFLTNKKGFP
            ****************  ***** ************************* *********

xPRMT5  241 VLSKVHQRLIFRLFKLEVQFVISGAHHHSEKDFCSYLQYLEYLSQNRPPPNAYEMFAKGY
xHsl7   241 VLTKVHQRLIFKLFKLEVQFVISGSHHHSEKDLCSYLQYLEYLSQNSPPPNAYEMFAKGY
            ** ******** ************ ******* ************* *************

xPRMT5  301 EDYLQSPLQPLMDNLESQTYEVFEKDPVKYSQYQQAVYKCLLDRVPEEEKETNIQVLMVL
xHsl7   301 EDYLQSPLQPLMDNLESQTYEVFEKDPVKYSQYQQAVYKCLLDRVPEEEKETNIQILMVL
            ********************************************************* ****

xPRMT5  361 GAGRGPLVNASLRAAKQAERKIKVYAVEKNPNAVITLEGWRYEEWGSQVTVVSGDMREWK
xHsl7   361 GAGRGPLVNASLRAAKQAERKIKVYAVEKNPNAVITLEGWRYEEWGSQVTVVSGDMREWK
            ************************************************************


xPRMT5  421 APEKADIIVSELLGSFGDNELSPECLDGAQHFLKEDGVSIPGEYTSFLAPISSSKLYNEV
xHsl7   421 APEKADIIVSELLGSFGDNELSPECLDGAQHFLKDDGVSIPGEYTSYLAPISSSKLYNEV
            ********************************** *********** *************

xPRMT5  481 RACREKDKDPEAQFEMPYVVRLHNFHQLSDPLPCFTFHHPNKDAVIDNNRYCCLQYRVDL
xHsl7   481 RACREKDRDPEAQFEMPYVVRLHNFHQLSDPLPCFTFHHPNKDDVIDNNRYCCLQYRVDL
            ******* ************************************ ****************

xPRMT5  541 NTVLHGFAGYFSTVLYKDVTLSICPESHSPGMFSWFPILFPIKQPISLREGDTVCVRFWR
xHsl7   541 NTVLHGFAGYFNTVLYKDVTLSICPESHSPGMFSWFPILFPIKQPIPMREGDTVCVRFWR
            *********** ********************************  ************

xPRMT5  601 CNNGKKVWYEWAVTSPVCSAIHNPTGRSYTIGL
xHsl7   601 CNNGKKVWYEWAVTSPVCSAIHNPTGRSYTIGL
            *********************************
```

Figure 3.3 72kD protein isolated with GST-PDCD4 from *Xenopus* egg extract corresponds to the two alleles of PRMT5 found in *Xenopus*. (A) List of peptides recovered from excised gel slice that correspond to *Xenopus* PRMT5. **(B)** Alignment of identified peptides within amino acid sequence of the two alleles of PRMT5 found in *Xenopus* laevis. At top is theoretical protein xPRMT5 (Q2VPH9) with alignments in yellow and below is xHsl7 (Q6NUA1) with alignments in red. Green highlights specific sequences recovered that are unique to each allele, confirming the expression (and binding) of both proteins. This demonstrates that the theoretical protein xPRMT5 is expressed.

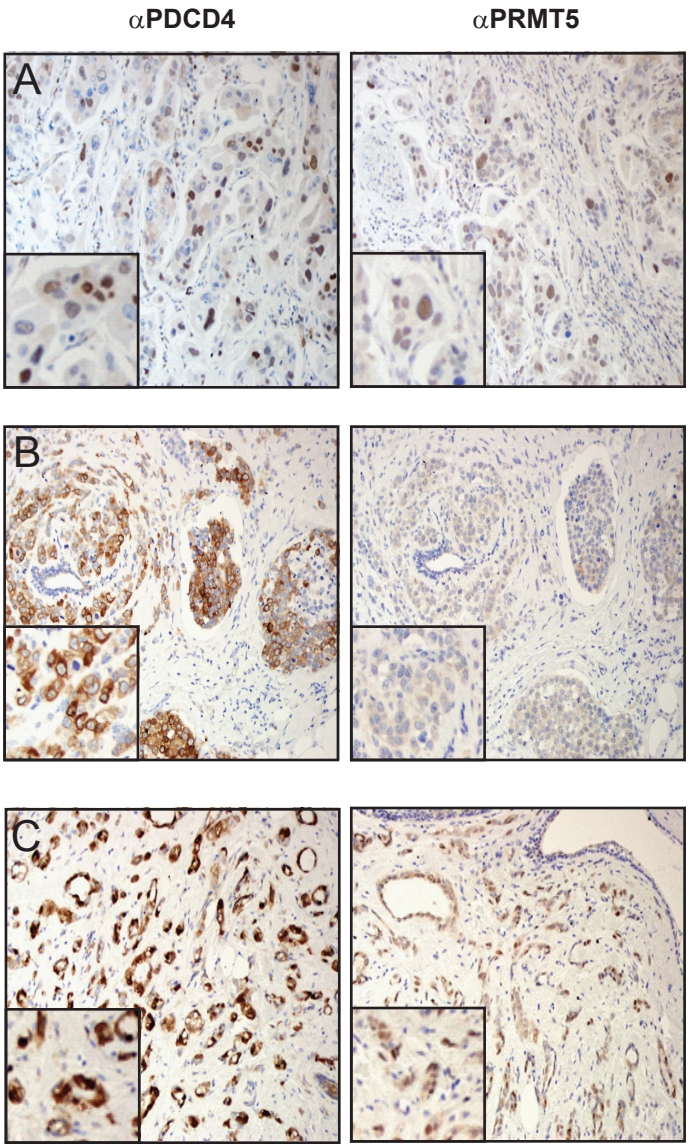

Figure 3.4. Immunohistochemical survey of tumor biopsies. **(A)** Invasive ductal carcinoma that is poorly differentiated with positive nuclear staining for both PDCD4 and PRMT5. **(B)** Invasive ductal carcinoma with lymphovascular invasion. PDCD4: Membranous positive staining in carcinoma and lymphovascular invasion. PRMT5: weak positive cytoplasmic blush. **(C)** Invasive ductal carcinoma. Both PDCD4 and PRMT5 display positive nuclear and cytoplasmic staining.

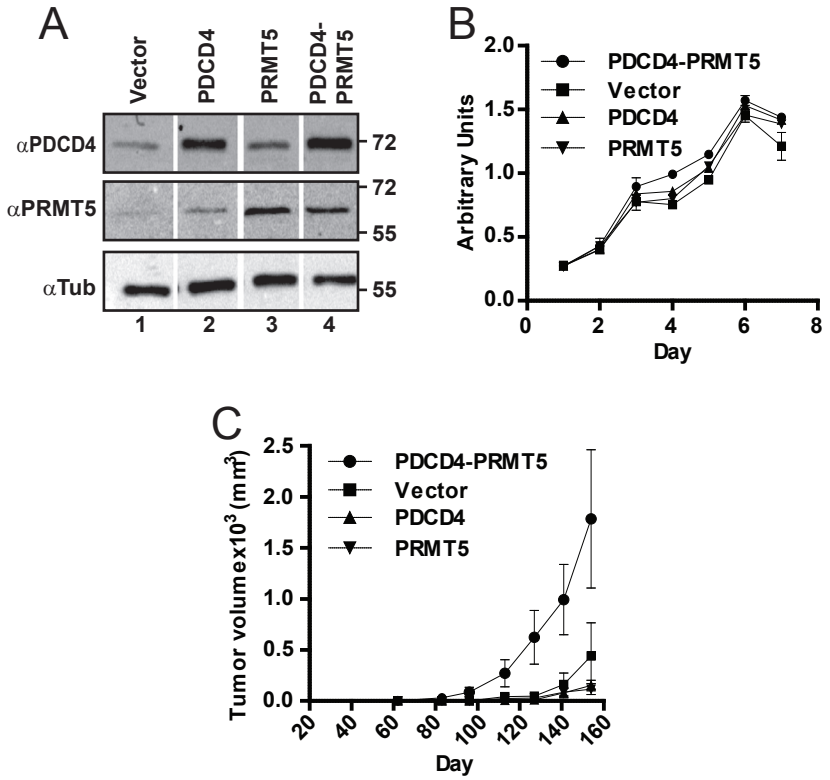

Figure 3.5 Co-expression of PDCD4 and PRMT5 enhances tumor growth in xenograft model. (A) MCF7e cells expressing PDCD4 and PRMT5 or empty constructs, as indicated, were assessed by immunoblot. Tubulin levels were tracked as a loading control. **(B)** Cell growth in tissue culture was measured for 7 days by a colorimetric assay tracking the cleavage of WST substrate (BioVision) by cellular mitochondrial dehydrogenase. **(C)** The cell panel was transplanted orthotopically and tumor volume was monitored over a 22 week period.

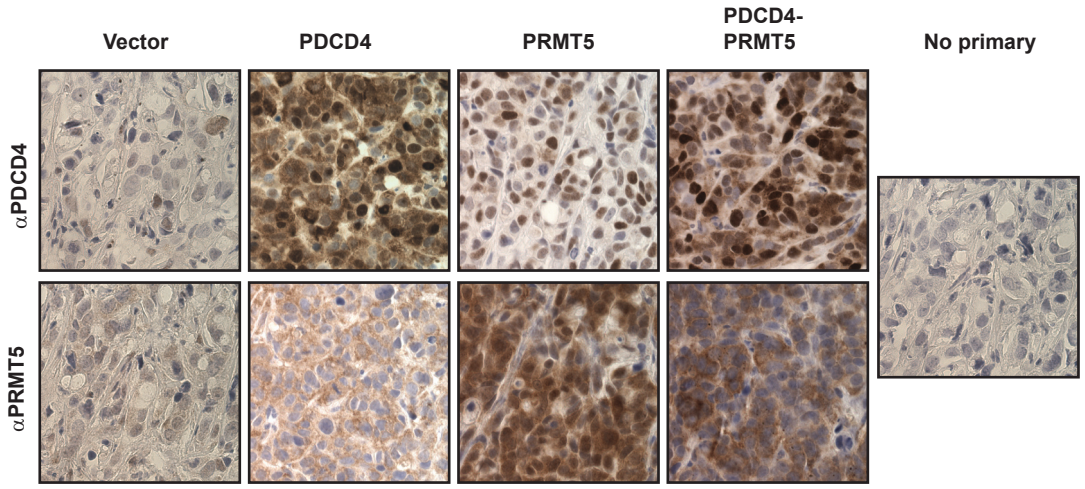

Figure 3.6 Immunohistochemical evaluation of harvested tumors. Immunohistochemical analysis of PDCD4 (antibody 1:5000) and PRMT5 (antibody 1:1000) expression in tumors recovered from mice (60x magnification). Expression constructs for each sample are listed at top. Panel at right is the no primary control.

Figure 3.7 PDCD4 can be methylated in its N-terminal domain and is a target of PRMT5. **(A)** Schematic of PDCD4, with arginine rich (RR) region and MA3 regions indicated. Amino acids 1-156 are shown, with the RR region underlined. **(B)** Upper panel: autoradiograph of reactions containing purified GST-PDCD4 (lane 1) or domain fragments (lanes 2, 3) along with HEK293 cell lysate and ^{3}H-SAM. Middle panel: immunoblot for tubulin, tracking lysate level in methylation reactions. Bottom panel: total protein in each reaction detected by Coomassie staining; * indicate recombinant protein present in each reaction. **(C)** Arg110 and/or Arg73 were mutated to lysines in full length PDCD4 or the N-terminal region (aa1-156), as indicated. These proteins, and wild-type (WT) counterparts, were incubated with cell lysates supplemented with ^{3}H-SAM. Top panel: samples were subjected to PAGE followed by autoradiography. Middle panel: immunoblot to detect GST fusion proteins. Lower panel: immunoblot for tubulin, to track levels of cell lysate used. **(D)** V5-PRMT5, the catalytically dead mutant (V5-PRMT5$_{cd}$), or control vector were transiently expressed and then cell lysates subjected to immunoprecipitation with anti-V5 antibody. Left panels are immunoblots of precipitated material using PRMT5 antibody (upper panel) or V5 antibody (lower panel). GST-PDCD4 (lanes 4-6) or GST-PDCD4$_{R110K}$ (lanes 7-9) were incubated with immunoprecipitates shown in lanes 1-3 along with ^{3}H-SAM. Methylation was monitored by autoradiography (upper panel). The presence of recombinant PDCD4 in all reactions was confirmed by immunoblot with anti-GST (lower panel).

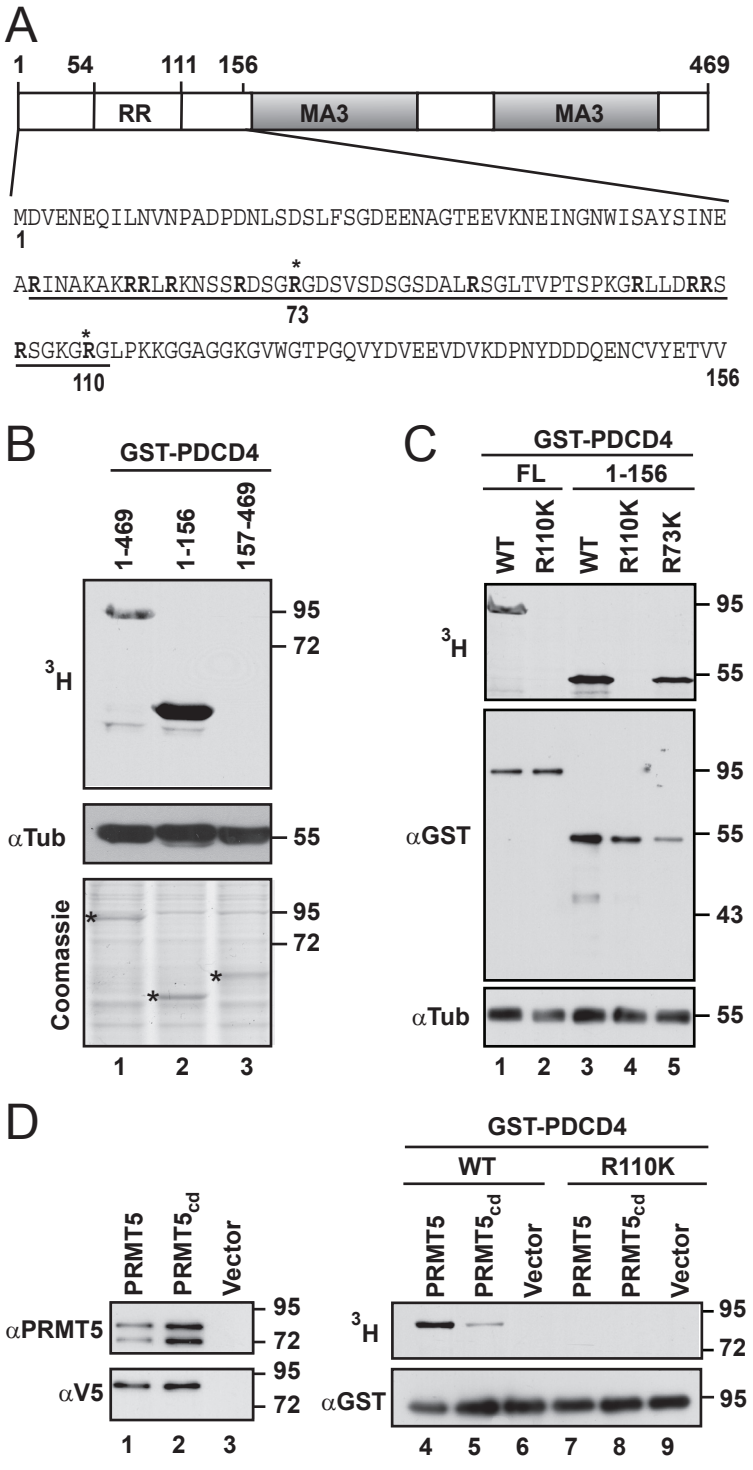
A
1
54
111
156
469
RR
MA3
MA3
MDVENEQILNVNPADPDNLSDSLFSGDEENAGTEEVKNEINGNWISAYSINE
1
ARINAKAKRRLRKNSSRDSGRGDSVSDSGSDALRSGLTVPTSPKGRLLDRRS
73
RSGKGRGLPKKGGAGGKGVWGTPGQVYDVEEVDVKDPNYDDDQENCVYETVV
110
156
B
GST-PDCD4
1-469
1-156
157-469
3H
95
72
αTub
55
Coomassie
95
72
1 2 3
C
GST-PDCD4
FL
1-156
WT
R110K
WT
R110K
R73K
3H
95
55
αGST
95
55
43
αTub
55
1 2 3 4 5
D
PRMT5
PRMT5cd
Vector
αPRMT5
95
72
αV5
95
72
1 2 3
GST-PDCD4
WT
R110K
PRMT5
PRMT5cd
Vector
PRMT5
PRMT5cd
Vector
3H
95
72
αGST
95
4 5 6 7 8 9

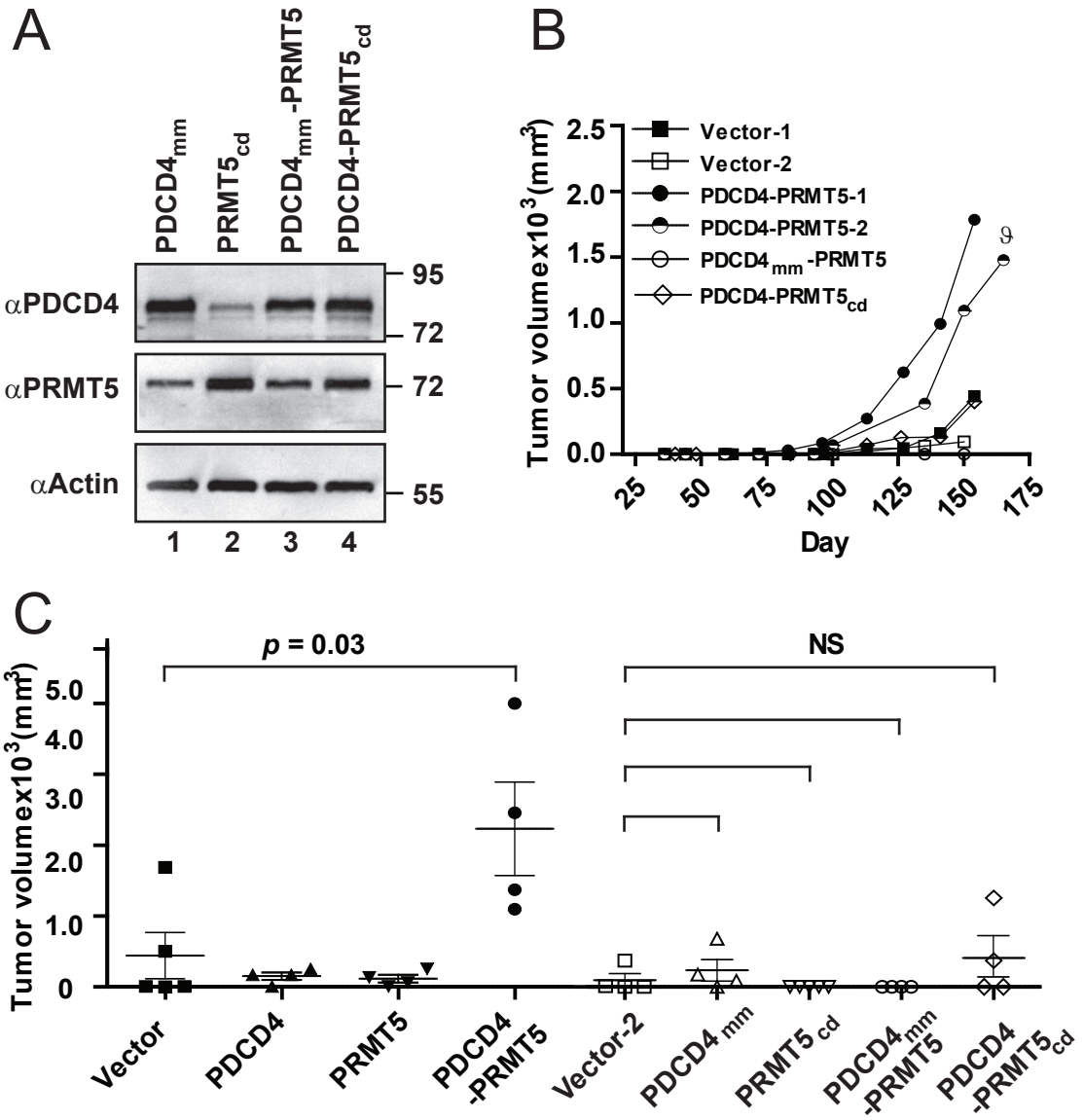

Figure 3.8 The catalytic activity of PRMT5 and arginine 110 of PDCD4 are necessary for synergistic tumor cell growth. (A) Immunoblot of MCF7e cells expressing R110K (methyl mutant) $PDCD4_{mm}$ and $PRMT5_{cd}$ with wild type PRMT5 or PDCD4 as indicated. **(B)** Tumor growth of $PDCD4_{mm}$-PRMT5 and PDCD4-$PRMT5_{cd}$ cell-lines is graphed along with repeats (-2) of vector only and PDCD4-PRMT5. Data from the first tumor growth experiment with these two cell-lines (Figure 3) is shown for comparison. Vector-2 and PDCD4-PRMT5-2 tumors were generated by injection of cells into both cleared inguinal fat pads of 2 mice (n=4 tumors for each cell line). One mouse injected with the PDCD4-PRMT5 cell line died at week 4 causing an n=2 tumors (9). These tumors tracked well with previous PDCD4-PRMT5 tumor growth rate, although the number was too low for statistical significance. **(C)** Size of tumors from both experiments at 22 weeks.

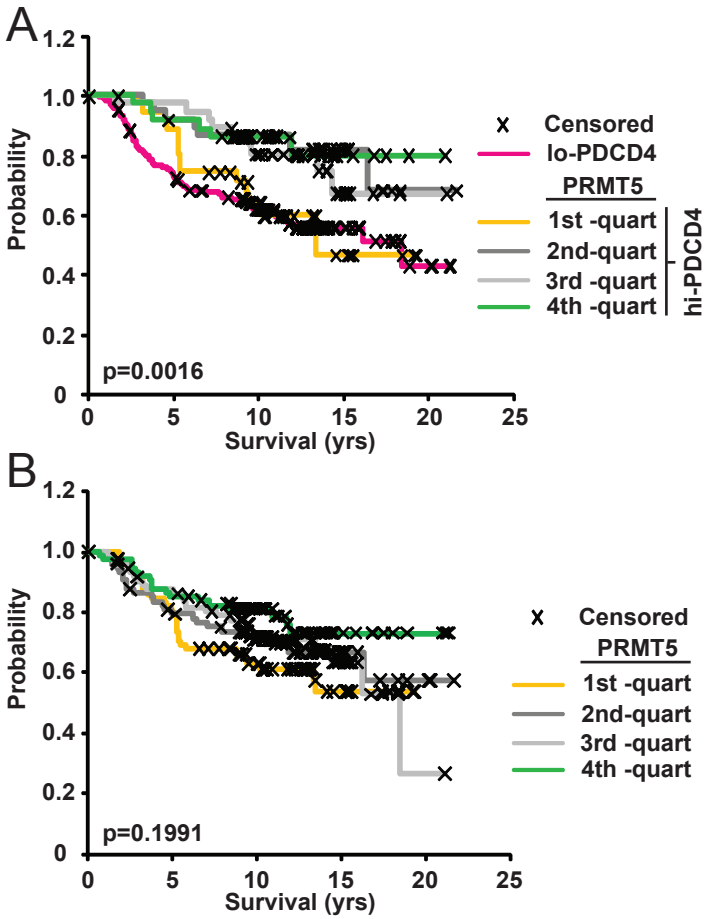

Figure 3.9 Expression of PRMT5, in conjunction with PDCD4, improves prediction of survival. mRNA expression data from the Netherlands Cancer Institute dataset (13) was analyzed with respect to both PDCD4 and PRMT5. **(A)** The "high" PDCD4 cohort of patients (see Figure 1) were stratified into quartiles based on PRMT5 expression, with the first quartile containing the highest levels of PRMT5 expression. **(B)** Patients from the entire dataset were stratified into quartiles based on PRMT5 expression alone.

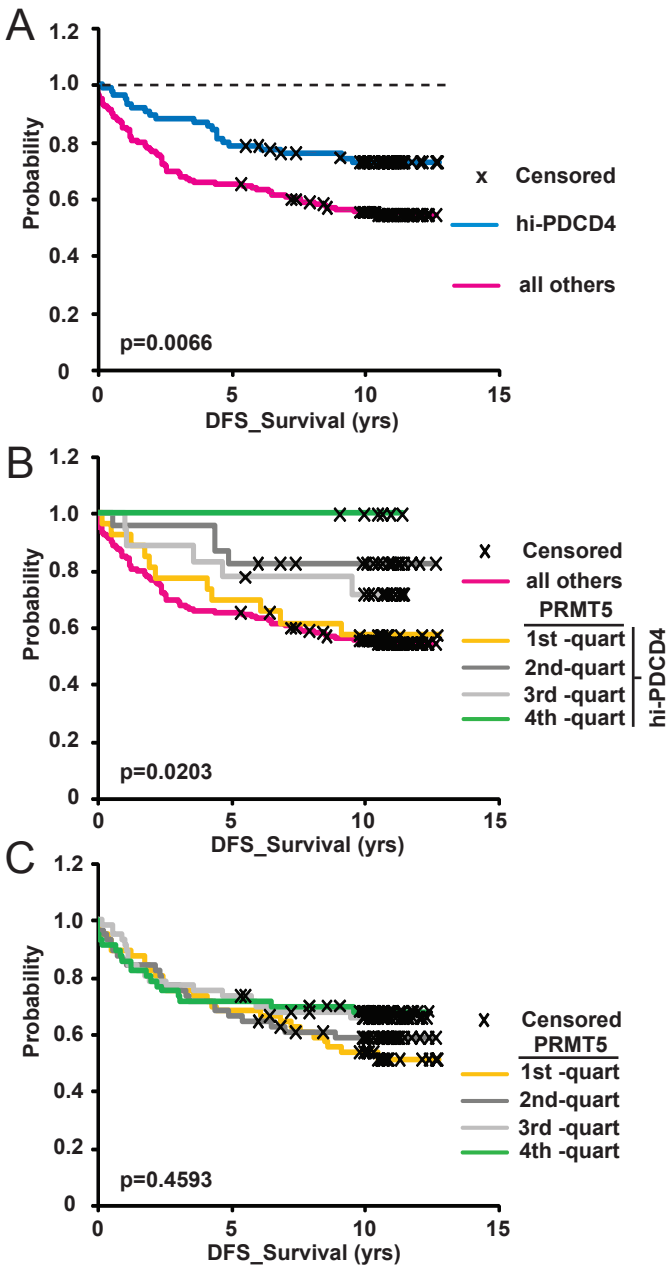

Figure 3.10 An independent dataset confirms the prognostic power of a combined PRMT5/PDCD4 expression signature. Analysis of a second dataset of mRNA collected from the tumors of 224 patients from Singapore and Sweden (1) selected based on availability of clinical follow-up data and PDCD4 and PRMT5 expression. **(A)** This dataset was stratified into thirds based on PDCD4 expression levels. Patients in the "high" expression cohort (top one-third) had greater probability of disease-free survival compared to all others. **(B)** The "high" PDCD4 cohort was further stratified into quartiles based on PRMT5 expression; less PRMT5 expression corresponded to increased probability of disease-free survival. **(C)** Patients stratified into quartiles based on tumor expression of PRMT5 alone did not show significant differences in survival.

CHAPTER 4

PDCD4-EIF4A MECHANISM IN TRANSLATION SUPPRESSION

4.1 Abstract

The ability of eIF4A to function as an RNA helicase is blocked when bound to PDCD4 resulting in the inhibition of efficient translation of mRNAs with structured 5'UTRs. The ability of PDCD4 to interact with eIF4A is dependent on the MA3 domain that is also found in other eIF4A binding proteins such as eIF4G. Curiously, PDCD4 contains two of these MA3 domains in tandem and it is unclear whether both MA3 domains are necessary for eIF4A binding or if the most distal C-terminal domain is sufficient. The studies described here demonstrate that both MA3 domains of PDCD4 are necessary for efficient, direct binding to eIF4AII. Furthermore, using RNA electrophoretic mobility shift assays, I found that PDCD4 inhibits the ability of eIF4AII to interact with RNA thereby inhibiting its RNA helicase activity. This experimental strategy also allowed the RNA binding activity of PDCD4 to be tracked and revealed that eIF4AII inhibits this function of PDCD4.

4.2 Introduction

PDCD4 was first characterized in a cancer context using a mouse epidermal cell model (1, 2). Exogenous expression of PDCD4 inhibited transformation and also blocked tumor forming cells from efficient anchorage independent cell growth (2-4). These tumor suppressor properties were found to be dependent on the ability of PDCD4 to bind the translation initiation factor 4A (eIF4A) (3). In conjunction with suppressing tumor phenotypes, PDCD4 also downregulated translation of mRNAs that contained structure in the 5'untranslated region (5'UTR) by blocking the ability of eIF4AII to function as a RNA helicase. The MA3 domain positioned closest to the C-terminus (the cMA3 domain) was found to be sufficient for translation inhibition in one study (5), while individual truncation mutations in either MA3 domain caused loss of translation inhibition in a second study (6). This discrepancy prompted us to further characterize the mechanism required for PDCD4-mediated disruption of eIF4A activity.

eIF4A is a component of a larger complex, eIF4F, that is instrumental in recruiting the ribosome to the start codon for translation initiation (7). eIF4F is composed of three proteins, eIF4A, eIF4E and eIF4G. eIF4E binds to the mRNA 5'methyl cap, bringing the eIF4F complex to the 5'UTR of transcripts. eIF4G is a large scaffold protein that links eIF4A to eIF4E. In addition to holding together the eIF4F complex, eIF4G also links this complex to the 40S ribosomal subunit (7). eIF4A has two isoforms in mammalian cells, eIF4AI and eIF4AII, that share 89% identity. They are differentially expressed in various tissues and can each rescue the depletion of the other (8, 9). eIF4AI or eIF4AII are often referred to as "eIF4A" when the known functions of both is being described. eIF4A unwinds secondary mRNA structures within the 5'UTR

by a process of conformational change catalyzed by ATP hydrolysis. When ATP is bound, eIF4A binds tightly to RNA due to a high affinity RNA binding conformation. When ATP is hydrolyzed to ADP, eIF4A changes shape and releases RNA allowing for processive movement along the 5'UTR (10). PDCD4 binds and blocks eIF4A RNA helicase function causing inefficient translation of mRNAs that contain structured 5'UTRs (6), but it was unclear what mechanism PDCD4 uses to inhibit eIF4A helicase activity.

More recently, eIF4A was recognized to be closely related to a different RNA helicase, eIF4AIII, that is a core component of the exon junction complex (11-13). Unlike eIF4A, eIF4AIII is not known to utilize its RNA helicase activity. Instead, eIF4AIII is an anchor molecule that clamps down on RNA in its role as a core member of the exon junction complex. This occurs through inhibition of eIF4AIII hydrolysis of ATP, locking it into a high affinity RNA binding state (14-16). This inhibition is mediated by the EJC core components MAGOH and Y14 when they bind to eIF4AIII (17). In an analogous manor, PDCD4 could bind to eIF4A and inhibit ATP hydrolysis thereby blocking RNA helicase activity. Alternatively, PDCD4 could interact with eIF4A in a way that interferes with RNA binding, disrupting efficient translation initiation. To distinguish between these possibilities, I tested the ability of eIF4AII to bind to RNA in the presence of PDCD4 and ATP or the non-hydrolyzable ATP analogue AMP-PNP. I found that PDCD4 inhibits the ability of eIF4AII to interact with RNA thereby blocking its ability to function as an RNA helicase. Furthermore, I found that both MA3 domains are necessary for efficient direct interactions between PDCD4 and eIF4A *in vitro*. Finally, I also monitored the effect of eIF4A on the ability of PDCD4 to

bind RNA. These results overlapped with those published by a different group while experiments were in progress (18). While the approaches here followed a different strategy (see Discussion), the conclusions were similar and so we changed the emphasis of the project to what is described in Chapter 3.

4.3 Experimental Procedures

4.3.1 Constructs

The PDCD4 open reading frame was purchased from Open Biosystems and eIF4AII open reading frame was cloned out of a human cDNA library. PDCD4 and eIF4AII were introduced into pDONR221 vectors by BP reactions (Invitrogen). pGEX4T was made gateway compatible using RFB oligos (Invitrogen) and eIF4AII was cloned into this vector by LR reaction to produce GST-recombinant proteins. To produce His-recombinant proteins, PDCD4 was cloned into pDEST-EXP1 by a LR reaction.

4.3.2 Recombinant protein purification

Recombinant proteins were expressed and purified as in section 2.3.2.

4.3.3 RNA gel purification

RNA oligos were run on a 12% acrylamide urea gel and the gel region where RNA migrates was excised (RNA migration was previously detected by ethidium bromide staining and successive gels were assessed by loading dye migration). Excised gel pieces were crushed using a pipet tip and RNA was allowed to elute from gel in 0.5 M ammonium acetate, 1 mM EDTA for 24 hours at room temperature. Gel fragments

were pelleted by low speed centrifugation and the supernatant was recovered. The RNA was precipitated out of solution with the addition of glycogen (Ambion) and EtOH and was incubated at -80°C for 15 minutes. RNA was pelleted by centrifugation at 20,000 x G for 30 minutes at 4°C. Pellets were washed with 80% EtOH and resuspended in DEPC treated H_2O.

4.3.4 RNA probe labeling

The 25 nucleotide hnRNP-A1 RNA binding site oligo was synthesized and gel purified. One nMol of The RNA oligo was incubated with T4 polynucleotide kinase in the presence of γ ^{32}P-ATP in kinase buffer (50 mM Tris pH 7.5, 10 mM $MgCl_2$, 50 mM DTT) at 37°C for 1 hour. The labeling reaction was stopped by the the addition of EDTA to a final concentration of 1 mM. RNA was precipitated with the addition of NaOAc, glycogen (Ambion) and EtOH. Pellets were washed with 80% EtOH. End labeling was checked by autoradiograph by running a portion of the sample on a denaturing urea gel and dehydrating onto Whatman paper.

4.3.5 Gel shift assays

Purified proteins were diluted 1:15 (approximately to 0.05 to 0.1 µg/µl) into gel shift salt buffer (25 mM HEPES pH 7.5, 100 mM KCl). Approximately 0.1-0.4 µg of protein was added to 100 pMol of labeled RNA and diluted in 20 µl gel shift buffer (100 mM KCl, 25 mM HEPES pH 7.5, 0.01% Triton X-100, 5% glycerol, 6 mM MgAOc, 0.3 µg/µl BSA, 1 x protease inhibitors (Roche), 1 x RNAse out (Invitrogen), 0.2 µg/ul heparin, 3 mM DTT, 2 mM AMP-PNP). Reactions were incubated 20 minutes at 30°C.

Reactions were terminated with the addition of native loading buffer. Samples were run on 6% acrylamide native gels and dehydrated onto Whatman paper. Gels were than subjected to autoradiograph.

4.4 Results

4.4.1 Both MA3 domains of PDCD4 are necessary for efficient eIF4A binding

To determine exactly what domains of PDCD4 were necessary for efficient eIF4A binding, I engineered subfragments of PDCD4 (specifically, 2MA3 domain, the nMA3 domain and the cMA3 domain, Figure 4.1) and expressed them as recombinant His-tagged proteins. eIF4AII was expressed as a recombinant GST-tagged protein and purified. GST-eIF4AII and the His-tagged PDCD4 domains were incubated together. A glutathione matrix was used to recover GST-eIF4AII and any interacting proteins were then separated by PAGE and immunoblotted with antibody directed against the 6-His tag. Full length PDCD4 and the 2MA3 domain interacted with eIF4AII (Figure 4.2A, lane 3 and Figure 4.2B, lane 1 and 3). The nMA3 and cMA3 domains did not interact with eIF4A (Figure 4.2A, lanes 1-2 and Figure 4.2B, lane 1). His-tagged recombinant proteins did not interact significantly with GST alone (Figure 4.2A and B, lanes 4-6).

4.4.2 PDCD4 blocks the ability of eIF4A to interact with RNA

To understand mechanistically how PDCD4 blocks eIF4AII RNA helicase ability, I first purified both proteins (Figure 4.3 lanes 10-11). To establish that recombinant purified GST-eIF4AII retained RNA binding and ability to hydrolyze ATP, GST-eIF4AII

was incubated with radiolabeled single-stranded RNA and ATP or the nonhydrolyzable analogue AMP-PNP. This mixture was run on a non-denaturing acrylamide gel to separate free RNA from eIF4AII shifted species. As expected, GST-eIF4AII efficiently shifted RNA in the presence of AMP-PNP but not with ATP (Figure 4.4, lanes 3-4). Inefficient RNA shifting in the presence of ATP indicates that GST-eIF4AII hydrolyzes ATP to ADP leaving eIF4AII in a low affinity RNA binding state. Binding to AMP-PNP locked eIF4A into a high affinity RNA binding state allowing robust RNA:protein interaction, seen as a shifted species in this assay. The specificity of the effect was confirmed by running a similar set of conditions with a control protein, hnRNP-A1. The ability of hnRNP-A1 to bind RNA was not perturbed by the addition of either ATP or AMP-PNP (Figure 4.4 lanes 5-6).

To determine the effect on eIF4AII RNA binding in the presence of PDCD4, GST-eIF4AII was incubated with radiolabeled RNA and AMP-PNP with increasing amounts of His-PDCD4. The addition of PDCD4 inhibited GST-eIF4AII from interacting with RNA (Figure 4.5, lanes 2-5). PDCD4 also has intrinsic RNA binding ability and shifts RNA (Figure 4.5, lanes 3-5 and 10). The lack of a super-shifted RNA species running at a different level than GST-eIF4AII indicates that a ternary complex of eIF4AII-PDCD4-RNA does not occur and, therefore, both PDCD4 and eIF4AII may block each other's ability to bind RNA. Addition of increasing amounts of His-PDCD4 did not affect the ability of hnRNP-A1 to bind to RNA, showing that the inhibition of eIF4AII is specific (Figure 4.5, lanes 6-9).

To test if eIF4AII blocks the ability of PDCD4 to interact with RNA, increasing amounts of GST-eIF4AII were added to PDCD4 and radiolabeled RNA. Separation by a

nondenaturing gel revealed that His-PDCD4 binding is inhibited with the addition of GST-eIF4AII (Figure 4.6 lanes 2-5). One caveat to this experiment is that there was RNA degradation with the addition of GST-eIF4AII with His-PDCD4, which may have skewed this result. This is very likely the case in lane 5 where greater addition of GST-eIF4AII does not correspond to a larger shifted band at the eIF4AII level indicating a reduced RNAs availability. Nevertheless, lanes 3 and 4 appear to have intact RNA and shows a decrease in PDCD4 shifted species. Together with a lack of super-shifted RNA species from Figure 4.4, this indicates that the ability of PDCD4 to bind RNA is inhibited by an interaction with eIF4AII. Had I pursued this line of investigation, I would have purified the recombinant protein to a greater extent in order to eliminate the RNase and clarify the result.

4.5 Discussion

The interaction of PDCD4 with eIF4A is thought to be critical for PDCD4 tumor suppressor function (3, 6). Determining how this interaction occurs, and how it modulates eIF4A function, is important in defining the effects of PDCD4 on oncogenesis. I have shown here that both MA3 domains within PDCD4 are necessary for efficient direct protein interaction with eIF4A. This confirms a study that was published while I was performing these experiments (18). In light of experiments where the transfection of the single cMA3 domain inhibited translation (5), however, the results of *in vitro* binding described here and by Suzuki *et al* (18) are surprising since individual MA3 domains have low affinity for eIF4A. This apparent discrepancy could result from stabilization of the cMA3 domain with eIF4A by other factors in the cell or by very high

exogenous expression forcing this interaction. Alternatively, the cMA3 domain may have translation suppression properties apart from eIF4A. Both scenarios need further investigation.

These seemingly contradictory results from *in vitro* and cell-based assays highlight that alternative roles for PDCD4 in cancer and translation regulation may occur *in vivo*. For example, post-translational modifications of PDCD4 or eIF4A may cause this complex to stimulate translation initiation rather than inhibiting it. We have shown that the co-expression of PDCD4 with PRMT5 causes accelerated tumors growth in an orthotopic model (see Chapter 3). This indicates that under these *in vivo* conditions PDCD4 becomes oncogenic. Whether this change is due to a switch from being an inhibitor to an enhancer of translation enhancer would be an interesting problem to explore.

The ability of PDCD4 to block eIF4A RNA helicase activity was also reported, when my experiments were in process, to occur through inhibiting the RNA binding activity of eIF4A. Suzuki *et al.* took a different strategy, namely, an N-terminal truncation mutant of PDCD4 (missing the putative PDCD4 RNA binding site) was shown to displace U6 RNA from the N-terminal fragment of eIF4A by NMR experiments (18). I confirmed and extended these result by using full length PDCD4 and full length eIF4A in RNA gel shift analysis. Furthermore, I have found that eIF4A may inhibit PDCD4 RNA binding. It has yet to be determined what role RNA binding plays in PDCD4 cellular function but it is of increasing interest due to a recent report that found PDCD4 binds to ribosomal subunits (19).

4.6 References

1. Cmarik JL, Min H, Hegamyer G, *et al.* Differentially expressed protein Pdcd4 inhibits tumor promoter-induced neoplastic transformation. Proc Natl Acad Sci U S A 1999;96(24):14037-42.

2. Yang HS, Jansen AP, Nair R, *et al.* A novel transformation suppressor, Pdcd4, inhibits AP-1 transactivation but not NF-kappaB or ODC transactivation. Oncogene 2001;20(6):669-76.

3. Yang HS, Jansen AP, Komar AA, *et al.* The transformation suppressor Pdcd4 is a novel eukaryotic translation initiation factor 4A binding protein that inhibits translation. Mol Cell Biol 2003;23(1):26-37.

4. Yang HS, Knies JL, Stark C, Colburn NH. Pdcd4 suppresses tumor phenotype in JB6 cells by inhibiting AP-1 transactivation. Oncogene 2003;22(24):3712-20.

5. LaRonde-LeBlanc N, Santhanam AN, Baker AR, Wlodawer A, Colburn NH. Structural basis for inhibition of translation by the tumor suppressor Pdcd4. Mol Cell Biol 2007;27(1):147-56.

6. Yang HS, Cho MH, Zakowicz H, Hegamyer G, Sonenberg N, Colburn NH. A novel function of the MA-3 domains in transformation and translation suppressor Pdcd4 is essential for its binding to eukaryotic translation initiation factor 4A. Mol Cell Biol 2004;24(9):3894-906.

7. Sonenberg N, Hinnebusch AG. Regulation of translation initiation in eukaryotes: mechanisms and biological targets. Cell 2009;136(4):731-45.

8. Nielsen PJ, Trachsel H. The mouse protein synthesis initiation factor 4A gene family includes two related functional genes which are differentially expressed. Embo J 1988;7(7):2097-105.

9. Yoder-Hill J, Pause A, Sonenberg N, Merrick WC. The p46 subunit of eukaryotic initiation factor (eIF)-4F exchanges with eIF-4A. J Biol Chem 1993;268(8):5566-73.

10. Caruthers JM, Johnson ER, McKay DB. Crystal structure of yeast initiation factor 4A, a DEAD-box RNA helicase. Proc Natl Acad Sci U S A 2000;97(24):13080-5.

11. Chan CC, Dostie J, Diem MD, *et al.* eIF4A3 is a novel component of the exon junction complex. Rna 2004;10(2):200-9.

12. Ferraiuolo MA, Lee CS, Ler LW, *et al.* A nuclear translation-like factor eIF4AIII is recruited to the mRNA during splicing and functions in nonsense-mediated decay. Proc Natl Acad Sci U S A 2004;101(12):4118-23.

13. Shibuya T, Tange TO, Sonenberg N, Moore MJ. eIF4AIII binds spliced mRNA in the exon junction complex and is essential for nonsense-mediated decay. Nat Struct Mol Biol 2004;11(4):346-51.

14. Andersen CB, Ballut L, Johansen JS, *et al.* Structure of the exon junction core complex with a trapped DEAD-box ATPase bound to RNA. Science 2006;313(5795):1968-72.

15. Le Hir H, Andersen GR. Structural insights into the exon junction complex. Curr Opin Struct Biol 2008;18(1):112-9.

16. Nielsen KH, Chamieh H, Andersen CB, *et al.* Mechanism of ATP turnover inhibition in the EJC. Rna 2009;15(1):67-75.

17. Ballut L, Marchadier B, Baguet A, Tomasetto C, Seraphin B, Le Hir H. The exon junction core complex is locked onto RNA by inhibition of eIF4AIII ATPase activity. Nat Struct Mol Biol 2005;12(10):861-9.

18. Suzuki C, Garces RG, Edmonds KA, *et al.* PDCD4 inhibits translation initiation by binding to eIF4A using both its MA3 domains. Proc Natl Acad Sci U S A 2008;105(9):3274-9.

19. Wedeken L, Ohnheiser J, Hirschi B, Wethkamp N, Klempnauer KH. Association of Tumor Suppressor Protein Pdcd4 With Ribosomes Is Mediated by Protein-Protein and Protein-RNA Interactions. Genes & Cancer 2010;1(3):293-31.

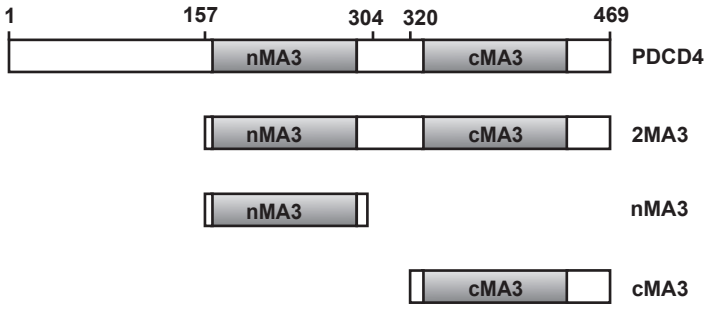

Figure 4.1 Schematic of PDCD4 showing nMA3 and cMA3 domains. The 2MA3 domain extends from amino acids 157 to 469. The nMA3 domain encompasses amino acids 157 to 304 while the cMA3 domain contains amino acids 320-469.

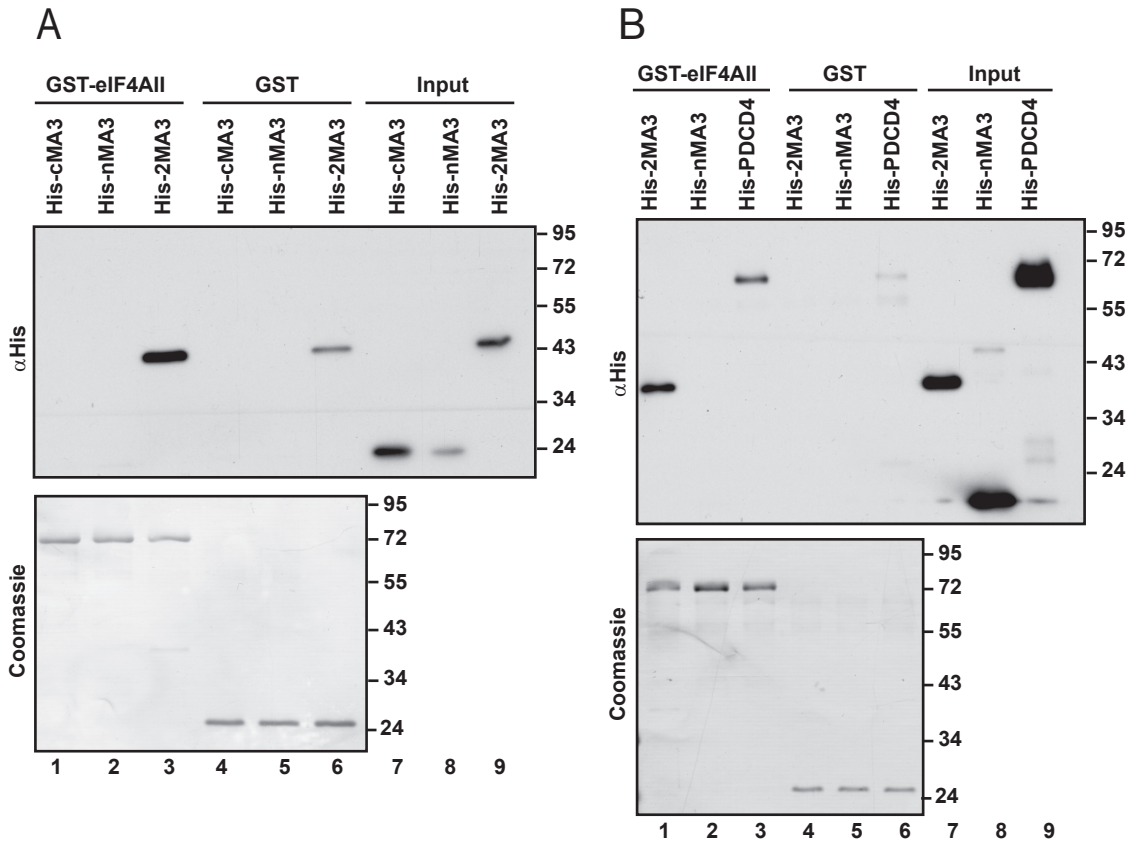

Figure 4.2 Both MA3 domains on PDCD4 are necessary for efficient direct binding to eIF4AII. (A) GST-eIF4AII is able to interact with His-2MA3 (top panel, lane 3) but not the His-cMA3 or His-nMA3 domains (top panel, lanes 2-3). GST-eIF4AII (bottom panel lanes 1-3) and GST (bottom panel, lanes 4-5) were loaded equivalently and visualized by Coomassie staining of immunoblot. Loading of His-nMA3 was low (top panel, lane 8) so a repeat of the experiment was performed using the 2MA3 and full length His-PDCD4 as controls. **(B)** GST-eIF4AII is able to interact with His-2MA3 (top panel, lane 1) and His-PDCD4 (top panel, lane 3) but not with His-nMA3 domain (top panel, lane 2). Input levels of His-tagged proteins were similar (top panel, lanes 7-9). GST-eIF4AII (bottom panel, lanes 1-3) and GST protein (bottom panel, lanes 4-6) were loaded similarly by Coomassie staining of immunoblot.

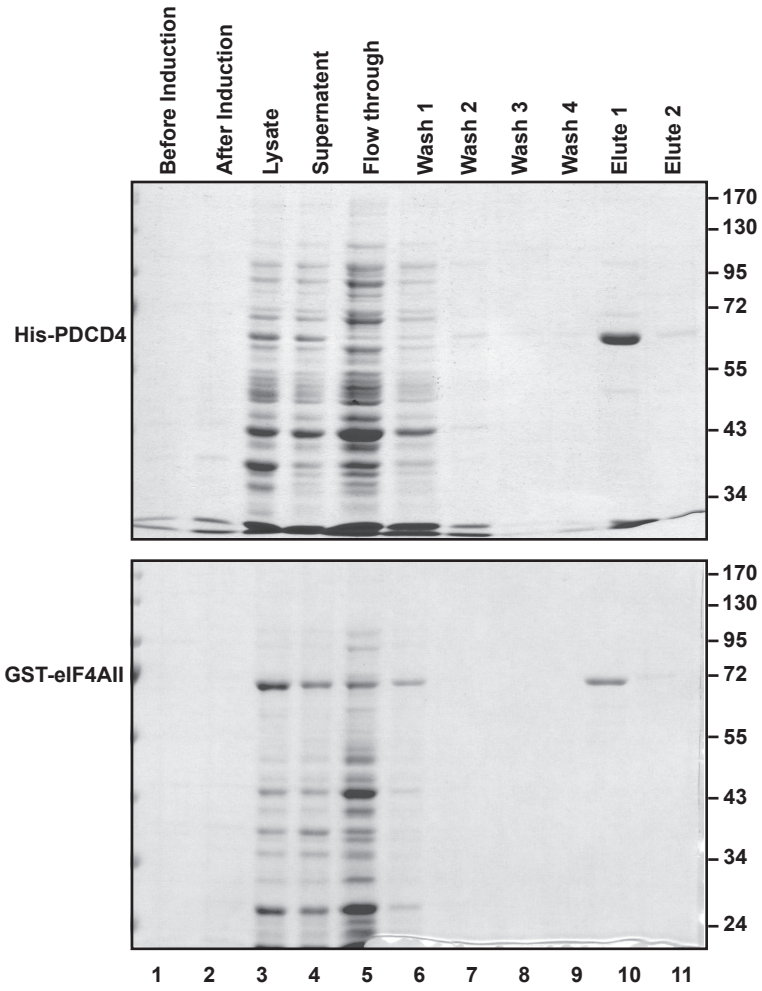

Figure 4.3 Purification of His-PDCD4 and GST-eIF4AII proteins. His-tagged PDCD4 (top panel) and GST-eIF4AII (lower panel) were expressed in BL21/RIL bacteria and, once fusion protein was captured on affinity matrix, the samples were extensively washed to reduce RNase contamination. His-PDCD4 and GST-eIF4AII from the first elution (lane 10) from nickel-NTA (top panel) and glutathione resin (lower panel), respectively, were used for analysis in RNA electrophoretic mobility shift assays.

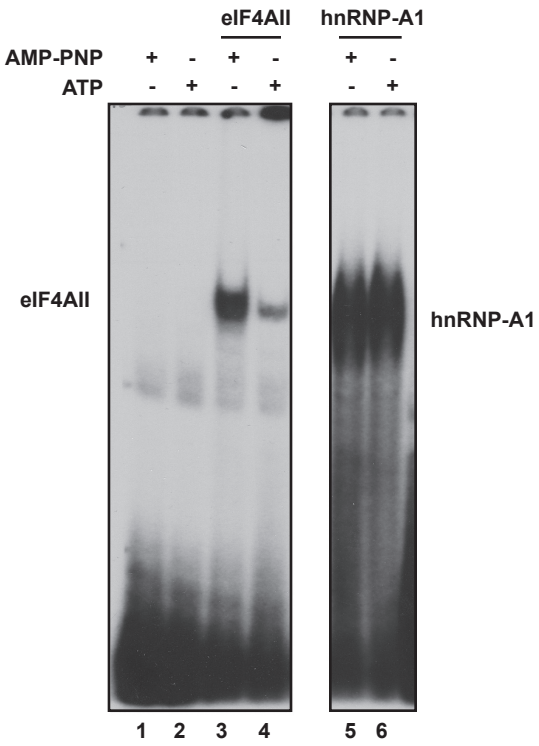

Figure 4.4 eIF4AII is locked onto RNA by addition of AMP-PNP. GST-eIF4AII binds stably to labeled RNA in the presence of the non-hydrolyzable ATP analogue AMP-PNP (lane 3) better than in the presence of ATP (lane 4). hnRNP-A1, which is insensitive to ATP, binds equally to RNA in the presence of ATP or AMP-PNP (lanes 5-6).

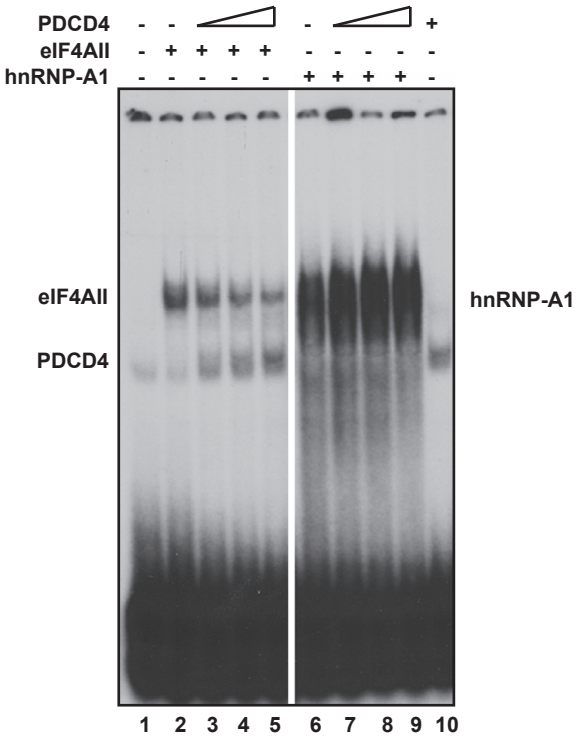

Figure 4.5 PDCD4 blocks the ability of eIF4AII to interact with RNA. GST-eIF4AII interacts with RNA in the presence AMP-PNP (lane 2). Increasing additions of His-PDCD4 causes loss of eIF4AII binding to RNA (lanes 3-5) without the appearance of a higher molecular weight species indicating that PDCD4, eIF4AII, and RNA do not make a complex. Increasing addition of His-PDCD4 does not inhibit hnRNP-A1 RNA binding (lanes 7-9), indicating that the PDCD4 induced inhibition of eIF4AII is specific. PDCD4 bands represent gel shifts when PDCD4 binds to radiolabeled RNA.

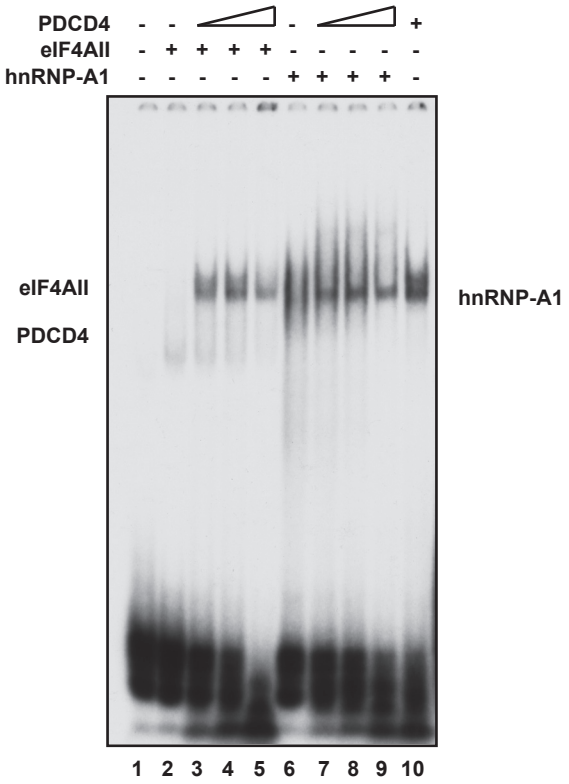

Figure 4.6 Evidence that eIF4AII may inhibit PDCD4 binding to RNA. His-PDCD4 binds RNA (lane 2) and this binding is decreased with increasing amounts of GST-eIF4AII (lanes 3-5). This experiment is not conclusive since there appears to be RNAse contamination (note alterations in free RNA, bottom bands lanes 3-5) when both PDCD4 and eIF4AII are added into the reaction.

CHAPTER 5

SUMMARY AND PERSPECTIVE

PDCD4 has been extensively studied in many types of *in vitro* assays for tumor suppression. This has resulted in multiple anticancer mechanisms being attributed to PDCD4. *In vivo*, PDCD4 knockout mice developed B-cell lymphoma. This has lead to observations that expression of PDCD4 in tumors is correlated with longer survival and/or better outcomes in cancer patients. Despite this, very few studies have directly tested in model organisms what has been discovered *in vitro*. Many questions remain; does PDCD4 inhibit cancer through growth suppression, invasion inhibition or apoptosis stimulation, and what factors modulate these possible tumor suppressor functions *in vivo*?

In Chapter 2, I describe new interacting partners of PDCD4: eIF4AIII, Nup153 and PRMT5. Interactions with these new proteins, along with eIF4G, eIF4AII, and ribosomes, places PDCD4 within the central framework of mRNA biogenesis from transcription through translation. Possible regulation of splicing and mRNA transport from the nucleus to the cytoplasm points to new mechanisms of cell growth regulation for PDCD4 beyond translation. Determining the role these interactions play in tumor suppression will involve separating the ability of PDCD4 to bind with each new partner independently and testing these mutants for tumor growth phenotypes.

Although I did not find a interaction between PDCD4 and the exon junction complex protein eIF4AIII using material from transformed tumor cell lines, this interaction could occur in normal cells or in other cancer contexts. A PDCD4 interaction with the exon junction complex in normal cells could regulate mRNA fate, contributing to the repertoire of transcripts that maintain normal cell growth. Disruption of this interaction in transformed cells may lead to enhanced potential for tumor growth. The first priority to follow this lead would be to test whether an interaction between eIF4AIII and PDCD4 occurs in normal cells, such as the nontransformed MCF10A breast cell line. Detecting mRNA expression in PDCD4 knockout mice versus normal mice could be useful in determining changes in mRNA trafficking or stability. Studies utilizing purified PDCD4 injected with intron-containing reporters into *Xenopus* egg nuclei could track any changes in mRNA fate directed by PDCD4.

The interaction with the nuclear pore protein Nup153 described in Chapter 2 further underscores the possibility that PDCD4 may sort and/or traffic classes of mRNAs as they transit through the nuclear pore. Changing the efficiency of mRNA transport from the nucleus to the cytoplasm would, by default, change the efficiency of translation as the polyribosome is loaded in the cytoplasm. Determining classes of mRNAs that experience altered transit through the nuclear pore upon perturbation of PDCD4 may help classify proteins involved in tumor suppression or oncogenesis. Nup153 also plays a novel role in mitotic control checkpoints (1). Alterations of these noncanonical roles of Nup153 may explain cell cycle disruption caused by upregulation or depletion of PDCD4.

Although not confirmed in mammalian cancer cell lines, the regulation of PDCD4 and PRMT5 interaction in Xenopus is clearly cell cycle dependent (see Chapter 2). Many proteins are hyperphosphorylated during mitosis and the lack of binding between PDCD4 and PRMT5 in this cell phase points to a role of phosphorylation in controlling this interaction. Determining what pathway is responsible for this binding inhibition, and promoting this pathway, may also block accelerated growth observed in tumors with high levels of PDCD4 and PRMT5. A cell cycle regulated interaction between PDCD4 and PRMT5 was not observed in transformed human cells. The difference observed between *Xenopus* egg extract and human cell lines could occur because of differences in differentiation, egg cells being embryonic and the human cell lines somatic, or could also be due to the human cells being transformed. Alternatively, the discrepancy observed could be due to a difference in species regulation. Determining the cell cycle regulation of PDCD4 and PRMT5 interaction in non-transformed human cells could help delineate if this discrepancy is due to misregulation in cancer or a species specific phenomena.

The use of PDCD4 as a prognostic biomarker may encompass a broad swath of cancer types (see Chapter 1). We have observed that elevated expression of PDCD4 transcript in breast cancer tumors correlates with longer survival (Chapter 3). This breast cancer analysis is very similar to observations in lung, colon and ovarian cancer where high levels of PDCD4 protein expression is correlated with longer survival (2-4). Despite these findings, in all cancer types, between 20 and 40% of patients with elevated tumor levels of PDCD4 have poor outcomes. This suggests that mechanisms within these tumors have counteracted the protective effect of PDCD4 expression. Our

discovery that PDCD4 interacts with PRMT5 provides one possible explanation for these observations. In breast cancer tumors where both PDCD4 and PRMT5 mRNAs are upregulated, the protective effect of PDCD4 is clearly negated (Chapter 3). This indicated that PRMT5 somehow deactivated PDCD4. I tested how co-expression affects breast cancer growth in an orthotopic model and found the PDCD4 and PRMT5 work synergistically to promote tumor growth. The enzymatic activity of PRMT5 and the site of PRMT5 modification on PDCD4 were both necessary for this accelerated tumor growth phenotype, providing a molecular mechanism for the correlations observed in clinical breast cancer data. Originally, the PRMT5/PDCD4 interaction appeared to be simple case of an oncogenic factor deactivating a tumor suppressor by post- translational modification. In effect, our theory was that the ratio of active oncogenic factors to tumor suppressors was tipped in the direction of tumor growth through this interaction. Instead, neither PDCD4 nor PRMT5 expression alone resulted in changes in tumor growth. Rather, the PDCD4-PRMT5 overexpressing cells gained a new growth phenotype. This is one of the first examples of clinical correlations in the PDCD4 cancer biology field that was then tested in a model organism. In the context of breast cancer, PDCD4 may have tumor suppressor properties when highly expressed but oncogenic functions when PRMT5 is also expressed. This is not unprecedented. The tumor suppressor p27 function can also have oncogenic properties when post-translationally modified and cytoplasmically localized (5, 6). This discovery also increases the accuracy of using PDCD4 as a predictive biomarker by pointing to the utility of tracking expression levels of PRMT5 at the same time. Yet, we still do not know what biological effect is occurring when PDCD4 interacts and is methylated by PRMT5.

The known PDCD4 tumor suppressor function results in inactivation of eIF4A and translation initiation. Could methylation by PRMT5 cause a reversal of function for PDCD4 from a translation suppressor to a translation activator? This is one possible scenario that will need to be explored. Also, these results do not rule out that a complex of methylated PDCD4 and PRMT5 alters PRMT5 targets or enzymatic activity and thereby cause an accelerated tumor growth phenotype.

PRMT5 belongs to the arginine methyl transferase (PRMT) family of enzymes. Type I PRMTs, such as PRMT1, mediates the addition of two methyl groups on one of the terminal nitrogens of arginine residues and this modification is termed an asymmetrical dimethylarginine (ADMA) (7). PRMT5 belongs to the type II class of enzymes. These enzymes catalyze the addition of a methyl groups onto both terminal nitrogens on an arginine residue and this modification is termed a symmetrical dimethylarginine (SDMA) (7). PRMT5 is known to methylate Sm proteins for efficient assembly of snRNPs (8) and also modulates transcription (9-12). Binding to the nuclear protein COPR5, PRMT5 is recruited to areas of the nucleosome and methylation of histone H4 leading to gene silencing of some targets (13). When associated with SWI/SNF chromatin remodeling complex, PRMT5 is thought to methylate histone H3 and H4 and also silence genes, notably, the tumor suppressors ST7 and NM23 (11). In the case of myogenesis, association of PRMT5 with SWI/SNF can activate transcription (14). PRMT5 also interacts with a transcription elongation factor hIws1 necessary for cell proliferation (15). Overexpression of PRMT5 can transform NH3T3 cells (11) and is highly expressed in some leukemia and lymphomas (10). Finally, PRMT5 has been found to be involved in development. In conjunction with Blimp1, PRMT5 has a role in

maintaining dedifferentiation in primordial germ cells (16, 17). An association with PDCD4 could alter some, or all, of these function of PRMT5 and contribute to tumor growth.

Finally, by RNA gel shift analysis, I describe the finding that PDCD4 interferes with the translation initiation protein, eIF4AII, by inhibiting its interaction with RNA (Chapter 4). This is a clear mechanism by which PDCD4 interferes with the helicase function of eIF4A. Furthermore, the intrinsic RNA binding function of PDCD4 appears blocked by binding to eIF4AII. While this line of experiments were being performed, Suzuki *et al.* published a report where a truncated version of PDCD4 (not including the RNA binding domain) displaced RNA from the eIF4A N-terminal truncation mutant by NMR spectra analysis (18). The RNA gel shift experiments here extend the findings of this result by using full length proteins and discovering that PDCD4 RNA interactions are also inhibited.

PDCD4 shows promise as a useful biomarker in cancer. In breast cancer, tracking PDCD4 and PRMT5 simultaneously increases the accuracy of prognosis based on these molecules. Developing tools to track PDCD4 methylation status in cancer my further increase the value of this biomarker. PRMT5 is a promising target for small molecule inhibitors due to its enzymatic activity and roles in oncogenesis. Inhibition of PRMT5 may well unleash the tumor suppressor function of PDCD4. Determining what mechanism PDCD4 and PRMT5 utilize to increase tumor growth may also lead to new targets of drug development.

5.1 References

1. Mackay DR, Elgort SW, Ullman KS. The nucleoporin Nup153 has separable roles in both early mitotic progression and the resolution of mitosis. Mol Biol Cell 2009;20(6):1652-60.

2. Wei NA, Liu SS, Leung TH, *et al.* Loss of Programmed cell death 4 (Pdcd4) associates with the progression of ovarian cancer. Mol Cancer 2009;8:70.

3. Mudduluru G, Medved F, Grobholz R, *et al.* Loss of programmed cell death 4 expression marks adenoma-carcinoma transition, correlates inversely with phosphorylated protein kinase B, and is an independent prognostic factor in resected colorectal cancer. Cancer 2007;110(8):1697-707.

4. Chen Y, Knosel T, Kristiansen G, *et al.* Loss of PDCD4 expression in human lung cancer correlates with tumour progression and prognosis. J Pathol 2003;200(5):640-6.

5. Lee J, Kim SS. The function of p27 KIP1 during tumor development. Exp Mol Med 2009;41(11):765-71.

6. Besson A, Hwang HC, Cicero S, *et al.* Discovery of an oncogenic activity in p27Kip1 that causes stem cell expansion and a multiple tumor phenotype. Genes Dev 2007;21(14):1731-46.

7. Gary JD, Clarke S. RNA and protein interactions modulated by protein arginine methylation. Prog Nucleic Acid Res Mol Biol 1998;61:65-131.

8. Friesen WJ, Paushkin S, Wyce A, *et al.* The methylosome, a 20S complex containing JBP1 and pICln, produces dimethylarginine-modified Sm proteins. Mol Cell Biol 2001;21(24):8289-300.

9. Wang L, Pal S, Sif S. Protein arginine methyltransferase 5 suppresses the transcription of the RB family of tumor suppressors in leukemia and lymphoma cells. Mol Cell Biol 2008;28(20):6262-77.

10. Pal S, Baiocchi RA, Byrd JC, Grever MR, Jacob ST, Sif S. Low levels of miR-92b/96 induce PRMT5 translation and H3R8/H4R3 methylation in mantle cell lymphoma. Embo J 2007;26(15):3558-69.

11. Pal S, Vishwanath SN, Erdjument-Bromage H, Tempst P, Sif S. Human SWI/SNF-associated PRMT5 methylates histone H3 arginine 8 and negatively regulates expression of ST7 and NM23 tumor suppressor genes. Mol Cell Biol 2004;24(21):9630-45.

12. Pal S, Yun R, Datta A, *et al.* mSin3A/histone deacetylase 2- and PRMT5-containing Brg1 complex is involved in transcriptional repression of the Myc target gene cad. Mol Cell Biol 2003;23(21):7475-87.

13. Lacroix M, El Messaoudi S, Rodier G, Le Cam A, Sardet C, Fabbrizio E. The histone-binding protein COPR5 is required for nuclear functions of the protein arginine methyltransferase PRMT5. EMBO Rep 2008;9(5):452-8.

14. Dacwag CS, Ohkawa Y, Pal S, Sif S, Imbalzano AN. The protein arginine methyltransferase Prmt5 is required for myogenesis because it facilitates ATP-dependent chromatin remodeling. Mol Cell Biol 2007;27(1):384-94.

15. Liu Z, Zhou Z, Chen G, Bao S. A putative transcriptional elongation factor hIws1 is essential for mammalian cell proliferation. Biochem Biophys Res Commun 2007;353(1):47-53.

16. Durcova-Hills G, Tang F, Doody G, Tooze R, Surani MA. Reprogramming primordial germ cells into pluripotent stem cells. PLoS One 2008;3(10):e3531.

17. Ancelin K, Lange UC, Hajkova P, *et al.* Blimp1 associates with Prmt5 and directs histone arginine methylation in mouse germ cells. Nat Cell Biol 2006;8(6):623-30.

18. Suzuki C, Garces RG, Edmonds KA, *et al.* PDCD4 inhibits translation initiation by binding to eIF4A using both its MA3 domains. Proc Natl Acad Sci U S A 2008;105(9):3274-9.